

https://dspace.org/

The development of strategic deoxygenation of seed oil for bio-energy use

Pedzisai, Standford Mirainashe

2022
https://hdl.handle.net/10539/34107

Downloaded from a DSpace repository. https://dspace.org/

The Development of Strategic Deoxygenation of Seed Oil for Bio-Energy Use

Submitted by

Standford Mirainashe Pedzisai (2380750)

A Dissertation submitted to the Faculty of Engineering and the Built Environment, University of the Witwatersrand, Johannesburg, South Africa, in fulfilment for the degree of Master of Science.

Supervisor: Prof. Diakanua Bavon Nkazi

Johannesburg, 2021

Declaration

I declare that this dissertation titled *"The Development of Strategic Deoxygenation of Seed Oil for Bio-Energy Use"* is the result of my own unaided research work, except as cited and acknowledged in the references. This dissertation has not been submitted for any degree.

Name: Standford Mirainashe Pedzisai

Student Number: 2380750

Signature: …  …….

Date:…….6 September 2021……..

Dedication

This work is dedicated to:

To my family for their unwavering love and support.

Acknowledgements

Firstly I would like to thank God for his faithfulness in directing the course of my life, and being an ever-present help in times of need.

I would like to express my sincere gratitude to the following individuals for availing their assistance which greatly contributed to the success of this work:

Professor Diakanua Nkazi; my supervisor, thank you so much for providing guidance and encouragement throughout the course of this work. This project benefitted immensely from your deep knowledge and expertise in organic chemistry, particularly in the oil and gas field. I could never thank you enough for funding my studies, you are much appreciated Prof.

Dr. Hembe Mukaya; I am so grateful for your availability to assist from the ordering of chemicals and gases, to the laboratory work, and in the editing of my manuscripts. Thank you for the rich discussions which greatly impacted this work.

My parents; you guys are gems! Thank you for your sacrificial financial provision to my sustenance, regardless of the harsh economic environment back home. Your moral support and prayers continue to help me each day, and I'm eternally grateful for that.

Mr. Motlatsi Phali; thank you for providing all the relevant apparatus in the laboratories for the success of this project. Thank you also for availing your prowess with the GC-MS for the oils used in this project. Your assistance with the BET, FTIR, TEM and XRD analyses for the catalysts used in this work is much appreciated.

Ms. Letta Ntuli; I am so grateful for your assistance in the labs with the provision of apparatus, as well as with the TGA characterization of this work's catalysts.

Miss. Sonia Mavhungu; thank you for lending your helping hand in mobilizing the apparatus for the experimental work of this project as well as with the AAS analysis of the catalysts used herein.

Mrs. Petra Dinham; thank you for diligently assisting with the SEM analysis of the catalysts used in this work.

Mr. Ngonidzashe Masunga; thank you for instilling confidence in me during the course of this work through the equipping discussions we would have.

Dr. Joshua Gorimbo; you are appreciated for letting me benefit from you and your vast network of academics. Thank you also, for assisting in the proof reading of my review paper.

Abstract

The growing demand for diesel fuel in the face of the rapidly dwindling fossil fuel reserves, oil price fluctuations and stringent pollution control regulations has stimulated the growth of the biofuels industry, particularly biodiesel production as it is presently the best commercially-produced renewable alternative to petroleum diesel. Biodiesel is a recognized complement and credible replacement of mineral diesel with overwhelming attributes relative to fossil diesel such as eco-friendliness, non-toxicity and good lubricity when used in diesel engines. Biodiesel is popularly produced as Fatty Acid Alkyl Esters through catalytic transesterification of triglycerides with an alkyl donor. However, Fatty Acid Alkyl Esters have limitations in oxidation stability, calorific value and cold flow properties relative to mineral diesel hence are throttled in their blending ratios with the latter to prevent engine damage and power losses during engine operation. The alternative renewable diesel synthesis strategy, deoxygenation, which yields n-alkanes and n-alkenes from fatty acids and triglycerides, produces better quality renewable diesel which can be employed in the currently existing engines at higher blending proportions or in its pure form without the aforementioned FAAEs problems. However, for this strategy to be economically viable for industrial scale production, there exists a need for its optimization with regards to the operating parameters and the diversity of the feedstock oils.

The deoxygenation of waste cooking oil was optimized using Design Expert® and the optimum conditions were applied on castor oil to investigate the influence of oil composition on its deoxygenation success. Five bimetallic catalysts of varying Ni:Co ratios were synthesized by impregnation to an alumina support. The optimum Ni:Co composition ratio for the catalyst was found to be 1:1 based on its selectivity for the deoxygenation of waste cooking oil. Various characterization techniques were employed to investigate the effects of catalyst composition on its physiochemical properties. The GC-MS was used for the characterization of the oils used in this work. Deoxygenation activity was discovered to be having a directly proportional relationship with reaction time, temperature and catalyst loading influence although to different magnitudes. Oil composition was also discovered to have considerable influence on the rate and extent of its deoxygenation. It was deduced therefore that catalysts behave differently with different oils. The highest deoxygenation extent for waste cooking oil (96.12%) was realized for the reaction conditions: 1Ni:1Co/Al_2O_3 catalyst, 300°C reaction temperature, 5 hours reaction duration, and a

catalyst loading of 1 wt.%. Under the same reaction conditions, a 37.4% oxygen content reduction from castor oil was realized.

Publications

- Review Paper titled *"Sustainable Production Strategies of Biodiesel for a Friendly Environment"* (Under Review with the Environmental Progress and Sustainable Energy Journal)

Nomenclature

AAS:	Atomic Absorption Spectometry
BET:	Brunauer-Emmet-Teller analysis
BJH:	Barrett-Joyner-Halenda analysis
CHMT:	School of Chemical and Metallurgical Engineering
Co:	Cobalt
CO:	Carbon Monoxide
$CO_{2:}$	Carbon Dioxide
Conc.%	Percentage Concentration
DCO_x:	Decarboxylation/ Decarbonylation
DCX:	Decarboxylation
DCN:	Decarbonylation
DO:	Deoxygenation
DoE:	Design of Experiments
EN:	European Standard
EU:	European Union
FFA:	Free Fatty Acid(s)
FT-IR:	Fourier Transform Infrared Spectra
GC-MS:	Gas Chromatography and Mass Spectrometry
GHG:	Greenhouse Gasses
H_2:	Hydrogen
HDO:	Hydrodeoxygenation

ml:	Millilitres
Mo:	Molybdenum
Ni:	Nickel
N_2:	Nitrogen
NO_x:	Nitrogen Oxides
rpm:	Revolutions per Minute
SEM:	Scanning Electron Microscopy
TEM:	Transmission Electron Microscopy
TGA:	Thermogravimetric analysis
USA:	United States of America
WCO:	Waste Cooking Oil
vol. %:	Volume Percentage
wt. %:	Weight Percentage
XRD:	X-Ray Diffraction

Table of Contents

Declaration i

Dedication ii

Acknowledgements iii

Abstract v

Publications vii

Nomenclature viii

Table of Contents x

List of Figures xiv

List of Tables xvi

Outline of the Dissertation xvii

Chapter 1: Introduction 18

1.1 Background 18

1.2 Problem Statement and Research Motivation 19

1.3 Aim and Objectives 20

1.4 Summary 20

Chapter 2: Literature Review 21

2.1 Introduction 21

2.2 Biodiesel Synthesis Feedstocks 21

2.2.1 Food competition 22

2.2.2 Land Competition 23

2.2.3 Oil Yield 23

2.2.4 Availability 24

2.2.5 Extraction 25

2.2.6 Lipid Composition 26
2.3 Biodiesel Synthesis Strategies 30
2.3.1 Transesterification 30
2.3.2 Deoxygenation 53
2.3.3 Hydrocracking 63
2.3.4 Development of the Biodiesel Synthesis Strategy 66
2.4 Conclusions 68
Chapter 3: Catalyst Synthesis and Selection 69
3.1 Introduction 69
3.2 Experimental Procedure 69
3.2.1 Catalyst Synthesis 69
3.2.2 Catalyst characterization 70
3.3 Results and Discussion 72
3.3.1 Catalyst Functional Groups 73
3.3.2 Catalyst Phases 74
3.3.3 Catalyst Morphology 75
3.3.4 Catalyst Surface Properties 77
3.4 Conclusions and Recommendations 81
Chapter 4: Deoxygenation of Waste Cooking Oil for Bio-Energy Production 69
4.1 Introduction 82
4.2 Experimental Procedure 82
4.2.1 Deoxygenation (DO) 82
4.2.2 Characterization of the DO Products 85
4.3 Results and Discussion 86
4.3.1 Influence of catalyst metal loading on DO activity 87

4.3.2 Influence of reaction time on DO activity 92
4.3.3 Influence of catalyst loading 96
4.3.4 Influence of reaction temperature 100
4.3.5 Kinetic Analysis of the Deoxygenation of Waste Cooking Oil 101
4.3.6 Hydrocracking of WCO 102
4.4 Conclusions and Recommendations 105
Chapter 5: Optimization of the Deoxygenation of Waste Cooking Oil 106
5.1 Introduction 106
5.2 Design of Experiments 106
5.3 Analysis 107
5.4 Optimization 110
5.5 Conclusions and Recommendations 111
Chapter 6: Strategic Method for the Deoxygenation of Seed Oil 112
6.1 Introduction 112
6.2 Deoxygenation of Castor Oil 112
6.3 Development of a Strategic Method for Seed Oil Deoxygenation 115
6.3.1 Method Development 115
6.3.2 Proposed Deoxygenation Mechanism for Addressing the Damping Behavior of Deoxygenation 117
6.4 Conclusions and Recommendations 118
Chapter 7: General Conclusions 119
7.1 Introduction 119
7.2 Conclusions and Recommendations 119
References 122
Appendices 137

List of Figures

Figure 2.1: Overall transesterification reactions of triglycerides; where R^1, R^2, R^3 are long chain hydrocarbons 31
Figure 2.2: Esterification reaction of fatty acid with alcohol; R^4 is an acyl residue, R' is the alcohol moiety 31
Figure 2.3: Interesterification reaction of TG with methyl acetate 31
Figure 2.4: Stoichiometric reaction schemes for the esterification of fatty acids with methyl acetate 32
Figure 2.5: Biodiesel production through transesterification block diagram 33
Figure 2.6:The three deoxygenation pathways for fatty acids 55
Figure 2.7: The Proposed Biodiesel Synthesis Strategy 67
Figure 3.1: FTIR spectra for the catalysts 73
Figure 3.2: Expanded view of the FTIR spectra 74
Figure 3.3: X-ray diffractograms of the catalysts 75
Figure 3.4: Scanning Electron Micrographs of the catalysts 76
Figure 3.5: Transmission Electron Micrographs of the catalysts 77
Figure 3.6: N_2 adsorption–desorption isotherms of $NiCo/Al_2O_3$ catalysts 78
Figure 3.7: BJH Desorption dA/dlog(D) Pore Area 79
Figure 3.8: BJH Desorption dV/dlog(D) Pore Volume 80

Figure 4.1: Deoxygenation apparatus setup 83
Figure 4.2: Deoxygenation with respect to catalyst composition 87
Figure 4 3: Functional group selectivity with respect to catalyst composition 89
Figure 4 4: Proposed DO mechanisms of Linoleic Acid and Oleic Acid 91
Figure 4.5: Deoxygenation response to reaction time 93
Figure 4.6: Deoxygenation relationship with reaction time 94
Figure 4.7: Functional group selectivity with respect to reaction time 95
Figure 4 8: Effect of catalyst loading on deoxygenation 97
Figure 4 9: Relationship between catalyst loading and deoxygenation 98

Figure 4 10: Functional group selectivity with catalyst loading 99
Figure 4 11: The relationship between deoxygenation and reaction temperature 100
Figure 4.12: Hydrocarbons selectivity with respect to catalyst composition 103

Figure 5.1: Surface Response from the optimization model..... 109
Figure 5 2: The optimization model..... 111

Figure 6.1: Proposed deoxygenation mechanisms of castor oil..... 114
Figure 6 2: Strategic method for seed oil deoxygenation 116

List of Tables

Table 2.1: Biodiesel Feedstocks Classification (Huang et al., 2015; Norjannah et al., 2016; Zhu, Li and Hiltunen, 2016). 22
Table 2.2: Lipid Composition Profiles of Vegetable Oils (Verma and Sharma, 2016; Mahmudul et al., 2017; Moazeni, Chen and Zhang, 2019; Nekhavhambe, Mukaya and Nkazi, 2019) 27
Table 2.3: Catalytic deoxygenation of Lipids 58

Table 3.1: Catalyst Active Metal Loading to 20g Alumina 70
Table 3.2: Catalyst Active Metal Composition Profiles 72
Table 3.3: Surface area, pore volume and pore size of the $NiCo/Al_2O_3$ catalysts 80

Table 4.1: Waste cooking oil deoxygenation parameters 84
Table 4:2: Fatty Acids Distribution of Waste Cooking Oil 86

Table 5 1: Design of Experiments Specifications 106
Table 5.2: Factors Summary 107
Table 5 3: Response Summary 107
Table 5 4: Model Summary Statistics 108
Table 5 5: ANOVA of the optimization model 109
Table 5 6: The Optimization Constraints 110

Outline of the Dissertation

The dissertation is delineated as follows:

Chapter 1: Introduction – This is the foundational chapter upon which this research work is built. It provides an insight into the current state of affairs which justifies the undertaking of this work, and the objectives that this work sought to achieve.

Chapter 2: Literature Review – An in-depth insight into literature studies that encompass the work in this project or similar scopes of study is given. The focus was on the biodiesel feedstocks and synthesis strategies, as well as its properties.

Chapter 3: Catalyst Synthesis and Selection – The procedures followed in synthesizing and characterizing the $NiCo/Al_2O_3$ catalysts for this project are outlined; the characterization results are also presented and discussed, leading to the selection of the catalyst with the most suited physiochemical properties for the deoxygenation of seed oil.

Chapter 4: Deoxygenation of seed oil for bio-energy production –The deoxygenation and characterization procedures for the waste cooking oil followed in this project are detailed. The results on the influence of catalyst metal composition ratios, catalyst loading, reaction temperature and duration on DO activity are presented and discussed.

Chapter 5: Optimization of deoxygenation method – The role played by Design Expert® is documented, from the design of experiments, analysis and optimization of the deoxygenation of waste cooking oil process.

Chapter 6: Strategic method for the deoxygenation of seed oil – A strategic method for the deoxygenation of seed oil is developed following the investigation of the influence of oil composition on its deoxygenation.

Chapter 7: Conclusions and Recommendations – A presentation of the conclusions reached from the analysis of results presented herein, and observations during the experimental stage of this work. Recommendations for future related works are also given.

Chapter 1: Introduction

1.1 Background

The growing demand for diesel fuel in the face of the rapidly depleting fossil fuel reserves, oil price fluctuations and stringent environmental pollution control regulations has engendered the growth of the biofuels industry globally (Huang *et al.*, 2015; Zhu, Li and Hiltunen, 2016; Damanik *et al.*, 2018; Makar and Ganda, 2018; Stephen and Periyasamy, 2018). Currently, about 80% of global primary energy demand is met by fossil fuels, whose growth is constrained by their finite nature (Collection, 2016). It is predicted that diesel fuel utilization will grow to about 5.7 million liters per day by the year 2035 as a result of the increasing number of heavy-duty trucks as well as the growing transportation and industrial sectors (Onoji *et al.*, 2016; Hajjari *et al.*, 2017). Diesel finds many uses in the South African economy, chiefly as the transportation fuel with the highest demand, for driving machinery in industry, as well as for power generation in some Eskom-run PowerStations such as Ankerlig and Gourikwa. Experts predict fossil oil scarcity within the next fifty years; due to the current estimated oil reserve (239400 million tonnes oil) depletion, so it is mandatory for alternatives to replace it (Banković-Ilić *et al.*, 2017; Hajjari *et al.*, 2017).

With small amounts of proved crude oil reserves, South Africa imports crude oil and refined fuels to meet its liquid fuel needs (Collection, 2016). As such, the security of supply also depends on the economic and political stability in the Organization of the Petroleum Exporting Countries (OPEC) countries (Herbert et al., 2019). South Africa, nonetheless envisages that it should be having adequate supply security in electricity and liquid fuels such that economic activity, transport and welfare are not disrupted, in the National Development Plan (NDP 2030: 163). The current total refining capacity amounts to 703 000 barrels per day, of which 72% is from crude oil refining, with the balance coming from synthetic fuel refining (Collection, 2016).

The Green Transport Strategy of South Africa identifies biofuels as one of the sustainable clean transport fuels for the transition towards a lower carbon transport future of the country, regardless the introduction of electric vehicles (Ca, 2020). Biodiesel has been recognized as the mainstream renewable supplement and credible alternative of fossil diesel because of its overwhelming

physiochemical properties that are comparable to petroleum diesel in addition to its good lubricity, biodegradability, non-toxicity and eco-friendliness when used in diesel engines (Mofijur *et al.*, 2016; Sehatpour, Kazemi and Sehatpour, 2017; Strzalka, Schneider and Eicker, 2017). Biodiesel is popularly produced in the form of Fatty Acid Alkyl Esters (FAAE) through the transesterification of triglycerides with an alkyl donor (mainly methanol or ethanol) in the presence a catalyst (Bagchi, Rao and Mallick, 2015; Serqueira *et al.*, 2015; Amin *et al.*, 2016; Liu *et al.*, 2016; Mujeeb, Vedamurthy and T, 2016; Laviola *et al.*, 2017; Mostafa and El-Gendy, 2017). It can effectively be blended with mineral diesel at practically any ratio, or can be used in its pure form in the preexisting diesel engines without prior modifications (Hegde *et al.*, 2015; Millo *et al.*, 2015; Amin *et al.*, 2016; Kumar and Rehman, 2016; Banković-Ilić *et al.*, 2017; Sehatpour, Kazemi and Sehatpour, 2017; Strzalka, Schneider and Eicker, 2017). In terms of the Mandatory Blending Regulations in South Africa; there is a minimum 5% mandatory blending of biodiesel into mineral diesel (subject to availability of locally produced biofuels) (Ca, 2020). Presently there are several small- and medium-scale biodiesel production plants utilizing waste cooking oil around South Africa (Herbert *et al.*, 2019), these supply their biodiesel to the refineries for blending with mineral diesel.

1.2 Problem Statement and Research Motivation

The mainstream biodiesel production strategy, transesterification, produces biodiesel which is not entirely favorable to the diesel engine (Viêgas *et al.*, 2015), due to its low oxidation stability, poor cold flow properties and low energy density, relative to mineral diesel (Li *et al.*, 2018). This is induced by the unsaturation in the fatty acid chains, and the presence of oxygen in the biodiesel. The oxygen in the biodiesel makes it corrosive to the engine, and susceptible to the formation gums and other impurities that result in poor storage stability, filter plugging, and the development of residue on fuel pumps (Zulkepli *et al.*, 2018). As such, the blending ratios for the biodiesel with fossil diesels are limited to 7 vol.% by the EN 590 standards (Goede *et al.*, 2015; Romero *et al.*, 2015, 2016; Makar and Ganda, 2018), in order to minimize engine damage, NO_x emissions, and low engine performance due to the low power density of the fuel (Hilbers, Sprakel and Ham, 2015). This restricts the realization of the benefits of using renewable sources of energy such as, lower environmental pollution and better energy security. The alternative renewable diesel synthesis strategy, deoxygenation, which yields n-alkanes and n-alkenes from fatty acids and triglycerides,

produces better quality renewable diesel which can be employed in the currently existing engines at higher blending proportions or in its pure form without the aforementioned FAAEs problems. However, for this strategy to be economically viable for industrial scale production, there exists a need for its optimization with regards to the operating parameters and the diversity of the feedstock oils.

1.3 Aim and Objectives

The aim of this research project was to develop a strategic method for the deoxygenation of seed oil as pretreatment of hydrocracking process for biofuel production for internal combustion engines. To achieve the set aim, the following objectives were the focus of this research project:

a. To investigate the effect of catalyst active metal ratio on its physiochemical properties hence deoxygenation catalytic activity;
b. To investigate the influence of catalyst loading on waste cooking oil deoxygenation;
c. To investigate the effect of reaction temperature on the deoxygenation of waste cooking oil;
d. To investigate the relationship between reaction time and the deoxygenation success of waste cooking oil;
e. To optimise the deoxygenation process using statistical tools;
f. To investigate catalyst selectivity on the seed oil type

1.4 Summary

In this chapter, the undertaking of this project was justified by outlining the problems associated with the current mainstream biodiesel synthesis strategy and highlighting the need for developing a better commercially viable synthesis strategy for South Africa to fulfil its biofuels policies and energy security obligations. The aim of this research and the objectives to be met in fulfilling this aim are defined as well in this chapter.

Chapter 2: Literature Review

2.1 Introduction

Research has shown that biodiesel combustion is CO_2 neutral, this is based on the concept that during the growth phase of biomass, it absorbs as much CO_2 as is released when burnt as a biofuel (Nwokoagbara, Olaleye and Wang, 2015; Mofijur et al., 2016; Ishak et al., 2017; Sehatpour, Kazemi and Sehatpour, 2017). The production of biodiesel is a function of many variables which include, the feedstocks, synthesis strategies, as well as the process parameters/ conditions. These variables have a considerable influence on the yield, cost and quality of the resultant fuel. In this chapter, a review of the literature from previous studies on the various aspects of biodiesel synthesis is presented.

2.2 Biodiesel Synthesis Feedstocks

The cost of the feedstocks and their availability have significant implications in the production of biofuels in the world's different regions (Stephen and Periyasamy, 2018). The feedstock supply cost alone contributes between 60% and 88% of the overall biodiesel production cost (Tabatabaei *et al.*, 2015; Mujeeb, Vedamurthy and T, 2016; Mahmudul *et al.*, 2017). The economic competitiveness of biodiesel relies significantly on the feedstock cost (Huang *et al.*, 2015; Hajjari *et al.*, 2017). Feedstock availability is a function of the geographical region and the nature of the available oil resources (Mata and Martins, 2015; Norjannah *et al.*, 2016; Hajjari *et al.*, 2017). Moreover, together with the production process; feedstock is a major determinant of the resultant biodiesel properties (Mahmudul *et al.*, 2017). Biodiesel feedstock comprises of fatty acid containing materials which include up to 350 oil producing crops globally, animal fats, waste oils and greases as well as algae and other microorganisms (Okoye and Hameed, 2016; Roy *et al.*, 2016; Skorupskaite, Makareviciene and Gumbyte, 2016), these feedstocks are classified into three distinct generations as presented in Table 2.1. The ideal biodiesel feedstock is one whose processing costs are the lowest, yet yielding the highest lipid quantity and quality (Verma, Sharma and Dwivedi, 2016). The most significant feedstock attributes with regards to biodiesel synthesis include: lipid content, fatty acids profiles, and availability of the feedstock (Go *et al.*, 2016).

Table 2.1: Biodiesel Feedstocks Classification (Huang et al., 2015; Norjannah et al., 2016; Zhu, Li and Hiltunen, 2016).

Generation	**1st**	**2nd**	**3rd**
Constituents	Edible Vegetable Oils	Non-Edible Vegetable Oils Animal Fats Waste oils Greases	Algae Other Microorganisms

2.2.1 Food competition

Previously the most popular biodiesel feedstocks were of the first generation (Huang *et al.*, 2015; Tabatabaei *et al.*, 2015; Maroa and Inambao, 2019). However, biodiesel production from edible oils is controversial for stimulating increased global food market prices and diminishing availability resultant of the food versus fuel competition (Hegde *et al.*, 2015; Millo *et al.*, 2015; Ishak *et al.*, 2017). Biodiesel obtained from edible oils has been reported in literature as being costly; to an extend of even being more expensive than petroleum diesel (Karmee, 2016; Onoji *et al.*, 2016; Strzalka, Schneider and Eicker, 2017). In South Africa for example, the use of corn for biofuel production is prohibited, all the corn produced is reserved for food production. Accordingly, a cheaper alternative route that employs second generation feedstocks for biodiesel production has been preferred, so as to curb the utilization of food-grade materials (Alaba, Sani and Ashri Wan Daud, 2016; Laesecke, Ellis and Kirchen, 2017; Mahmudul *et al.*, 2017). Waste oils for example, have been found to be low cost sustainable feedstock, that reduce feedstock costs by up to 70% (Stephen and Periyasamy, 2018). Non-edible oils such as castor oil have seen an increase in value and interest in the biofuels industry of South Africa in the recent past. Millo *et al.*, (2015) reported that some international biofuel regulations have been reviewed with the objective of expanding the share of second generation biofuels, for example, the European Parliament limited the utilization of biofuels synthesized from agricultural feedstock to 6%, against a 10% target so that the balance would be compensated by second-generation biofuels.

2.2.2 Land Competition

The sustainability of using first and second generation crop-feedstocks for biofuel production is threatened by the competition for arable land and freshwater the cultivation thereof tends to present with food crops for human consumption (Zhu, Li and Hiltunen, 2016; Hajjari *et al.*, 2017; Stephen and Periyasamy, 2018). In addition, the clearing of forests and the other unoccupied land for biodiesel feedstocks cultivation reduces biodiversity (Mata and Martins, 2015; Katiyar *et al.*, 2017). Some non-edible oil plants, however, such as jatropha are able to grow on arid land since they are drought-resistant (Huang *et al.*, 2015; Norjannah *et al.*, 2016), and using other waste oriented second generation feedstocks for biodiesel production is in fact a sustainable solution to waste management issues (Mujeeb, Vedamurthy and T, 2016; Hajjari *et al.*, 2017; Katiyar *et al.*, 2017). Microalgae also, as an alternative biodiesel production feedstock can assist in settling the food versus fuel debate accompanying food crop feedstocks, and the land competition since it can be cultured on marginal land or wastewater (Huang *et al.*, 2015; Nwokoagbara, Olaleye and Wang, 2015; Salam, Velasquez-Orta and Harvey, 2016). However, it is important also to note that microalgae promotes eutrophication in the water, which is an unfavorable occurrence to aqua life.

2.2.3 Oil Yield

The lipid content of the feedstock is directly proportional to its biodiesel yield (Nwokoagbara, Olaleye and Wang, 2015) and inversely proportional to the production cost (Moazeni, Chen and Zhang, 2019). Higher lipid content feedstocks with higher growth rates, thus better availability, are preferable for synthesizing biodiesel. The various yield characteristics for some of the common feedstocks are shown in Appendix A1. Clearly, first and second generation feedstocks have inferior oil yields in comparison with microalgae (Hegde *et al.*, 2015; Kumar and Sharma, 2016; Laviola *et al.*, 2017). This means that large quantities of feedstock are required for fulfilling the demand for petroleum-based fuels with plant derived biodiesel, thus large acreage for their cultivation (Kumar and Sharma, 2016; Katiyar *et al.*, 2017; Mostafa and El-Gendy, 2017). Microalgae, on the other hand, can produce up to 23-300 times more oil per acre than other plants used for biodiesel (Skorupskaite, Makareviciene and Gumbyte, 2016; Jayakumar *et al.*, 2017; Katiyar *et al.*, 2017). Reasons for this are, microalgae have a higher photosynthetic response and higher oil content (Abd-Alla *et al.*, 2015; Jayakumar *et al.*, 2017; Katiyar *et al.*, 2017). They grow rapidly, to the extent of 100 times faster than terrestrial energy plants and they can double their

biomass in less than one day (Bhatia *et al.*, 2015; Nwokoagbara, Olaleye and Wang, 2015; Mujeeb, Vedamurthy and T, 2016). Thus, in terms of oil yields and growth rates, microalgae are preferable and cost effective when compared with other conventional biodiesel feedstocks (Mata and Martins, 2015). It is worth noting that lipid content is a function of the strain of the feedstock used and the culturing thereof (Nwokoagbara, Olaleye and Wang, 2015; Go *et al.*, 2016; Katiyar *et al.*, 2017). Lipid content thus can be modified through genetic engineering technology means, as well as environmental condition modification, such as provision or deprivation of nutrients, sunlight exposure and water supply (Hegde *et al.*, 2015; Li, Backes and Wachtmeister, 2015; Zhu, Li and Hiltunen, 2016). Although some genetic engineering interventions to improve biodiesel synthesis have been successful at laboratory scale, commercialization necessitates scaling up of these interventions without performance losses (Hegde *et al.*, 2015; Katiyar *et al.*, 2017).

2.2.4 Availability

The feedstock choice for the synthesis of biodiesel is generally influenced by the regional climate (Norjannah *et al.*, 2016; Mahmudul *et al.*, 2017). In temperate regions, rapeseed, sunflower, corn, and other legumes or cereals are used as feedstocks, whereas in tropical regions, palm oil, and soybeans are used due to their availability (Cai *et al.*, 2015; Roy *et al.*, 2016; Sierra-Cantor and Guerrero-Fajardo, 2017). Lately, feedstocks such as microalgae, jatropha, and waste oils, have been growing in prominence because they can be harvested in a broad range of geographical conditions (Hegde *et al.*, 2015; Mata and Martins, 2015). Microalgae have much higher growth rates, productivity, and their supply is independent of the seasonal fluctuations relative to conventional forestry, and agricultural crops (Maymandi and Rahimpour, 2015; Mujeeb, Vedamurthy and T, 2016). Jatropha, on the other hand, can be grown at almost any altitude and has several agronomic morphological traits, such as tolerance to drought, ease of propagation, and rapid growth (Kumar and Rehman, 2016; Laviola *et al.*, 2017). However, regular irrigation, fertilization and good management practices may improve the oil yield. (Mujeeb, Vedamurthy and T, 2016). Waste oils are an unavoidable consequence of human activity, examples being waste oils from machinery, tallow, and waste cooking oil (Lam *et al.*, 2016; Hajjari *et al.*, 2017). Waste cooking oils are a widely available feedstock (Singh and Patel, 2015; van Dyk *et al.*, 2019), with the total global production approximately around 18.6 million tonnes per year (Cai *et al.*, 2015; Hajjari *et al.*, 2017; Stephen and Periyasamy, 2018). Bulk waste cooking oil can be sourced from

food manufacturers such as potato processing plants at snack food factories, and industrial deep fryers such as fast-food establishments (Singh and Patel, 2015; Hajjari *et al.*, 2017). Waste cooking oil is about 40–70% cheaper than fresh vegetable oils (Cai *et al.*, 2015), and its use for biodiesel production is a prudent waste management strategy (Norjannah *et al.*, 2016; César *et al.*, 2017; Hajjari *et al.*, 2017).

2.2.5 Extraction

After harvest the oil seeds undergo drying, decortication, and subsequently oil extraction (Mata and Martins, 2015; Amin *et al.*, 2016). The lipid extraction can be effected by either or a combination of mechanical; chemical; or enzymatic techniques. Also, other methods for example ultrasound-assisted extraction; supercritical fluid extraction; and microwave-assisted extraction have been used as complementary techniques to extract oils from vegetal sources (Mata and Martins, 2015; Mahmudul *et al.*, 2017). The mechanical press extraction technique can be combined with solvent extraction to produce oil with a higher degree of purity but it is more expensive (Mata and Martins, 2015). The solvent extraction technique employs chemical solvents that have high selectivity and solubility towards lipids, some of which are hexane, dichloromethane, chloroform and toluene (Mata and Martins, 2015; Katiyar *et al.*, 2017). However, the use of chemical solvents exposes humans and the environment to their high toxicity (Mujeeb, Vedamurthy and T, 2016). The solvent can be recovered and separated from the oil by distillation after the lipid extraction process (Mata and Martins, 2015). Supercritical extraction, on the other hand is an excellent technique, but it is economically unfeasible for industrial scale application (Jayakumar *et al.*, 2017). At supercritical phase, thermophysical properties of the fluid change drastically so that it becomes a super-solvent with enhanced extraction efficiency. The most common supercritical extraction technique employs supercritical CO_2, and this is advantageous relative to chemical solvent extraction in the following regard: (a) easy post-extraction separation with the product at ambient conditions; (b) non-toxicity, offering a non-oxidizing atmosphere to avert the oxidation of extracts ; and (c) the low critical temperature of CO_2 suppresses thermal decomposition of products (Mujeeb, Vedamurthy and T, 2016).

In the case of microalgae, its harvest is followed by the drying of the microalgae biomass step before lipid extraction can be done (Mujeeb, Vedamurthy and T, 2016; Katiyar *et al.*, 2017). The drying step of the microalgal biomass, which contains approximately 90% water is one of the most

time- and energy-consuming processes in the production of biodiesel (Bagchi, Rao and Mallick, 2015; Moreno-Garcia *et al.*, 2017). Microalgal drying is accomplished by various techniques which include solar drying, lyophilization, oven based drying, drum drying, spray drying, and vacuum drying (Mata and Martins, 2015). The microalgae cells are subsequently subjected to a cell disruption process after drying, this enhances the lipid extraction process against the thick cell walls that tends to inhibit the release of intra-lipids during extraction (Mujeeb, Vedamurthy and T, 2016). Several techniques can be employed for the cell breakdown process such as bead beating, pressing, autoclaving, homogenizer etc. (Kesaano *et al.*, 2015; Mujeeb, Vedamurthy and T, 2016; Katiyar *et al.*, 2017), after which the released lipids and the other cellular components are separated (Katiyar *et al.*, 2017). Chemical solvent extraction is usually employed for dry microalgae biomass, while supercritical fluid extraction is suitable for wet-paste microalgae biomass (Mujeeb, Vedamurthy and T, 2016). However, the industrial scale usage of microalgae as a biodiesel feedstock is still not economically viable, due to its intensive processing requirements (Jayakumar *et al.*, 2017; Moreno-Garcia *et al.*, 2017). Thus it has been proposed that wet microalgae biomass be converted directly into biodiesel as a cost reduction measure, as it eliminates the need for the drying process (Moreno-Garcia *et al.*, 2017).

2.2.6 Lipid Composition

The lipid composition profiles of the feedstock oils for the production of biodiesel are unique to their sources (Nekhavhambe, Mukaya and Nkazi, 2019), and these in turn are the major determinant of the resultant fuel properties (Hegde *et al.*, 2015; Mahmudul *et al.*, 2017). The lipid composition is a function of the feedstock source strain and its culturing (Norjannah *et al.*, 2016; Mahmudul *et al.*, 2017). Table 2.2 shows the lipid composition profiles of some of the popular biodiesel feedstocks. The physiochemical properties of resultant biodiesel are mainly determined by the fatty acid attributes such as the degree of saturation, length of the carbon chains, and the extend of branching in the chains (Norjannah *et al.*, 2016; Verma and Sharma, 2016; Mahmudul *et al.*, 2017). High levels of saturation in the fatty acids usually results in biodiesel with poor cold flow behavior (Sierra-Cantor and Guerrero-Fajardo, 2017), though it possesses excellent oxidation stability (Verma and Sharma, 2016). The quality of biodiesel can be enhanced by blending with other diesel fuels from other sources, as a way of altering its fatty acid composition (Hegde *et al.*, 2015).

Table 2.2: Lipid Composition Profiles of Vegetable Oils (Verma and Sharma, 2016; Mahmudul et al., 2017; Moazeni, Chen and Zhang, 2019; Nekhavhambe, Mukaya and Nkazi, 2019)

Fatty Acid	**Castor**	**Coconut**	**Cotton Seed**	**Jatropha**	**Mustard**	**Neem**	**Olive**	**Palm**	**Polanga**	**Pongamia**	**Rapeseed**	**Soybean**	**Sunflower**	**Tallow**	**UCO**
Arachidic	0.3			0.2-0.3	0.7	1.9		0.06-0.11		2.2-4.7		0.3	0.4		0.55-2.3
Behemic										4.2-5.3		0.1			0.65
Erucic					32.81			0							
Gadolic				3.6	10.44			0.33		9.5-12.4					3.6
Gondoic	0.7														
Lauric		46.5		0.1				0.2-0.9					0.5		
Lignoceric						0.3			2.6						0.04

Linoleic	4.2	2.2	55.2	31.9-36.0	11.64	17.9	5.8	9.59-12.2	13.7	10.8-18.3	14.1-32	51.8-53.7	52.34-66.2	2.9	13.5-36.0
Linolenic	0.3	0	0.6	0.2-0.3	8.61	0.4		0.17-0.2	2.1	1.1-3.5	1.8-8.8	6.5-8.6	0.8-8.19	0.9	0.2-0.8
Myristic		19.2	0.7	0.1	0.05	0.2-0.26		0.9-1.14			1	0.1	0.2		0.19-0.9
Oleic	3.0	6.9	19.2	38.6-44.7	24.98	43.9	82.3	39.9-42.6	42.7	44.5-72.2	55.0-77.8	16.5-24.8	20.6-22.52	42.4	18.3-52.9
Palmiric		9.8	20.1					42.8			5.5	0.2			20.4
Palmitic	1.0	9.8		14.1-14.6	2.8	14.9	9.7	37.8-43.79	17.9	3.7-9.8	3.49-4.0	10.4 – 24.8	4.8-10.58	23.3	4.1-26.5
Palmitoleic				0.5-0.7	0.16	0.1	0.46	0.15-0.4	2.5			0.1-2.0	0.8	0.1	0.8-2.4
Ricinoleic	89.5														

Stearic	1.0	3	2.6	6.8-7.6	1.09	20.6	1.74	2.7-4.76	18.5	2.4-8.9	0.55-2.3	2.6-4.7	4.76-5.7	19.3	1.6-4.8

2.3 Biodiesel Synthesis Strategies

Presently, there are several techniques available for biodiesel production from biomass-derived oils and these include direct blending, micro-emulsion, pyrolysis, and transesterification (Mofijur *et al.*, 2016; César *et al.*, 2017; Laesecke, Ellis and Kirchen, 2017). Amongst the techniques listed above, transesterification produces a fuel whose characteristics are closely comparable to the petroleum diesel properties, in terms of viscosity, purity and volatility (Mofijur *et al.*, 2016; Mahmudul *et al.*, 2017). As such, the transesterification process is the universal and established method for synthesizing biodiesel, it is widely used for commercial biodiesel synthesis by reason of its relatively low cost and high conversion efficiency (Daramola, Nkazi and Mtshali, 2015; Singh and Patel, 2015; Roy *et al.*, 2016). The transesterification reaction entails the reaction of triglycerides with an alkyl donor (usually short chain alcohol), to produce biodiesel in the form of fatty acid alkyl esters, and glycerol as a byproduct (Lam *et al.*, 2016; Lee *et al.*, 2017; Lotti *et al.*, 2018). Other variants of transesterification used for biodiesel synthesis are esterification and interesterification; the former being a reaction of fatty acids with an alcohol to produce water as a byproduct (He *et al.*, 2015; Han *et al.*, 2016; Ishak *et al.*, 2017); and the later entailing the exchange of alkyl groups between two different esters (Norjannah *et al.*, 2016).

2.3.1 Transesterification

(Trans)esterification or alcoholysis is a chemical process of transforming lipids (triglycerides) and free fatty acids into fatty acid alkyl esters (biodiesel), by exchanging the alkyl moiety with an alcohol source (Marx, 2016; Roy *et al.*, 2016; Moazeni, Chen and Zhang, 2019). It is a sequence of three reversible reactions whereby, triglycerides are firstly reduced to diglycerides, which in turn are converted to monoglycerides, and finally fatty acid esters and glycerol (Mata and Martins, 2015; Mujeeb, Vedamurthy and T, 2016). An ester molecule is produced in each reaction step so that three fatty acid alkyl monoester (FAAE) molecules and a glycerol molecule are produced from a triglyceride molecule (Alaba, Sani and Ashri Wan Daud, 2016; Okoye and Hameed, 2016; Verma and Sharma, 2016). Since the transesterification reactions are equilibrium reaction, excess amounts of the alkyl donor are needed for maximizing biodiesel yield by offsetting the equilibrium towards the products side (Mata and Martins, 2015; Mujeeb, Vedamurthy and T, 2016). Figures

below illustrate the general mechanisms for the transesterification process and its variants, the ensuing sections provides an in-depth review of the process:

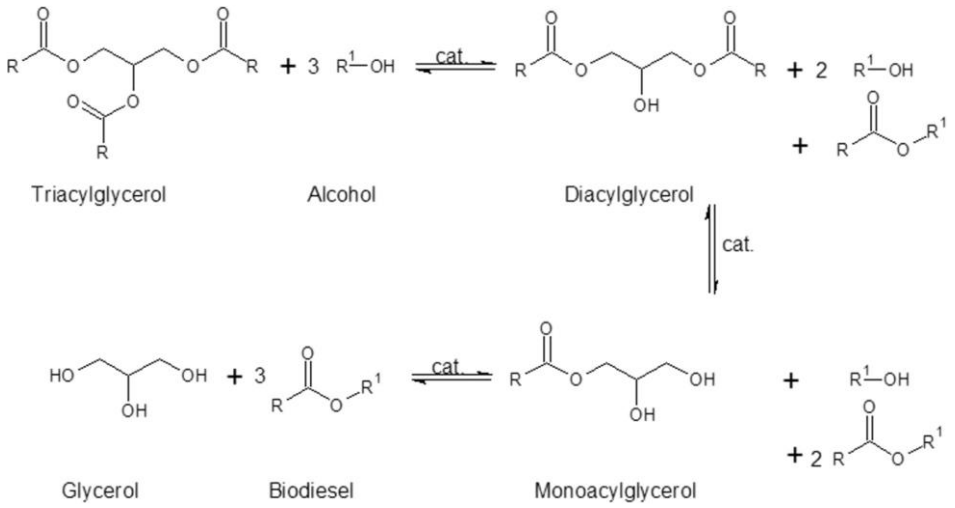


Figure 2.1: Overall transesterification reactions of triglycerides; where R^1, R^2, R^3 are long chain hydrocarbons (Nanda et al., 2016; Palmer and Brigham, 2016; Sierra-Cantor and Guerrero-Fajardo, 2017)

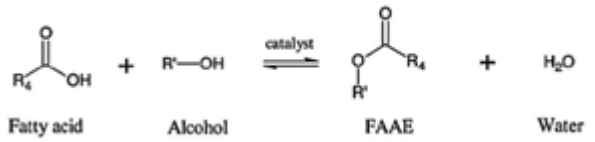


Figure 2.2: Esterification reaction of fatty acid with alcohol; R^4 is an acyl residue, R' is the alcohol moiety (Alaba, Sani and Ashri Wan Daud, 2016; Salam, Velasquez-Orta and Harvey, 2016; Lotti et al., 2018)

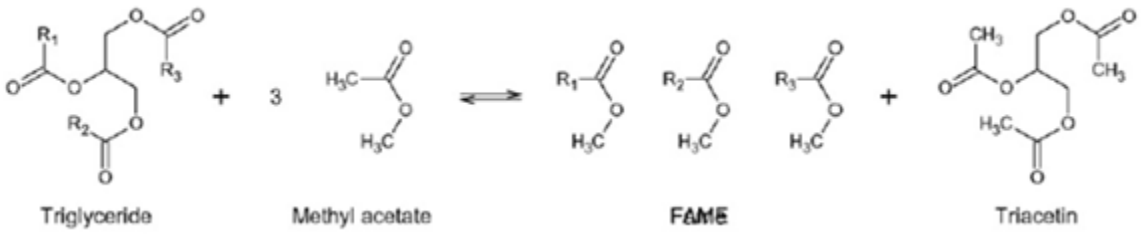


Figure 2.3: Interesterification reaction of TG with methyl acetate (Campanelli, Banchero and Manna, 2010; Marx, 2016; Norjannah et al., 2016)

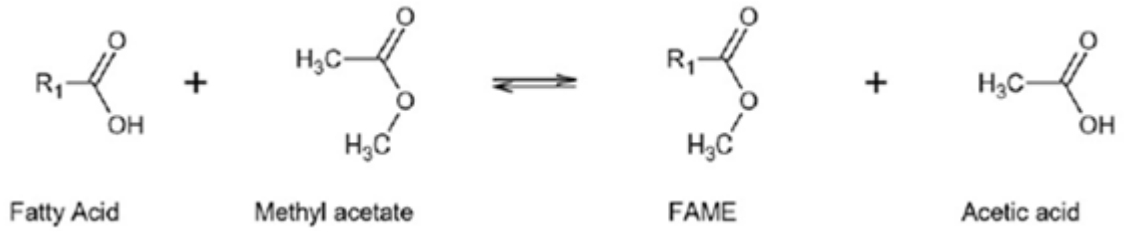


Figure 2.4: Stoichiometric reaction schemes for the esterification of fatty acids with methyl acetate (Campanelli, Banchero and Manna, 2010; Marx, 2016)

2.3.1.1 Process Description

Generally, the oil and an alcohol are essentially mixed in a reaction vessel, and two polar phases are formed due to the immiscibility between alcohol and oil (Mata and Martins, 2015), the immiscibility is inhibitory in effect to the transesterification reaction leading to low biodiesel yields (Stephen and Periyasamy, 2018). Various techniques are used to improve mass transfer between oil and alcohol during transesterification, and these include: catalyzing the reaction, temperature elevation, agitation of the mixture, as well as the use of a solvent; these techniques can be employed as a combination or singularly in order to optimize the reaction. Upon reaction completion, the products are allowed to settle and form two phases so that glycerol can be removed. Then, any excess alcohol that did not react and catalyst are removed from both phases (of esters and glycerol) and recycled back to the reactor (Mata and Martins, 2015). Subsequently, purification and drying processes are employed so that the produced biodiesel complies with the market approved quality standards for the preservation of engine integrity, performance, and the environment, through controlled combustion emissions (Gomes *et al.*, 2015).

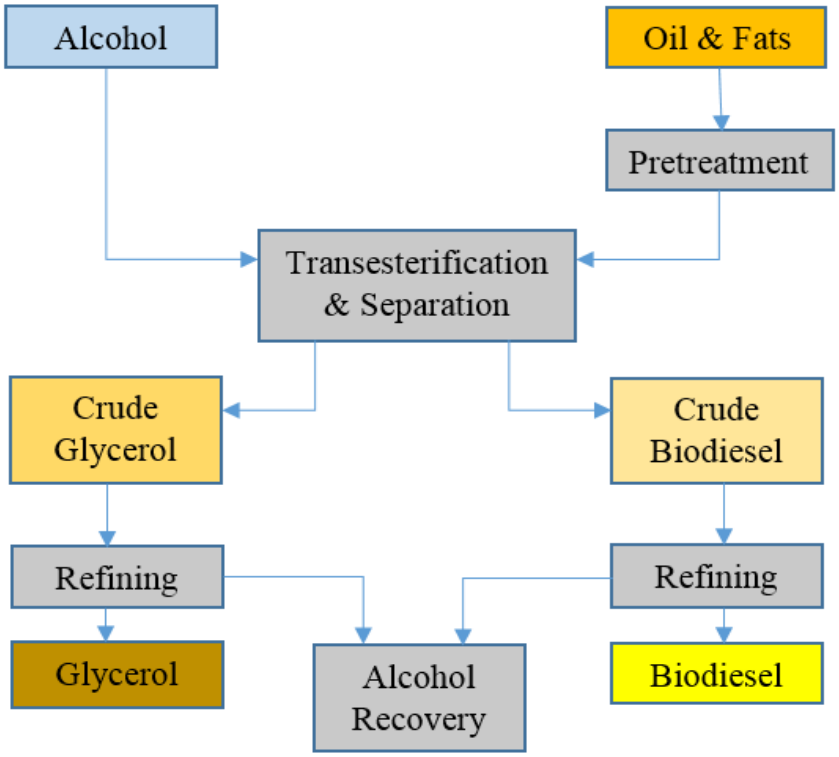


Figure 2.5: Biodiesel production through transesterification block diagram (Mofijur et al., 2016; Mahmudul et al., 2017; Stephen and Periyasamy, 2018)

The transesterification process can be catalytic or non-catalytic (Daramola, Nkazi and Mtshali, 2015; Sierra-Cantor and Guerrero-Fajardo, 2017; Moazeni, Chen and Zhang, 2019), the former being attainable through either chemical or enzyme catalysts (Xu, Gao and Xiao, 2015; Mofijur *et al.*, 2016; César *et al.*, 2017). Chemical catalysts such as acids and alkalis can be employed in the transesterification reaction (Micic *et al.*, 2015; Katiyar *et al.*, 2017); enzymes such as lipase can be used likewise (Lam *et al.*, 2016; Palmer and Brigham, 2016; Moazeni, Chen and Zhang, 2019). The non-catalytic reaction is characterized by supercritical conditions (Norjannah *et al.*, 2016), whereas the catalytic reaction allows for milder conditions, with a better control of the resulting products (Mata and Martins, 2015). A catalyst is usually employed to enhance the rate of reaction and the yield thereof, by splitting the reactant molecules to merge with the separated esters (Mujeeb, Vedamurthy and T, 2016; Katiyar *et al.*, 2017).

2.3.1.2 Chemical Catalytic Transesterification

Conventionally, the synthesis of biodiesel through the transesterification reaction occurs in the presence of a chemical catalyst (Abd-Alla *et al.*, 2015). These chemical catalysts can be classified

as being homogeneous or heterogeneous, depending on their nature (Marx, 2016; Verma and Sharma, 2016; Moazeni, Chen and Zhang, 2019). Homogeneous catalysts are used in their liquid form whereas their heterogeneous counterparts are used in solid form; both can either be basic or acidic (Norjannah *et al.*, 2016; Verma, Sharma and Dwivedi, 2016). Accordingly, the heterogeneous catalysis reaction involves three phases, i.e. the alcohol phase, the lipid phase, and the catalyst phase, resulting in mass transfer resistance among the phases; so that higher optimum conditions are required for competitive conversion (Verma, Sharma and Dwivedi, 2016; Stephen and Periyasamy, 2018). The conversion rate during heterogeneous catalysis is dependent on the catalyst's particle size: smaller particle sizes result in higher conversion rate due to the increased specific surface area hence active sites (Micic *et al.*, 2015; Verma, Sharma and Dwivedi, 2016; Banković-Ilić *et al.*, 2017). Heterogeneous acid catalysts include heteropoly acids, tungstated zirconia, and sulphated zirconia whereas the examples for heterogeneous alkali catalysts include basic zeolites, oxides of aluminum and zinc, hydrotalcites, and calcium based mixed metal oxides (CaO–MgO)(He *et al.*, 2015; Mata and Martins, 2015; Verma, Sharma and Dwivedi, 2016). The homogeneous acid catalysts examples include hydrochloric, phosphoric, and sulphuric acids, whereas the homogenous alkali catalysts include sodium hydroxide, potassium hydroxide, potassium methoxide, and sodium methoxide (E. Wang *et al.*, 2015; Katiyar *et al.*, 2017; Mahmudul *et al.*, 2017). The most common setback in the chemical catalysis is the poor product purity which emanates from side reactions such as hydrolysis and saponification, these consequently complicate the downstream product recovery processes (Abd-Alla *et al.*, 2015; Ishak *et al.*, 2017; Sierra-Cantor and Guerrero-Fajardo, 2017). The economic sustainability of the process thus is mainly determined by the product recovery cost, as it covers more than half of the entire production process (Alaba, Sani and Ashri Wan Daud, 2016).

Heterogeneous vs Homogeneous

Homogeneous catalysts are preferred in industrial scale transesterification processes to heterogeneous catalysts which require higher pressure and temperature reaction conditions, as well as excessive amounts of alcohol (Micic *et al.*, 2015; Stephen and Periyasamy, 2018; Moazeni, Chen and Zhang, 2019). Heterogeneous catalysts are characterized by low biodiesel yields relative to the homogeneous catalysts due to mass transfer resistance and the leaching of the active sites of the catalyst (He *et al.*, 2015; Alaba, Sani and Ashri Wan Daud, 2016). Homogeneous catalysts

display relatively high catalytic activity in general, which is characterized by high reaction rates and product yield, also they are cost-effective compared to the currently-available heterogeneous catalysts (Marx, 2016; Verma, Sharma and Dwivedi, 2016; Hajjari *et al.*, 2017). However, the homogeneous catalyzed reaction is sensitive to the free fatty acids and the water content in the feedstocks (Aguieiras, Cavalcanti-Oliveira and Freire, 2015); it also requires additional complex post-reaction treatments for product finalization (neutralization, flushing and separation) (Han *et al.*, 2016; Lee *et al.*, 2017). These purification procedures are ecologically unfriendly because of their excessive water demand, and disposal of strong alkalis and acids into the environment (Aguieiras, Cavalcanti-Oliveira and Freire, 2015; He *et al.*, 2015; Micic *et al.*, 2015). Heterogeneous catalysts on the other hand, are eco-friendly due to their relatively easy downstream product and catalyst recovery, non-corrosivity, and reusability (Micic *et al.*, 2015; Verma, Sharma and Dwivedi, 2016; Ishak *et al.*, 2017). Moreover, heterogeneous catalysts can tolerate extreme reaction conditions more than the homogeneous and enzyme catalysts (Verma, Sharma and Dwivedi, 2016). As for the homogeneous catalyzed reaction, the alcohol and the catalyst are premixed in the relevant proportions as per the free fatty acids (FFA) composition of the feedstock, before being mixed with the oil in the biodiesel reactor. The reaction can be carried out with high reaction rates under ambient pressure and within the temperature range of 60-80°C (Mujeeb, Vedamurthy and T, 2016; Verma, Sharma and Dwivedi, 2016).

Base Preference

In industrial scale transesterification processes homogeneous alkaline catalysts are preferred to both acid homogeneous catalysts and enzyme catalysts by reason of their relatively low cost and high reactive efficiency in mild conditions (Cai *et al.*, 2015; Micic *et al.*, 2015; Lam *et al.*, 2016). According to Mujeeb, Vedamurthy and Shivasharana, 2016, alkaline metal alkoxides have the highest catalytic activity since they give very high yields in short reaction durations even under low catalyst loading. Acid catalysts, on the contrary have low catalytic activity consequently requiring higher temperatures and excess amounts of alcohol for significant biodiesel yield. Also, mineral acid catalysts are extremely corrosive and contaminative, as such, they present complications in the product biodiesel purification.

However, regardless of the several advantages that alkaline catalysts have against their acidic counterparts, they are extremely sensitive to moisture and FFA presence in the feedstock oil (Cai

et al., 2015; Verma and Sharma, 2016; Verma, Sharma and Dwivedi, 2016). The presence of water induces hydrolysis of triglycerides instead of transesterification (Ishak *et al.*, 2017; Katiyar *et al.*, 2017), resulting in the production of FFA and glycerol. Basic catalysts, on the other hand react with the free fatty acids to produce soap (E. Wang *et al.*, 2015; Lee *et al.*, 2017; Stephen and Periyasamy, 2018) which complicates biodiesel separation (Maymandi and Rahimpour, 2015; Verma, Sharma and Dwivedi, 2016) since the soap can gel under ambient conditions (Moazeni, Chen and Zhang, 2019). Accordingly, the catalytic activity of the base catalyst is reduced by the free fatty acids, which resultantly reduces the biodiesel yield (Lam *et al.*, 2016; Mujeeb, Vedamurthy and T, 2016; Verma and Sharma, 2016). Therefore, feedstock oils with lower than 0.06 wt.% and 0.5 wt.% moisture and free fatty acids content, respectively, are recommended for alkaline metal hydroxides catalytic transesterification (Mujeeb, Vedamurthy and T, 2016; Verma, Sharma and Dwivedi, 2016; Ishak *et al.*, 2017). The conventional transesterification processes feedstocks thus need a water and free fatty acids removal pretreatment to ensure adherence to the limits (Katiyar *et al.*, 2017; Lee *et al.*, 2017). The following Equations illustrate the respective saponification reactions of free fatty acids and esters in the presence of water and heat (Mata and Martins, 2015).

Equation 2.1

$$R - COOH + NaOH \rightarrow R - COONa + H_2O$$

Equation 2.2

$$R - COOR' + NaOH \rightarrow R - COONa + H_2O$$

Oil feedstocks with high FFA content can be converted into biodiesel through acid-catalyzed esterification with an alcohol, since the FFA do not react with the acid catalysts (Lam *et al.*, 2016; Verma, Sharma and Dwivedi, 2016; Moazeni, Chen and Zhang, 2019). Acid catalysis can be employed for both esterification of FFA and transesterification of complex lipids (Alaba, Sani and Ashri Wan Daud, 2016; Norjannah *et al.*, 2016; Katiyar *et al.*, 2017), invariably these reactions occur concurrently when an acid catalyst is used (Verma, Sharma and Dwivedi, 2016; Moazeni, Chen and Zhang, 2019). A combination of acid catalysis for the esterification of free fatty acids and subsequently base catalysis for the transesterification of triglycerides i.e. the two step method, can be employed for feedstock oils with greater than 1 wt.% FFA (Karmee, 2016; Norjannah *et al.*, 2016; Verma and Sharma, 2016). However, since water is a by-product of the esterification reaction, continual water removal is necessary for the maintenance of catalyst activity as well as

offsetting the equilibrium towards the continuous production of biodiesel, consequently keeping to a minimum the amount of alcohol required for the reaction (Campanelli, Banchero and Manna, 2010; Mata and Martins, 2015). Relative to base catalysis, acid-catalyzed (trans)esterification is only preferred for feedstock oils with high FFA content, nonetheless is characterized by low reaction rates, poor selectivity, and high oil:alcohol molar ratios (Aguieiras, Cavalcanti-Oliveira and Freire, 2015; Mata and Martins, 2015). Therefore, the choice of the transesterification process as well as its catalysis are largely influenced by the FFA and moisture content of the feedstock oil (Lam *et al.*, 2016; Mujeeb, Vedamurthy and T, 2016; Verma, Sharma and Dwivedi, 2016).

Two-Step Method

The two-step chemical catalysis method entails acid-catalyzed esterification of FFA in the first step so as to reduce the free fatty acids content to below 0.5 wt.%, and then followed by alkali-catalyzed transesterification of the remaining triglycerides in the feedstock (Go *et al.*, 2016; Laviola *et al.*, 2017; Silitonga *et al.*, 2018). The main merit of the two-step method is its insensitivity to the quality of the feedstock oil in terms oil moisture and FFA content (Aguieiras, Cavalcanti-Oliveira and Freire, 2015), since the acid-catalyzed esterification serves as a pretreatment procedure for the base-catalyzed transesterification in order to inhibit saponification (Moazeni, Chen and Zhang, 2019). Therefore the two-step method is a tactic to realize high biodiesel yield from feedstock oils with high fractions of free fatty acids and moisture (Go *et al.*, 2016; Verma and Sharma, 2016), whereby the water byproduct of the esterification reaction is discarded before introducing the alkaline catalyst into the reaction (Mata and Martins, 2015; Go *et al.*, 2016; Moazeni, Chen and Zhang, 2019). According to Shiu *et al.*, 2010, an excess amount of the alkaline catalyst can be added directly to neutralize the acid catalyst after the esterification step, so that the remaining alkaline catalyst will be used to catalyze the transesterification step. When H_2SO_4 is used for the acid catalysis, the neutralization step may provide better moisture tolerance as the resultant metal sulfates may act as sorbents for moisture present in the reaction (Go *et al.*, 2016).

2.3.1.3 Enzyme Catalyzed

Enzymes are biocatalysts that can be employed to catalyze the synthesis of biodiesel (Karmee, 2016; Mujeeb, Vedamurthy and T, 2016). Lipases are a type of enzymes which can catalyze hydroesterification, interesterification and transesterification reactions (Abd-Alla *et al.*, 2015; Su

et al., 2015; Karmee, 2016) with high specificity, under mild conditions which are in most cases ambient (Maymandi and Rahimpour, 2015; Verma, Sharma and Dwivedi, 2016; Moazeni, Chen and Zhang, 2019). Generally, the prime forms of biocatalysts used in the production of biodiesel are the free lipases, immobilized lipases (Mata and Martins, 2015; Karmee, 2016), whole-cells, and the fermented solids (Aguieiras, Cavalcanti-Oliveira and Freire, 2015; Serqueira *et al.*, 2015). Sources of lipases range from various plants, animals, fungal and bacterial species (Norjannah *et al.*, 2016), however the microbial lipases are the most commonly used in synthesizing biodiesel (Aguieiras, Cavalcanti-Oliveira and Freire, 2015; Moazeni, Chen and Zhang, 2019). This follows that microbial lipases are relatively cheap, quick to produce, and can be immobilized low-cost media. They are characterized by high yields, more stability, and can be genetically modified for performance improvement compared to lipases from other sources (Mata and Martins, 2015; Su *et al.*, 2015; Moazeni, Chen and Zhang, 2019). Lipase catalytic transesterification has reduced feedstock restrictions since lipases are immune to moisture and FFA fractions in the feedstock oil, relative to alkaline catalysts (Aguieiras, Cavalcanti-Oliveira and Freire, 2015; Karmee, 2016; Verma, Sharma and Dwivedi, 2016). Additionally, the product purity for enzyme catalysis is superior compared to those of the chemical catalysis methods (Huang *et al.*, 2015; Karmee, 2016; Marx, 2016), this may be due to the suppression of side reactions such as saponification (Lam *et al.*, 2016; Ishak *et al.*, 2017; Lotti *et al.*, 2018). As such, relatively simple downstream processing procedures for product recovery and purification are required (Norjannah *et al.*, 2016; Verma, Sharma and Dwivedi, 2016; Mahmudul *et al.*, 2017). Moreover, enzymes are environmentally benign unlike the chemical catalysts (Go *et al.*, 2016; Lotti *et al.*, 2018; Moazeni, Chen and Zhang, 2019). they can also be reused repeatedly with optimum performance (Su *et al.*, 2015; Verma, Sharma and Dwivedi, 2016).

However, enzyme catalysis of transesterification is limited because of drawbacks which include low catalytic activity, consequently leading to long reaction times and high catalyst quantity requirement for a significant biodiesel yield; and the high cost of the lipases (Abd-Alla *et al.*, 2015; Maymandi and Rahimpour, 2015; Lam *et al.*, 2016). These drawbacks threaten the feasibility for their industrial application in biodiesel production (Daramola, Nkazi and Mtshali, 2015; Go *et al.*, 2016; Mujeeb, Vedamurthy and T, 2016). Moreover, the inhibitory effect of short-chain alcohols and glycerol is the other problem associated with enzyme catalysis for biodiesel synthesis (Maymandi and Rahimpour, 2015; Marx, 2016; Norjannah *et al.*, 2016). The most popular alkyl

donor, methanol, has a toxic effect on enzyme catalysts and tends to deactivate them at high concentrations (Abd-Alla *et al.*, 2015), it is of paramount importance therefore, to control the alcohol concentration throughout the duration of the reaction so as to avert lipase deactivation (Abd-Alla *et al.*, 2015; Norjannah *et al.*, 2016; Moazeni, Chen and Zhang, 2019). The stepwise alcohol addition as the reaction progresses is generally employed for maintaining optimal levels alcohol to keep the reaction running (Lotti *et al.*, 2018); while retaining lipase activity for extended periods (Mata and Martins, 2015). Alcohol-impregnated silica gel could be used to effect the step-wise alcohol addition as it will gradually release the alcohol during the course of the reaction, thereby restricting the alcohol concentration to a minimum (Norjannah *et al.*, 2016). A co-solvent can also be employed to control the concentration of methanol for the prevention of lipase deactivation. Alternatively, using longer chain alkyl donors such as methyl acetate or dimethyl carbonate instead of methanol may also result in higher conversions without lipase deactivation from the reagents (Marx, 2016).

Different enzymes have different capacities of thermal stability, reaction speeds and methanol tolerance (Abd-Alla *et al.*, 2015; Mata and Martins, 2015). Actually, very few lipases are stable in the presence of methanol to withstand the optimal methanol: oil ratios for the process i.e. higher than 3:1 (Lotti *et al.*, 2018). Enzymes are most often immobilized when used, immobilization of lipase simplifies its recovery from reaction products, enables its repeated reuse (Marx, 2016; Verma, Sharma and Dwivedi, 2016; Mahmudul *et al.*, 2017), and promotes high quality reaction products (Karmee, 2016). Lipase immobilization also increases its stability in organic solvents (Norjannah *et al.*, 2016), i.e. tolerance to the inhibitory effect of polar short chain alcohols and glycerol (Abd-Alla *et al.*, 2015) (Ishak *et al.*, 2017). The improvement may be attributed to the stabilization of the enzyme hyper-activated form, dispersion of enzyme on the support surface, protection against harsh conditions owing to the rigidification, and/ or promotion of diffusional limitation and component partition by porous support (Norjannah *et al.*, 2016). Lipase immobilization can be done using various methods on different supports such as encapsulation on silica aerogel, adsorption on microporous resin, chemical binding on chitin, and entrapment on hydrophobic sol-gel (Norjannah *et al.*, 2016; Ishak *et al.*, 2017). Studies show that a high biodiesel yield is obtainable from enzyme-catalyzed transesterification through the immobilization of the lipases on a suitable support, and the optimization of reaction conditions (Mujeeb, Vedamurthy and T, 2016; Moazeni, Chen and Zhang, 2019). However, immobilization in some cases can

negatively affect the enzyme activity, selectivity and also alter its structural form resulting in poor biodiesel yield. The economics of enzyme catalysis for transesterification can be improved by finding efficient methods to regenerate lipase activity for reuse (Moazeni, Chen and Zhang, 2019).

2.3.1.4 Non catalytic

The non-catalytic transesterification reactions usually occur under supercritical conditions. Under supercritical conditions the alcohol will be in a supercritical gaseous state and the triglycerides will somehow be dissolved in a homogeneous phase (Mata and Martins, 2015). Transesterification with help of super critical alcohols is more superior than the conventional process in terms of enhanced solubility properties of triglycerides in supercritical alcohol (Mata and Martins, 2015; Go *et al.*, 2016; Verma, Sharma and Dwivedi, 2016), thus higher reaction rate (Mujeeb, Vedamurthy and T, 2016; Norjannah *et al.*, 2016; Stephen and Periyasamy, 2018). Supercritical methanol overcomes the mass transfer issues of normal alcohol/oil mixtures by forming a homogeneous phase due to the lower value of the dielectric constant of supercritical methanol (Mujeeb, Vedamurthy and T, 2016). The elimination of the catalyst requirement in the supercritical non catalytic transesterification results in a simplified downstream product separation and purification process (Campanelli, Banchero and Manna, 2010; Stephen and Periyasamy, 2018; Moazeni, Chen and Zhang, 2019), since there is no formation of side products such as soap (Mata and Martins, 2015; Norjannah *et al.*, 2016). Moreover, this process is insensitive to the moisture and FFA contents of the feedstock oil so that transesterification of triglycerides and esterification of free fatty acids can concurrently occur rapidly (Verma, Sharma and Dwivedi, 2016); comparatively it is more environmentally friendly than the conventional process (Mujeeb, Vedamurthy and T, 2016). Conversely, utilizing supercritical conditions is capital and energy intensive (Mata and Martins, 2015; Stephen and Periyasamy, 2018). The reaction demands the use of excessive amounts of alcohol compared to the conventional transesterification process, the excess of which needs to be recovered and reused, further complicating the process design (Mata and Martins, 2015). The typical reaction conditions are temperatures of 200-400°C, pressures of 10-60 MPa, and 20:1-45:1 alcohol to oil ratio (Go *et al.*, 2016; Mujeeb, Vedamurthy and T, 2016; Norjannah *et al.*, 2016). These process conditions require specialized equipment that can handle them which is obviously more expensive than those of conventional transesterification (Mata and Martins, 2015; Moazeni, Chen and Zhang, 2019). Apart from its clear advantages over other

processes, significant hurdles remain for full scale implementation of supercritical biodiesel production units (Mata and Martins, 2015).

2.3.1.5 Alkyl Donor

The most widely used alkyl donors in the transesterification reactions are low molecular mass primary alcohols i.e. methanol and ethanol (Mata and Martins, 2015; Norjannah *et al.*, 2016), however higher molecular mass alcohols, secondary and branched chain alcohols can be also employed as alkyl donors. The alkyl donor selection influences the process conditions as well as the biodiesel yield (Verma, Sharma and Dwivedi, 2016). Various factors are considered in the exploration of alternative alkyl donors, including the following: solubility between the reactants; toxicity towards the catalyst; its renewability; health and environmental issues; the obtainable fuel quality; and overall economics of the process (Go *et al.*, 2016).

Alcohols

Methanol popularity as the alkyl donor for commercial biodiesel synthesis is motivated by its relatively cheap price (Salam, Velasquez-Orta and Harvey, 2016; Verma and Sharma, 2016), as well as simple post-transesterification separation of glycerol by settling (Mata and Martins, 2015). Ethanol is synthesized from biomass thus it is renewable and environmentally friendly relative to methanol, which is a fossil fuels derivative (Huang *et al.*, 2015; Skorupskaite, Makareviciene and Gumbyte, 2016; Verma, Sharma and Dwivedi, 2016). Biodiesel can only be fully renewable if all its reagents are from renewable sources. Employing longer chain alcohols as biodiesel synthesis reagents produces biodiesel with superior thermal stability but poor oxidation stability, particularly if they have branched chains (Mujeeb, Vedamurthy and T, 2016; Norjannah *et al.*, 2016; Verma, Sharma and Dwivedi, 2016). Linear chain alcohols also produce better ignition qualities in the product fuel relative to their branched chain isomers (Sierra-Cantor and Guerrero-Fajardo, 2017). The miscibility of alcohols with oils increase with increasing alcohol chain length (Salam, Velasquez-Orta and Harvey, 2016); however post-reaction product separation and purification is difficult relative to that of methanol (Sanli *et al.*, 2015; Verma and Sharma, 2016), as such, lower biodiesel yields are attained with increasing chain length (Abd-Alla *et al.*, 2015; Verma, Sharma and Dwivedi, 2016). Reactions with secondary alcohols as reagents, are slower than those of primary alcohols, and this could be attributed to steric hindrance in the former (Norjannah *et al.*, 2016). The low solubility of methanol in oil can be explained by its relatively high polarity,

compared to higher molecular mass alcohols (Huang *et al.*, 2015; Go *et al.*, 2016; Skorupskaite, Makareviciene and Gumbyte, 2016). Numerous methods can be employed to improve mass transfer during transesterification, such as the addition of a solvent, stirring, heating etc. Methanol itself is a toxic solvent (Lee *et al.*, 2017), and as has been aforementioned, lipase exposure to more than one molar equivalent of methanol induces enzyme deactivation and denaturation (Norjannah *et al.*, 2016). As such, ethanol or higher alcohols could be better reagents for enzyme-catalyzed transesterification than methanol based on its less hostility to lipase (Aguieiras, Cavalcanti-Oliveira and Freire, 2015; Norjannah *et al.*, 2016). Methanol and ethanol can be employed as transesterification reagents in the same reaction in order to realize the benefits of both solvents concurrently, however, methanol is consumed faster (Norjannah *et al.*, 2016).

Short Chain Esters

Recently, short chain esters such as acetates and alkyl carbonates have been used as alkyl donors for the synthesis of biodiesel and high yields have been realized together with some valuable byproducts (Go *et al.*, 2016; Norjannah *et al.*, 2016; Lee *et al.*, 2017). The problems associated with the glycerol production as a byproduct in transesterification reactions such as lipase deactivation can be avoided when esters are used as alkyl donors instead of alcohols (Abd-Alla *et al.*, 2015; Lee *et al.*, 2017), thus presenting an opportunity for lipase recycling without additional pretreatment (Aguieiras, Cavalcanti-Oliveira and Freire, 2015). Valuable byproducts such as triacetylglycerol (triacetin) are obtained from the interesterification of lipids (Campanelli, Banchero and Manna, 2010; Norjannah *et al.*, 2016; Okoye and Hameed, 2016), which serves as a cold flow properties and viscosity improver of biodiesel, and can be used as an anti-knock agent in petroleum (Marx, 2016). The saponification reaction also, is suppressed when methyl acetate is employed as the alkyl donor since it reacts with the FFA in the oil to produce biodiesel and acetic acid (Campanelli, Banchero and Manna, 2010; Go *et al.*, 2016). However, despite the high biodiesel yields attained, the interesterification reaction is characterized by low reaction rates as well as high ester to oil ratio and catalyst concentration requirements relative to when alcohols are used as alkyl donors (Aguieiras, Cavalcanti-Oliveira and Freire, 2015; Norjannah *et al.*, 2016). It can be assumed that the lower reactivity of ester-alkyl donors relative to short chain alcohol-alkyl donors is due to steric hindrance in the former as a result of their relatively large and complex molecular structure. Additionally, since the ester-alkyl donors are derivatives of alcohols, they are

obviously expensive relative to the commonly used alcohol-alkyl donors (Abd-Alla *et al.*, 2015; Go *et al.*, 2016). Employing alkyl carbonates leads to the generation of byproducts such as glycerol carbonate and glycerol dicarbonate whose separation from the FAAE and fatty acid glycerol carbonate monoesters mixture requires environmentally unfriendly solvents such as methyl tert-butyl ether (Marx, 2016). There is therefore a need to find better means to regulate the product selectivity during interesterification with reagents such as dimethyl carbonate, as well as production of methyl acetate from renewable sources.

2.3.1.6 Factors that affect transesterification

The conversion, selectivity and reaction rate of the biodiesel synthesis process can be influenced by a number of process variables such as: the alkyl donor to oil molar ratio, reaction temperature, free fatty acid and moisture content, catalyst type and concentration, mass transfer, co-solvent, and the reaction time, (Huang *et al.*, 2015; Skorupskaite, Makareviciene and Gumbyte, 2016; Sodhi, Tripathi and Kundu, 2017). Out of these, the main parameters used for the optimization of the transesterification reaction include reaction temperature, alkyl donor to oil molar ratio, catalyst concentration, reaction time, and mixing rate (Karmee, 2016; Norjannah *et al.*, 2016; Verma and Sharma, 2016). Analysis of the interactions between these variables and selection for process optimization can considerably improve biodiesel yield and minimize the operational costs (Skorupskaite, Makareviciene and Gumbyte, 2016).

Molar Ratio

The molar ratio of alcohol to oil is a pivotal parameter that greatly influences the biodiesel yield (Marx, 2016; Verma and Sharma, 2016; Sodhi, Tripathi and Kundu, 2017). The transesterification reaction being an equilibrium reaction requires an excess amount of the alkyl donor to skew the reaction towards the continuous production of biodiesel (Campanelli, Banchero and Manna, 2010; Maymandi and Rahimpour, 2015; Skorupskaite, Makareviciene and Gumbyte, 2016). Singh and Patel, (2015) studied the effect of the methanol to oil molar ratios and observed that, higher methanol fractions in the reaction mixture reduces its viscosity, thereby promoting greater mass transfer rate through enhanced contact between the reagents and the catalyst. However, the biodiesel yield increases with alcohol molar ratio to a certain optimum point beyond which the yield starts dropping due to the polar hydroxyl group-induced emulsification of the transesterification products, thus aiding the reverse reaction resulting in low overall FAAE yield

(Verma and Sharma, 2016). Also, in the case of enzyme-catalyzed transesterification, excessive polar short chain alcohol concentrations may deprive the lipase of the aqueous environment which upholds the conformation of lipase, triggering an irreversible deactivation of the proteins (Aguieiras, Cavalcanti-Oliveira and Freire, 2015; Huang *et al.*, 2015). The stoichiometric alcohol to oil ratio needed for transesterification is 3:1, but the optimum molar ratios required for maximum yield and rate vary depending on the reaction conditions (Kumar and Ali, 2015; Marx, 2016; Verma and Sharma, 2016). The most commonly used molar ratio in conventional transesterification methods is 6:1 (Mujeeb, Vedamurthy and T, 2016; Salam, Velasquez-Orta and Harvey, 2016; Skorupskaite, Makareviciene and Gumbyte, 2016). In reactions whereby methanol will be having dual functions i.e. an extraction solvent as well as a transesterification reagent, the molar ratios required for high biodiesel yield can be very high to the tune of several hundreds or even thousands (Salam, Velasquez-Orta and Harvey, 2016; Skorupskaite, Makareviciene and Gumbyte, 2016). The optimum alcohol: oil molar ratios also increase with increasing reaction temperature and higher biodiesel yields are attained with the increment of both molar ratio and temperature, as such, typical molar ratios for supercritical transesterification are 42:1 (Marx, 2016). The process economy may be improved by recovering, purifying, and recycling the unreacted alkyl donor for the synthesis of more biodiesel (Cai *et al.*, 2015; Verma and Sharma, 2016).

Reaction Temperature

The reaction temperature considerably influences the rate of reaction and biodiesel yield (Verma and Sharma, 2016; Moazeni, Chen and Zhang, 2019), depending on the catalyst used (Salam, Velasquez-Orta and Harvey, 2016). Low reaction rate and biodiesel yield characterize reactions run under ambient temperatures because of the mass transfer resistance between the oil and methanol, however, higher reaction yields and rates are obtainable with increasing reaction temperatures (Xu, Gao and Xiao, 2015; Skorupskaite, Makareviciene and Gumbyte, 2016). Increasing reaction temperature tends to offset the reaction equilibrium towards perpetuating the production of biodiesel, this behavior is consistent with the endothermic nature of esterification (Huang *et al.*, 2015; Karmee, 2016). Accordingly, high reaction rates and short reaction durations are attained at high reaction temperatures (Mujeeb, Vedamurthy and T, 2016; Sodhi, Tripathi and Kundu, 2017). Mass transfer between oil and alcohol is enhanced with increasing reaction

temperatures due to the inverse variation of oil viscosity with temperature (Cai *et al.*, 2015; Marx, 2016; Verma, Sharma and Dwivedi, 2016). Also, the frequency of collisions between substrate molecules increases with temperature, resulting in improved material transfer thus an enhanced reaction rate (Huang *et al.*, 2015). However, research reveals that the influence of temperature changes to the reaction kinetics is limited to certain temperature ranges (Skorupskaite, Makareviciene and Gumbyte, 2016), depending on the catalysis of the reaction. In general, catalyzed reactions are conducted between ambient temperature and the boiling temperature of the alkyl donor (Go *et al.*, 2016). Additional temperature increments may result in the evaporation of the alcohol thereby effecting no significant change in the biodiesel yield (Singh and Patel, 2015; Salam, Velasquez-Orta and Harvey, 2016; Verma, Sharma and Dwivedi, 2016). On the contrast, enzyme catalysts undergo thermal denaturation as temperature rises above 60°C (Marx, 2016), resulting in decreased reaction rate (Huang *et al.*, 2015; Norjannah *et al.*, 2016). Thermal decomposition of transesterification products begins after the attainment of equilibrium under high temperatures, extended reaction times thus increases decomposition resulting in a low biodiesel yield (Marx, 2016). The optimization of reaction temperature and duration results in rapid biodiesel production and high yields, due to the suppression of products thermal decomposition.

Moisture Content

The moisture fraction in the transesterification reaction mixture significantly affects the reaction rate and the resultant biodiesel yield (Su *et al.*, 2015). Generally, lipase catalytic activity relies on the aqueous-organic interfacial area, so a minimum moisture content is required in the reaction mixture to preserve lipase active conformation hence optimum catalytic activity (Aguieiras, Cavalcanti-Oliveira and Freire, 2015; X. Wang *et al.*, 2015). Higher moisture content results in more water-organic interfacial which would be expected to increase lipase catalytic activity, hence higher biodiesel yield (Marx, 2016). However, excessive moisture content in the reaction mixture may induce enzyme aggregation, which results in reduced catalytic activity (Aguieiras, Cavalcanti-Oliveira and Freire, 2015; Su *et al.*, 2015). Additionally, excessive moisture in the reaction system leads to the reversal of the transesterification reaction by hydrolysis of the produced biodiesel into free fatty acids and methanol (Huang *et al.*, 2015; Alaba, Sani and Ashri Wan Daud, 2016; Lam *et al.*, 2016). As such, the optimum moisture content for enzyme catalysis is one that minimizes hydrolysis as much as possible while maintaining active lipase conformation for maximum

biodiesel yield (Aguieiras, Cavalcanti-Oliveira and Freire, 2015; Huang *et al.*, 2015; Norjannah *et al.*, 2016). Hydrolysis of triglycerides into soap and glycerol may also occur during alkaline-catalyzed transesterification in the presence of excessive moisture content, thus lowering resultant FAAE yield (Marx, 2016), and increasing the complexity in the product separation train (Mata and Martins, 2015; Salam, Velasquez-Orta and Harvey, 2016). Excessive moisture content has a dilution effect to homogeneous acid catalysts such that high alkyl donor amounts will be required to retain an optimum biodiesel yield. As such, utilizing moisture-free raw feedstock results in savings in the amounts of reagents and catalysts required for the optimization of the reaction (Skorupskaite, Makareviciene and Gumbyte, 2016). Thus, the acid esterification system which produces water as a byproduct needs to have a water management strategy, for example, carrying the reaction out in a membrane reactor to enable the removal of water as the reaction progresses (Mata and Martins, 2015).

Reaction Pressure

The effect of reaction pressure may be based on its influence with fluid density, hence its solubility under supercritical conditions. The improvement of a supercritical fluid's solubility stems from the increment in its density with increasing reaction pressure, which ultimately translates to a high biodiesel yield (Campanelli, Banchero and Manna, 2010; Marx, 2016). Thus, yield increases with pressure up to an optimum pressure, beyond which further pressure increments do not significantly increase the yield (Campanelli, Banchero and Manna, 2010). The typical optimum pressure used for supercritical transesterification is 20 MPa, at this point the entire system will be in a supercritical state (Marx, 2016).

Additional Solvent

The utilization of solvents such as hexane during transesterification reactions expedites extraction, in the case of reactive extraction, and improves the solubility between the reagents, thus ensuring intensified biodiesel formation under mild conditions (Mata and Martins, 2015; Norjannah *et al.*, 2016; Skorupskaite, Makareviciene and Gumbyte, 2016). Better solubility is achieved due to the diminishing of the mixture polarity by the non-polar additional solvents. Owing to the solubility improving effects of co-solvents, it therefore implies that the optimum alcohol to oil molar ratios required for the reaction may be lowered (Go *et al.*, 2016; Salam, Velasquez-Orta and Harvey, 2016). Also, solvents are useful during enzyme-catalyzed transesterification in minimizing the

inhibitory effects of methanol and glycerol on lipase activity (Mata and Martins, 2015; Marx, 2016; Norjannah *et al.*, 2016). The use of supercritical CO_2 as a co-solvent during supercritical in situ transesterification engenders a reduction in the temperature and pressure required to attain the supercritical state (Marx, 2016). However, employing co-solvents can alter the transesterification product selectivity, and may pose post-reaction product recovery and separation problems thereby compromising the resultant biodiesel purity (Salam, Velasquez-Orta and Harvey, 2016). Also, some solvents are toxic and have significant environmental effects, which can adversely affect the life cycle carbon emissions of the biodiesel produced (Norjannah *et al.*, 2016; Salam, Velasquez-Orta and Harvey, 2016). The solvent loading into the reaction mixture should be controlled in order to prevent reaction productivity loss through catalyst and reagent dilution (Go *et al.*, 2016). The additional solvent by itself is an additional cost factor to the overall production cost, through its purchasing and the additional product recovery and purification implications; however, if the benefits outweigh the additional costs, it maybe noble to adopt it.

Stirring

The agitation of the reaction mixture through stirring promotes mass transfer during the reaction by enlarging the interfacial area between the reactant phases with increasing mixing intensity, which is resultant in high reaction rates and biodiesel yields (Mata and Martins, 2015; Salam, Velasquez-Orta and Harvey, 2016; Skorupskaite, Makareviciene and Gumbyte, 2016). Employing co-solvents, coupled with a high mixing intensity lowers the optimum temperature required for the reaction owing to the improved mass transfer and solubility between the transesterification reagents (Mata and Martins, 2015). However, the agitation intensity only positively affects the reaction to a certain optimum point beyond which no significant improvement is realized. The shear stress from excessive agitation may disrupt the enzyme structure, for the lipase catalyzed reaction, thereby reducing its catalytic activity, translating to lower overall biodiesel yield (Norjannah *et al.*, 2016; Skorupskaite, Makareviciene and Gumbyte, 2016). Continuous stirring and alternating stirring essentially yields the same results, therefore (Salam, Velasquez-Orta and Harvey, 2016) suggested the alternating stirring treatment for the purposes of energy savings.

Catalyst Concentration

Transesterification generally requires a catalyst in order to attain a reasonable reaction rate and realize high yields under mild conditions (Salam, Velasquez-Orta and Harvey, 2016). Generally,

employing chemical homogeneous catalysts has less methanol to oil molar ratio demands than enzyme and heterogeneous chemical catalysts (Go *et al.*, 2016), this may be resultant of phase transfer limitations. Biodiesel yield increases with catalyst concentration until an optimum point, beyond which further catalyst concentration increments diminishes the yield (Singh and Patel, 2015; Salam, Velasquez-Orta and Harvey, 2016; Verma and Sharma, 2016). Excessive use of the catalysts promotes side reactions which results in emulsions, gel formation etc. which further complicates the product recovery processes as well as reducing the biodiesel yield (Verma and Sharma, 2016; Sodhi, Tripathi and Kundu, 2017), the homogeneous alkaline catalysts are more susceptible to such (Verma, Sharma and Dwivedi, 2016). Strong acid catalysis usually demands higher catalyst concentrations but however presents the need for its neutralization in the product streams, thereby increasing operating costs (Salam, Velasquez-Orta and Harvey, 2016).

2.3.1.7 Biodiesel Characterization

Biodiesel is a clear amber yellow, non-aromatic, and non-toxic liquid fuel with comparable physiochemical characteristics to petroleum diesel, and is derived from renewable oils through transesterification (Mata and Martins, 2015; Kumar and Rehman, 2016; Mujeeb, Vedamurthy and T, 2016). Biodiesel quality can be characterized by its physiochemical properties; such as cold flow properties, density, cetane number, heating value, oxidation stability and viscosity (Mata and Martins, 2015; Mofijur *et al.*, 2016; Mahmudul *et al.*, 2017). These properties are measured against and must comply with the globally prescribed certification standards, i.e. the EN 14214 (2003) and the ASTM D 6751 shown in Appendix A2; as a prerequisite for commercial use (Altaie *et al.*, 2015; Kumar and Ali, 2015; Sierra-Cantor and Guerrero-Fajardo, 2017). Biodiesel quality is a function of several factors such as feedstock traits, production process and post-production processes, as well as handling and the storage environment (Hajjari *et al.*, 2017). Some of the crucial properties of biodiesel are discussed in the ensuing sections.

Cold Flow Properties

The cold flow properties describe the flow performance of a fuel in low temperature environments (Sierra-Cantor and Guerrero-Fajardo, 2017). This property is a major deciding factor of the utilization of biodiesel as a neat fuel in cold regions (Altaie *et al.*, 2015). Biodiesel tends to crystallize when exposed to low temperatures such that it blocks the filters or becoming highly viscous, resisting flow, and thereby causing operational problems such as engine fuel starvation

and fuel pump overload (Kumar and Sharma, 2016; Verma, Sharma and Dwivedi, 2016; Mahmudul *et al.*, 2017). The cold flow properties can be defined in terms of Cloud Point (CP), Pour Point (PP), and Cold filter plugging Point (CFPP) (Altaie *et al.*, 2015; Kumar and Sharma, 2016; Verma, Sharma and Dwivedi, 2016; Sierra-Cantor and Guerrero-Fajardo, 2017). The cold-flow performance of biodiesel is relatively lower than that of petroleum diesel (Altaie *et al.*, 2015; Mahmudul *et al.*, 2017). The CFP of biodiesel is a function of the length and saturation extent of its fatty acid chains (Kumar and Sharma, 2016). The level of saturation of the fatty acid chains relates inversely with the cold flow behavior of biodiesel (Altaie *et al.*, 2015; Kumar and Sharma, 2016; Sierra-Cantor and Guerrero-Fajardo, 2017). Conversely, high levels of saturation in the fatty acid chains of imparts high oxidation stability and heat of combustion onto biodiesel, though with poor CFPs (Sierra-Cantor and Guerrero-Fajardo, 2017). The cold flow properties of biodiesel also varies inversely with its fatty acids chain lengths, i.e. CFPs improve with reducing fatty acid chain lengths (Altaie *et al.*, 2015). Cold flow properties of biodiesel can be improved by employing various methods such as blending (with mineral diesel or biodiesels with better CFPs) (Mahmudul *et al.*, 2017), using branched chain alcohols as alkyl donors for transesterification (Sierra-Cantor and Guerrero-Fajardo, 2017), and winterization to reduce the amount of saturated fatty esters (Kumar and Sharma, 2016).

i. Cloud Point

The cloud point of a fuel can be defined as the temperature whereby the smallest visible cluster forms in the fuel in a low temperature environment, i.e. the highest melting point of its constituents (Altaie *et al.*, 2015; Kumar and Sharma, 2016; Verma, Sharma and Dwivedi, 2016). Additional temperature reductions from this point increases the cluster formation in the fuel, resultantly thickening the fuel so that it blocks the fuel filters and injectors in engines (Kumar and Sharma, 2016). Cloud Point can be determined using numerous ASTM standards including D2500, D5771, D5772, and D5773 (Sierra-Cantor and Guerrero-Fajardo, 2017). The fatty acid composition of biodiesel can be used to predict its cloud point as illustrated in Equation 2.3 below (Verma, Sharma and Dwivedi, 2016). As can be deduced from Equation 2.3 the cloud point of biodiesel increases with the degree of saturation in its fatty acid chains.

Equation 2.3

$$Cloud\ Point = (1.44 \times \%\ Saturated\ Fatty\ Acids) - 24.8$$

ii. Pour Point

The pour point of a fuel is a temperature lower than CP, whereby the clusters formed begins to coagulate, becoming a semi-solid which can neither be pumped nor flow (Kumar and Sharma, 2016; Mofijur *et al.*, 2016; Verma, Sharma and Dwivedi, 2016). PP can be measured using various ASTM standards such as D97, D5949, D5950, D5985, D6749 and D6982 (Sierra-Cantor and Guerrero-Fajardo, 2017). Biodiesel has a relatively high pour point to that of petroleum diesel (Mofijur *et al.*, 2016).

iii. Cold Filter Plugging Point

The CFPP is the minimum temperature which enables a specified fuel flowrate through a standard filter when subjected to low temperature in a controlled environment (Kumar and Sharma, 2016; Mofijur *et al.*, 2016; Verma, Sharma and Dwivedi, 2016). Altaie *et al.*, (2015) and Sierra-Cantor and Guerrero-Fajardo, (2017) defined it as the highest temperature, whereby 20 ml of fuel fails to flow through a 45μm wire mesh filter under 0.02atm vacuum within 60s. The cold filter plugging point is a low temperature performance measuring parameter for fuel which increases with increasing saturation in the fatty acid chains of the biodiesel (Verma, Sharma and Dwivedi, 2016). Thus, a low degree of saturation in biodiesel is ideal for cold climate as it implies a low filter plugging point. Equation 2.4 below can be used to estimate the cold filter plugging point.

Equation 2.4

$$CFPP = (0.8537 \times CP) - 4.72$$

Kinematic Viscosity

The kinematic viscosity of a fuel is an important parameter which influences its atomization in the engine (Altaie *et al.*, 2015), hence the combustion efficiency (Mahmudul *et al.*, 2017; Damanik *et al.*, 2018). High viscosity suppresses the extent to which fuel can be atomized so that combustion efficiency is reduced, resulting in low engine power and high exhaust emissions (Kumar and Rehman, 2016; Skorupskaite, Makareviciene and Gumbyte, 2016; Moazeni, Chen and Zhang, 2019). Conversely, fuel has better lubricity when the kinematic viscosity is high, which implies lower engine wear-rate and fuel leakages (Mofijur *et al.*, 2016; Mahmudul *et al.*, 2017). Kinematic

viscosity of biodiesel varies inversely with temperature, i.e. viscosity increases with lower temperatures (Mahmudul *et al.*, 2017). Biodiesel has a high kinematic viscosity relative to that of petroleum diesel (Mata and Martins, 2015; Mofijur *et al.*, 2016), and this could be attributed to its larger chemical structure and higher molar mass (Mahmudul *et al.*, 2017). According to the ASTM D6751 and EN14214 standards, the acceptable kinematic of biodiesel at 40°C may vary within the ranges of 1.9-6 mm^2/s and 3.5–5 mm^2/s respectively (Skorupskaite, Makareviciene and Gumbyte, 2016; Moazeni, Chen and Zhang, 2019). The kinematic viscosity of biodiesel is influenced by the level of saturation in its fatty acid chains as well as their length (Kumar and Rehman, 2016). Kinematic viscosity increases with the saturation degree of biodiesel (Sierra-Cantor and Guerrero-Fajardo, 2017; Sodhi, Tripathi and Kundu, 2017; Damanik *et al.*, 2018).

Density

Density being a ratio of the fuel mass to its volume, greatly influences its atomization and combustion efficiency, hence the resultant engine power output since the fuel injection system's operation is volume-based (Kumar and Rehman, 2016; Mahmudul *et al.*, 2017). Generally the flow resistance of a fuel increases with its density, i.e. the fuel injection efficiency deteriorates with higher density (Mofijur *et al.*, 2016), consequent in poor combustion quality and therefore high engine emissions (Mahmudul *et al.*, 2017). Petrodiesel has lower density compared to biodiesel and this could be attributable to its lower molecular mass (Mofijur *et al.*, 2016).

Flash Point

The flash point of a fuel is a safety indicator for its handling and storage, which can be defined as the lowest temperature at which the fuel vapors ignite with the flame propagating beyond the source of ignition when heated under standard test conditions (Altaie *et al.*, 2015). The higher flash point of biodiesel relative to petrodiesel is an indicator that it is less flammable than the later, thus is safer for handling and storage (Kumar and Rehman, 2016; Mostafa and El-Gendy, 2017). The minimum acceptable flash point for biodiesel and its blends, in accordance with the ASTM D6751-12 and EN14214 standards, is 93°C and 120°C respectively (Mofijur *et al.*, 2016; Moazeni, Chen and Zhang, 2019).

Cetane Number

The cetane number (CN) of a fuel is defined as the relative measure of the duration before its auto ignition from its injection into the combustion chamber i.e. the ignition delay time (Maymandi and Rahimpour, 2015; Mostafa and El-Gendy, 2017). It is indicative of a fuel's ignition quality in cold operation conditions (Altaie *et al.*, 2015; Mujeeb, Vedamurthy and T, 2016; Mahmudul *et al.*, 2017). A high CN implies a shorter ignition delay (Kumar and Rehman, 2016; Mostafa and El-Gendy, 2017); which simply means the engine starts rapidly and runs smoothly (Mofijur *et al.*, 2016; Mujeeb, Vedamurthy and T, 2016; Mahmudul *et al.*, 2017). Accordingly, fuels having lower cetane numbers suffer from longer ignition delays (Altaie *et al.*, 2015), and are susceptible to higher hydrocarbons and particulate matter emissions (Mofijur *et al.*, 2016; Mahmudul *et al.*, 2017; Mostafa and El-Gendy, 2017). Cetane number increases with the degree of saturation in the fuel's carbon chains as well as their length (Skorupskaite, Makareviciene and Gumbyte, 2016; Zhu, Li and Hiltunen, 2016; Mostafa and El-Gendy, 2017). The cetane number of biodiesel is high relative to that of petrodiesel, this may be as a result of oxygen and long fatty acid chains present in biodiesel (Mofijur *et al.*, 2016; Mahmudul *et al.*, 2017). The cetane numbers of biodiesel normally range from 40 to 70 while of diesel range from 47 to 55 (Maymandi and Rahimpour, 2015; Mofijur *et al.*, 2016; Mujeeb, Vedamurthy and T, 2016). Cetane number enhancement in diesel is achievable through additives such as fatty acid amides (Kumar and Ali, 2015). Equation 2.5 below may be employed in calculating the cetane number of biodiesel.

Equation 2.5

$$CN = \sum X_{ME(wt.\%)} \times CN_{ME}$$

where CN is the overall cetane number of biodiesel, X_{ME} is the weight percentage of the individual methyl esters constituting the biodiesel, and CN_{ME} is the cetane number of individual methyl esters (Altaie *et al.*, 2015).

Oxidation Stability

The oxidation stability of a fuel is a measure of its resistance to reacting with atmospheric oxygen during storage for a predetermined duration. The oxidation stability of biodiesel is a function of its composition in terms of natural antioxidants and fatty acid esters (Altaie *et al.*, 2015; Verma, Sharma and Dwivedi, 2016). Biodiesel with high weightage of unsaturated content is more

susceptible to oxidation degradation, this is because unsaturated molecules promote auto-oxidation (Serqueira *et al.*, 2015; Spacino *et al.*, 2015; Sodhi, Tripathi and Kundu, 2017). The oxidation of unsaturated fatty acids/esters produces hydro-peroxide, sediments and gums, whose presence in biodiesel negatively affects the engine performance (Spacino *et al.*, 2015; Kumar and Sharma, 2016; Sierra-Cantor and Guerrero-Fajardo, 2017). The oxygenated functional groups also in the biodiesel reacts with refinery and engine metallurgy leading to corrosion, as well as the formation gums and other impurities that result in poor storage stability, filter plugging, and the development of residue on fuel pumps (Zulkepli *et al.*, 2018). However the oxidation stability of biodiesel is not only limited to the degree of unsaturation, the presence of water and other compounds derived from external contamination or from thermal degradation can also promote oxidation (Altaie *et al.*, 2015). Fuel oxidation can be suppressed by restricting moisture, oxygen and light access from the fuel, as well as employing antioxidant additives (Serqueira *et al.*, 2015; Spacino *et al.*, 2015; Sierra-Cantor and Guerrero-Fajardo, 2017).

Heating Value

The heating value of fuel is the thermal energy emitted from the complete combustion of its unit quantity (Mahmudul *et al.*, 2017). The gross heating value can be predicted by cooling all the combustion products down to the initial temperature before combustion; while the net heating value only focuses on gaseous water vapor as the byproduct which can be predicted by subtracting the heat of vaporization of the water vapor from the gross heating value (Altaie *et al.*, 2015; Mahmudul *et al.*, 2017). The heating values of biodiesel (39–40 MJ/kg) are about 10% lower than fossil diesel fuel (42–46 MJ/kg) (Mata and Martins, 2015). The lower heating value is induced by oxygen presence in the biodiesel composition, which is resultant in reduced carbon and hydrogen contents for the same mass of mineral diesel (Ali *et al.*, 2015; Wang *et al.*, 2018), thereby necessitating the injection of higher biodiesel quantities into the engine so as to attain the same engine power as that of petroleum diesel (Kumar and Rehman, 2016) (Aldhaidhawi, Chiriac and Badescu, 2017; Gharehghani, Mirsalim and Hosseini, 2017). According to the EN14313 standards, the acceptable heating value for biodiesel is at least 35 MJ/kg (Mahmudul *et al.*, 2017).

2.3.2 Deoxygenation

The deoxygenation (DO) of biomass-derived oils is an oxygen removal process in the form of water molecules (hydrodeoxygenation), carbon dioxide molecules (decarboxylation), and/or

carbon monoxide molecules (decarbonylation), in the presence of a catalyst to produce hydrocarbons whose composition and behavior is similar to that of mineral diesel. The diesel-like hydrocarbon-products of deoxygenation which comprise of n-alkanes and n-alkenes are also known as Renewable Diesel (Kumar, Singh and Korstad, 2017).The renewable diesel is more similar to petroleum diesel than the transesterification-produced biodiesel in terms of composition and combustion behavior (Pattanaik and Misra, 2017; Li *et al.*, 2018); thus, can be employed in the preexisting diesel combustion infrastructure without further processing (Li *et al.*, 2015). The transesterification-produced biodiesel emits low particulate matter and carbon dioxide but high NO_x and hydrocarbons relative to renewable diesel (Kumar, Singh and Korstad, 2017). Furthermore, the net heating value, oxidation stability, and cold flow properties of renewable diesel are better than those of the transesterification biodiesel (Viêgas *et al.*, 2015). The hydrodeoxygenation (HDO) process entails oxygen removal by reacting lipids with hydrogen to produce diesel range n-alkanes and water in the presence of metal catalyst or oxide catalysts (Dawes *et al.*, 2015; Hermida, Abdullah and Mohamed, 2015). The hydrotreatment of triglycerides involves its decomposition primarily by β-elimination to produce fatty acids, and the subsequent deoxygenation of intermediate fatty acids yielding n-alkanes (Wang *et al.*, 2018). Conversely, decarboxylation (DCX) and decarbonylation (DCN) are typically hydrogen-free oxygen removal processes in the presence of a catalyst, yielding CO_2 and CO, respectively, as well as diesel range n-alkanes and n-alkenes (Hermida, Abdullah and Mohamed, 2015). Practically, the deoxygenation process may follow more than one pathway depending on the reaction conditions, though one pathway will be dominant (Li *et al.*, 2018; Oh *et al.*, 2018). However, using hydrogen deoxygenation is costly since large amounts of H_2 (typically 300–420m^3 H_2/m^3 vegetable oil) (Oh *et al.*, 2018), and an expensive reactor is required for the HDO reaction (Zulkepli *et al.*, 2018); also, H_2 is largely a product of fossil fuels (Rogers and Zheng, 2016). In that regard, research efforts have been expended to minimize or eliminate the usage of H_2 in the DO process (Rogers and Zheng, 2016), thereby promoting DCX and DCN so as to improve on the process economy and sustainability. The deoxygenation reactions may be run in batch or continuous configurations within a conducive temperature range of 250–450°C (Pattanaik and Misra, 2017). The three main DO reaction pathways are shown on Figure 2.6 and a discussion of the mechanisms ensues in the subsequent sections.

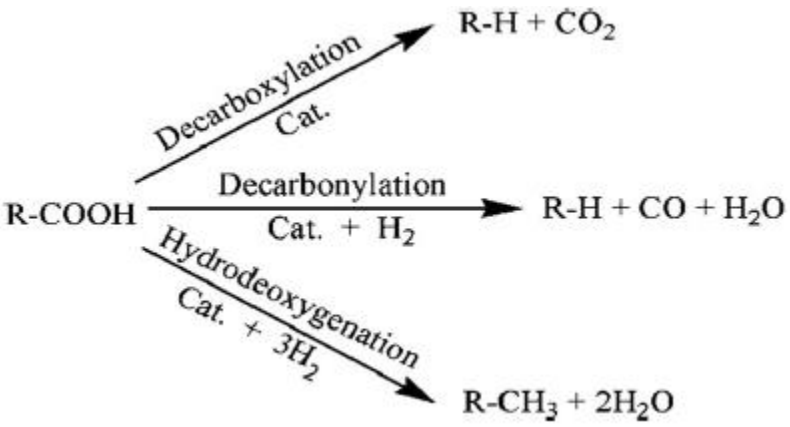


Figure 2.6:The three deoxygenation pathways for fatty acids (Hermida, Abdullah and Mohamed, 2015; Li et al., 2015, 2018; Pattanaik and Misra, 2017)

2.3.2.1 Hydrodeoxygenation (HDO)

Hydrodeoxygenation is an exothermic chemical reaction during which the carboxyl groups in triglycerides and/or fatty acids are reduced by hydrogenation and oxygen removal to produce diesel range n-alkanes and water (Online *et al.*, 2017; Pattanaik and Misra, 2017), in the presence of a catalyst (Hermida, Abdullah and Mohamed, 2015; Kumar, Singh and Korstad, 2017). HDO is the most hydrogen intensive DO pathway which is characterized by a series of hydrogenation and hydrogenolysis reactions (Rogers and Zheng, 2016; Kong *et al.*, 2020) at higher temperature and H_2 pressures compared to other pathways (Rogers and Zheng, 2016; Ng *et al.*, 2017; Li *et al.*, 2018). During the hydrogenation process, the hydrogen dissolves in the oil and diffuses onto the catalyst surface where molecular hydrogen is dissociated into hydrogen atoms (Nekhavhambe, Mukaya and Nkazi, 2019). Hydrodeoxygenation may be accompanied by indirect decarbonylation so that the resultant n-alkanes have one carbon number less than the initial fatty acids, otherwise the product retains the reactant's carbon number (Hachemi *et al.*, 2017; Li *et al.*, 2018). It is suggested in literature that the hydrogenation of the hydroxyl group produces the water and an aldehyde intermediate, which subsequently undergoes indirect DCO if the intermediate experiences C-C scission (Rogers and Zheng, 2016; Ng *et al.*, 2017). Alternatively, the separation of oxygen happens via the C=O bond hydrogenation followed by the C–O bond rupture during the HDO reaction (Ng *et al.*, 2017; Pattanaik and Misra, 2017); the selective formation of larger hydrocarbons is enabled by catalyst's presence which restrains the C–C bond breaking while facilitating the hydrogenation of the C=O bond and splitting of the C–O bond (Pattanaik and Misra,

2017). The reduction of the Oxygen to Carbon ratio while increasing the Hydrogen to Carbon ratio leads to the production of higher energy hydrocarbons. Elevating the reaction temperature and the hydrogen to oil ratio facilitates HDO, however extremely high reaction temperatures may induce thermal cracking thereby negatively impacting the reaction selectivity (Li *et al.*, 2018). Hydrodeoxygenation require continuous hydrogen supply for the attainment of a satisfactory product selectivity, however, optimum amounts should be used in order for the process to remain economically viable (Pattanaik and Misra, 2017). Recently, hydrogen donor solvents or coreactants have been employed for in situ hydrogen generation through aqueous phase reforming or decomposition, as a hydrogen gas requirement reduction technique for the HDO reactions (Oh *et al.*, 2018).

2.3.2.2 Decarboxylation/Decarbonylation (DCO_x)

Decarboxylation/Decarbonylation is an effective way to decompose the carboxyl groups in the fatty acids structure to release CO_2 or CO to produce n-alkanes in the presence or absence of H_2 (Hermida, Abdullah and Mohamed, 2015; Li *et al.*, 2018; Kong *et al.*, 2020). Oxygen is abstracted from the fatty acids structure in the form of Carbon Dioxide during the DCX reaction, and Carbon Monoxide during the DCN reaction (Ng *et al.*, 2017). The deoxygenation via DCO_x reactions is analogous to hydrocarbon chain cracking reactions whereby at least one C-C bond is broken during the liberation of oxygen from the fatty acids (Online *et al.*, 2017), to produce hydrocarbons with at least one less carbon unit (Rogers and Zheng, 2016; Ng *et al.*, 2017). A catalytic DCO_x reaction requires little or no hydrogen thereby simplifying the process and improving its economics relative to HDO (Online *et al.*, 2017; Kong *et al.*, 2020). The presence hydrogen has an inhibitory effect on the DCX reaction which increases with an increase in hydrogen pressure (Rogers and Zheng, 2016). The CO_2 and CO are released upon the rupture of the C-C bond during the respective decarboxylation and decarbonylation reactions (Romero *et al.*, 2015), and in both cases the hydrocarbon product is released after the hydrogenation of the carbon pool (Rogers and Zheng, 2016). High hydrogen pressure during the deoxygenation process significantly suppresses the production of aromatic compounds which in effect improves hydrocarbon selectivity (Pattanaik and Misra, 2017). Hydrogen-free deoxygenation of lipids, though feasible, has efficiency issues due to the rapid catalyst deactivation. Other than maintaining catalyst activity, hydrogen is also essential for the full decomposition of triglycerides into fatty acids (Rogers and Zheng, 2016).

Direct decarboxylation and direct decarbonylation reactions occur concurrently during hydrogen-free deoxygenation, while a combination of direct hydrogenation and indirect decarbonylation reactions characterize the deoxygenation process in the presence of hydrogen (Pattanaik and Misra, 2017). Indirect decarbonylation is the fastest reaction of all the DCO_x reaction pathways. In terms of hydrogen demand, the DCO_x pathways are favorable than the more environmentally friendly HDO pathway (Li *et al.*, 2018).

2.3.2.3 Factors that affect DO

The conversion and selectivity of the deoxygenation process for any feedstock is determined by a number of process variables which include the nature and quantity of the catalyst, the reaction atmosphere, pressure and temperature, and the reaction duration (Pattanaik and Misra, 2017; Li *et al.*, 2018). Some of the deoxygenation reactions reported in literature are presented in Table 2.3 below, the influence of the process variables are discussed in the ensuing passages.

Table 2.3: Catalytic deoxygenation of Lipids

Catalyst	**Support**	**Feed**	**Conditions**			**Atm**	**Reactor Mode**	**Conversion**	**Selectivity**	**Ref**
			Temperature	**Pressure**	**Time**					
NiMoCe (5wt.%Ni, 15wt.%Mo, Ce 5wt.%)	Al_2O_3	Jatropha Oil	370°C	3.5MPa	0.9/h	H_2	Fixed bed	89%	80% C15-C18	(Liu *et al.*, 2012)
NiMoLa	Al_2O_3	Jatropha Oil	370°C	3.5MPa	0.9/h	H_2	Fixed bed	83%	78% C15-C18	(Links *et al.*, 2012)
Ni-PTA	Al_2O_3	Jatropha Oil	360°C	3.0MPa	0.8/h	H_2	Fixed bed	98.5%	84.5% C15-C18	(J. Liu *et al.*, 2015)
Sulphided NiMo	γ-Al_2O_3	Soyabean Oil	400°C	9.2MPa	2h	H_2	Batch	92.9%	93.5-97.8% Diesel	(Veriansyah *et al.*, 2012)
10 wt% NiCo	γ-Al_2O_3	Jatropha FAME	400°C	2MPa		H_2	Fixed bed	78.2%	79% C12-C20	(Hari and Yaakob, 2015)

10 wt% NiCo	SiO_2	Jatropha FAME	400°C	2MPa		H_2	Fixed bed	76.1%	73% C12-C20	(Hari and Yaakob, 2015)
5 wt% Pd	C	Castor oil FAME	340°C	25bar	6hrs	H_2	Batch	100%	96% C17-C18	(Meller *et al.*, 2014)
25 wt% Ni	SAPO-11	Castor oil	300°C	3MPa	2/hr	H_2	Fixed bed	99%	96% C16-C19	(S. Liu *et al.*, 2015)
Sulphided 3Ni15Mo	AC	Jatropha oil	350°C	90 bar	3hrs	H_2	Batch	99.7%	81% C17-C18	(Tapia *et al.*, 2017)
25 wt% Ni	MAC	Stearic acid	260°C	6 bar	10hrs	H_2	Batch	100%	94% C17	(Li and Luo, 2015)
Ni	γ-Al_2O_3	Stearic acid	270°C	8 bar	6hrs	H_2	Batch	100%	90.3 C17	(Kumar *et al.*, 2014)
Ni	MFI type Zeolites	Fatty acid esters	280°C	40 bar	8hrs	H_2	Batch	100%	100 C17-C18	(Schreiber *et al.*, 2016)

Catalyst

While non-catalytic deoxygenation is possible, it is unfavorable compared to the catalytic process due to its low product selectivity and high thermal energy demand (Dawes *et al.*, 2015). The nature of the catalyst is a critical determinant of the deoxygenation pathway, conversion and product selectivity (Pattanaik and Misra, 2017; Li *et al.*, 2018). Catalysts used in the catalytic deoxygenation process consist of a metal component and the support component which work in synergy; the metal being the active constituent of the catalyst, and the support being responsible for hydrogen dissociation or adsorption of the oxygenated compounds (Rogers and Zheng, 2016; Pattanaik and Misra, 2017). A wide range of metals have been employed for the active metal component of the catalyst either in monometallic configuration or as combinations of different metals, these include noble and non-noble metals. Catalytic behavior varies with reaction conditions, thus it is important to understand the catalytic mechanism of a catalyst when optimizing the deoxygenation conditions (Li *et al.*, 2018). The main deciding factors however of the catalytic options are its activity and cost/availability (Rogers and Zheng, 2016).

Sulphided $CoMo/Al_2O_3$ and $NiMo/Al_2O_3$ are preferred for hydrodeoxygenation reactions because of their exceptionally high catalytic activity in hydrogen atmospheres (Hachemi *et al.*, 2017; Pattanaik and Misra, 2017). However, sulphided catalysts are not ideal for low hydrogen or hydrogen free reactions due to their limited catalytic activity towards DCO_x reactions as well as rapid deactivation that occurs in the absence of hydrogen (Rogers and Zheng, 2016). Also, sulphided catalysts tend to produce sulphur-contaminated hydrocarbon products and this is highly detrimental from an environmental preservation outlook (Pattanaik and Misra, 2017). In literature, Carbon-supported noble metals like Pd and Pt were demonstrated to be the best catalysts for deoxygenation of lipids due to their relatively high catalytic activity, even without the need for sulphidation (Hachemi *et al.*, 2017; Pattanaik and Misra, 2017). However, in spite of the high catalytic activity of noble metals during the deoxygenation of lipids even in inert reaction atmospheres, their high cost and scarcity is restrictive to their application in industrial scale processes (Hachemi *et al.*, 2017; Zulkepli *et al.*, 2018). Accordingly non-noble metal catalysts such as, Co-, Mo-, and Ni- based catalysts, are preferred owing to their high catalytic activity and availability at lower cost (Li *et al.*, 2015). Ni/ZrO_2 has been reported by Rogers and Zheng, (2016) to favor indirect DCN presumably due to its bifunctionality, which supports the hydrogenolysis

step and the subsequent decarbonylation of the aldehyde intermediate. Furthermore, Hachemi *et al.*, (2017) studied the catalyst reusability of Ni supported on Y zeolites by regenerating the spent catalyst from the hydrodeoxygenation of fatty acids; the catalyst demonstrated the possibility of restoring the rates per unit of surface area after regeneration. It is claimed however, that nickel based bimetals on suitable supports such as $NiMo/\gamma\text{-}Al_2O_3$, have better catalytic activity than the nickel monometallic catalysts, which is comparable to that of noble metal catalysts (Rogers and Zheng, 2016). Employing alkali metal and alkaline earth metal catalysts for the deoxygenation of lipids can also be considered due to their unique basic properties; the carbon dioxide adsorption/desorption ability of basic catalysts is favorable for the decarboxylation reaction (Online *et al.*, 2017). Amongst the alkaline catalytic materials, Mg–Al mixed oxides produced by calcining hydrothalcite are industrially available at a cheap price (Romero *et al.*, 2015).

The major drawback of catalytic deoxygenation processes is the deactivation of the catalyst (Li *et al.*, 2015; Rogers and Zheng, 2016). The catalyst's activity can be hindered by the unstable intermediates and aromatic compounds that are formed due to insufficient hydrogen presence in the reaction (Oh *et al.*, 2018), which leads to rapid coke deposition on the catalyst surface and therefore its deactivation. This phenomenon is more pronounced under inert atmospheres whereby the absence of hydrogen for the hydrogenation of the carbon pool prompts massive coke formation (Rogers and Zheng, 2016). Even minimal coke formation is enough to induce deactivation, noble and non-noble metal catalyst alike; this therefore necessitates the development of catalysts which can be resistant to coke deactivation or be regenerated by simple processes (Li *et al.*, 2015). As such, the viability of hydrogen free deoxygenation processes is threatened by the inevitable formation of coke in catalytic reactions of long chain reactants, and that complete conversion of triglycerides is difficult because of limitations in terms of b-elimination reactions (Rogers and Zheng, 2016). Ultimately, hydrogen-free deoxygenation processes may not be as economical as they seem relative to the HDO process, and this is because of their low catalytic activity thus low conversion and selectivity of the desired products. Deactivation, for sulphided metal catalysts, may be induced by the exhaustion of sulphur from the surface due to oxidation and coking; the regeneration of the sulphur sites on the catalyst may be achieved through the addition of a source of sulphur into the reaction, such as H_2S. However, catalyst regeneration is limited to the extent of degradation, beyond certain limits the degradation of the sulphur sites is irreversible (Rogers and

Zheng, 2016). The rate of catalyst deactivation may be reduced through higher catalyst loading during the deoxygenation process.

As has been aforementioned, the active metal of the catalyst and its support should work in synergy for the best catalytic performance. The commonly used supports include carbonaceous and SiO_2 supports, and this may be due to their inertness towards the deoxygenation reactants and products (Rogers and Zheng, 2016). Zeolites and alumina, likewise, have been used as supporting materials for the deoxygenation of lipids (Zulkepli *et al.*, 2018); these are regarded as acidic supports, with zeolites containing abundant Brønsted acid sites while alumina supports consisting of more Lewis acid sites (Rogers and Zheng, 2016). There is a general consensus in literature that the acidity of catalyst support materials has significant influence on the formation of active sites for both decarboxylation and hydrogenation of carboxyl groups. Alumina support for example, is reported to have some significant catalytic activity alone without metal loading, and this is due to its Lewis acid sites (Zhang, Lin and Zheng, 2014). Reducible oxide catalyst supports such as ZrO_2, TiO_2, CeO_2, and Cr_2O_3 are not ideal for hydrogen-free reaction atmospheres, as they are activated by hydrogen (Rogers and Zheng, 2016).

Reaction Temperature

The reaction temperature is the primary means of controlling catalytic activity and product selectivity during the deoxygenation process (Dawes *et al.*, 2015). By virtue of the DCO_x reactions being endothermic in nature, the generally favor high temperatures compared to the exothermic HDO reaction whose selectivity may decline with high temperatures (Rogers and Zheng, 2016). Excessively high temperatures though negatively impacts the DO selectivity regardless of the reaction pathway, and this is caused by the rate of thermal cracking and formation of aromatic compounds that increase with reaction temperature (Pattanaik and Misra, 2017). Accordingly, higher H_2 to lipids molar ratios will be required to suppress the thermal decomposition and formation of aromatic compounds during the deoxygenation process. The optimization of the reaction conditions remain imperative so as to attain the best reaction rate, product selectivity, and reaction economics.

2.3.3 Hydrocracking

Hydrocracking is a catalytic process whereby complex organic molecules such as heavy hydrocarbons are broken down into simpler light hydrocarbons under an elevated hydrogen pressure (Hassan *et al.*, 2017). It is one of the most versatile petroleum refining processes for upgrading mixtures of hydrocarbons into more valuable product streams such as diesel, gasoline and jet fuel (Rasyid *et al.*, 2015; Sahu *et al.*, 2015; Hassan *et al.*, 2017). The hydrocracking process is characterized by cracking and hydrogenation reactions, which lead to phase separation of the products (Kim, Kim and Lee, 2017). Hydrogenation occurs in compounds of olefins, aromatics, sulfur, nitrogen and oxygen while cracking occurs at C–C bonds (Sahu *et al.*, 2015), this results in the saturation of double bonds, removal of hetero atoms and isomerization (Hari and Yaakob, 2015). Non-catalytic hydrocracking (thermal hydrocracking) is almost impossible, this is because a catalyst is needed to stimulate the hydrogenation reaction (Munir, Irfan and Usman, 2018). The hydrocracking process is able to yield better quality products than other cracking processes because of the hydrogenation reaction that accompanies it (Rasyid *et al.*, 2015), as such, the products of hydrocracking are saturated hydrocarbons (Hassan *et al.*, 2017) that can be used without subsequent processing (Munir, Irfan and Usman, 2018). The catalysts used for the hydrocracking reactions are bi-functional in nature, i.e. they have acid and metal functions (Hassan *et al.*, 2017); these functions significantly influence the product distribution of the process (Agudelo *et al.*, 2015). The acid function conducts the cracking and isomerization, while the metal function conducts the hydrogenation-dehydrogenation during the hydrocracking process (Rasyid *et al.*, 2015; Peng *et al.*, 2018).

Hydrocracking is highly susceptible to the thermodynamic equilibrium between the endothermic cracking reactions and the exothermic hydrogenation reactions, thus hydrogen consumption is a function of the reaction temperature (Kim, Kim and Lee, 2017). Employing high hydrogen partial pressure suppresses the undesirable coking, catalyst fouling and/or repolymerization (Hassan *et al.*, 2017; Munir, Irfan and Usman, 2018). The heat energy input facilitates the cracking of the long hydrocarbon chains (Munir, Irfan and Usman, 2018). The hydrocracking extent, thus the product selectivity, is influenced by the reaction temperature, catalyst properties, hydrogen partial pressure, and the reaction time (Hassan *et al.*, 2017).

2.3.3.1 Reaction Temperature

The hydrogenation reaction is favored in a lower temperature environment because of its exothermic nature, this implies that the consumption of H_2 increases with lower reaction temperatures. Despite the low reaction rates that characterize lower reaction temperatures, they also suppress coke and aromatic compounds formation (Nguyen *et al.*, 2016; Kim, Kim and Lee, 2017). Conversion increases with temperature at the expense of valuable liquids product selectivity due to overcracking at excessively high reaction temperatures (Nguyen *et al.*, 2016; Munir, Irfan and Usman, 2018). At excessively high reaction temperatures, the influence of the catalyst is overridden and control of products is difficult. The optimum hydrocracking temperature is one whereby the highest conversion and selectivity are mutually realized.

2.3.3.2 Hydrogen pressure

Hydrogen presence suppresses the formation of free radicals that are responsible for the cracking and overcracking of a hydrocarbon molecules (Munir, Irfan and Usman, 2018). Hydrogen also promotes the increased yield of saturated hydrocarbons, and stifles coke and aromatic compounds formation, by saturating the olefins (Nguyen *et al.*, 2016; Munir, Irfan and Usman, 2018). Increasing hydrogen pressure enhances catalyst activity during the reaction by regenerating the catalyst's active sites through the conversion of the coke deposits on the catalyst surface into gaseous organic compounds which subsequently leave the surface of the catalyst, thereby lengthening of its life time (Sahu *et al.*, 2015).

2.3.3.3 Catalyst

Catalyst activity significantly influences the product distribution, the total conversion as well as the production costs (Nguyen *et al.*, 2016; Lopez *et al.*, 2017). A typical hydrocracking catalyst is a heterogeneous solid powder consisting of an acidic support with metal impregnated over it (Nguyen *et al.*, 2016; Munir, Irfan and Usman, 2018); homogeneously dispersed catalysts have also been reported in slurry phase hydrocracking processes. The acidic support conducts the cracking reactions, while the loaded metal catalyzes the hydrogenation reactions during the hydrocracking process (Rasyid *et al.*, 2015; Sahu *et al.*, 2015). A strong hydrogenation function minimizes coke formation by hydrogenating the coke precursors and improves product selectivity

by quenching the free radicals formed during the cracking reactions, to prevent their additional cracking which may promote unrestrained gas formation (Sahu *et al.*, 2015; Nguyen *et al.*, 2016; Munir, Irfan and Usman, 2018). During catalytic hydrocracking, other acid catalyzed reactions such as dehydrocyclization reactions can also occur (Munir, Irfan and Usman, 2018).

Catalyst performance is a function of its composition, preparation procedure, and the reaction conditions (Sahu *et al.*, 2015). The metallic component of the catalyst can be a noble metal or non-noble metal of groups VI-A and VIII-A of the periodic Table (Sahu *et al.*, 2015; Online *et al.*, 2017; Munir, Irfan and Usman, 2018). It can be made up of singular or a combination of metals, such as a combination of cobalt and molybdenum (Rasyid *et al.*, 2015; Hassan *et al.*, 2017). As discussed earlier, the application of noble metals for catalytic purposes is economically unattractive due to their high cost constrains (Online *et al.*, 2017). The acidic support is usually an amorphous oxide such as silica-alumina (ASA), ultra-stabilized Y (USY) zeolite, a strong solid acid such as sulfated zirconia, or a fusion of these materials (Agudelo *et al.*, 2015; Nguyen *et al.*, 2016; Hassan *et al.*, 2017). Hydrocracking product selectivity is largely influenced by the Brønsted acidity of the support; a high Brønsted acidity induces increases the product selectivity for lighter products (Peng *et al.*, 2018). Low acidity of the catalyst support usually result in low rates of reaction and this can be compensated by higher reaction temperature (Agudelo *et al.*, 2015). The acidity and shape-selectivity of the catalyst also determines the catalyst's resistance to deactivation (Kim *et al.*, 2017; Lopez *et al.*, 2017).

A hydrocracking catalyst enables the realization of high hydrocarbon conversion and product selectivity under moderate process conditions thereby improving the process efficiency(Lopez *et al.*, 2017; Munir, Irfan and Usman, 2018). An ideal catalyst improves the hydrocracking reaction rate while suppressing overcracking and the olefins content in the resultant products. Generally, deactivation of the catalyst occurs when carbonaceous materials such as coke are deposited and blocks its pores during the reaction (Nguyen *et al.*, 2016). Catalyst regeneration for some catalysts may be realized by burning in air or passing hydrogen over it at high temperature (Hassan *et al.*, 2017). Additionally, changing the textural properties of a catalyst may extend its lifespan (Sahu *et al.*, 2015). Catalysts with long lifespans are economically preferable from the operational and maintenance perspective (Nguyen *et al.*, 2016).

2.3.4 Development of the Biodiesel Synthesis Strategy

Following the study of literature in this work, it was understood that the main demerits of the transesterification-produced biodiesel, namely, poor cold flow properties, oxidation stability, and energy density, are influenced by the degree of saturation and the length of the carbon chains, as well as the presence of oxygen in its structure. The oxygen content in the biodiesel stems from its vegetable-mother oils, which contain oxygen atoms in the form of carboxyl or carbonyl groups (Romero *et al.*, 2015) as well as from the alcohol used for transesterification. The essential reaction in the synthesis of high-quality diesel-like hydrocarbons is the deoxygenation reaction, which entails the removal of oxygen from biomass-derived oils through either or a combination of hydrodeoxygenation, decarboxylation and decarbonylation (Dawes *et al.*, 2015; Ng *et al.*, 2017; Oh *et al.*, 2018). The hydrocarbon fuels attained from the deoxygenation process usually have a high cetane number (CN), but restrictions on its usage still exist due to the poor cold flow properties which may be attributed to their long carbon chains (Li *et al.*, 2018). If deoxygenation is tailed by mild hydrocracking to enhance cold properties, the product biodiesel of the process may have almost identical properties to petrochemical diesel (Romero *et al.*, 2015). A similar process chronology was reported by Kim *et al.*, (2017) and Li *et al.*, (2018) to be prominent in the synthesis of biojet fuel; whereby the products of the deoxygenation of triglycerides are subsequently hydrocracked to produce biojet fuel which is permitted by ASTM specification D7566-14 for blending into commercial jet fuel at proportions of up to 50%. The removal of oxygen improves the calorific value and reduces the corrosiveness of the resultant fuel, while carbon chain saturation through hydrogenation improves its oxidation stability. The cold flow properties are improved by the reduction of the carbon chain length to match that of petroleum diesel, C13-C20 (Online *et al.*, 2017; Li *et al.*, 2018), during the hydrocracking reaction. Other researchers, in a quest to improve the properties of the transesterification-produced biodiesel, have subsequently subjected it to hydrotreatment. However, the transesterification route is susceptible to saponification for cheap feedstocks such as waste cooking oils, due to its high sensitivity to fatty acids, and it requires more investment in terms of reactors, catalysts, the alcohol and energy. The strategy depicted in Figure 2.7 below, is therefore suggested for synthesizing biodiesel from castor oil.

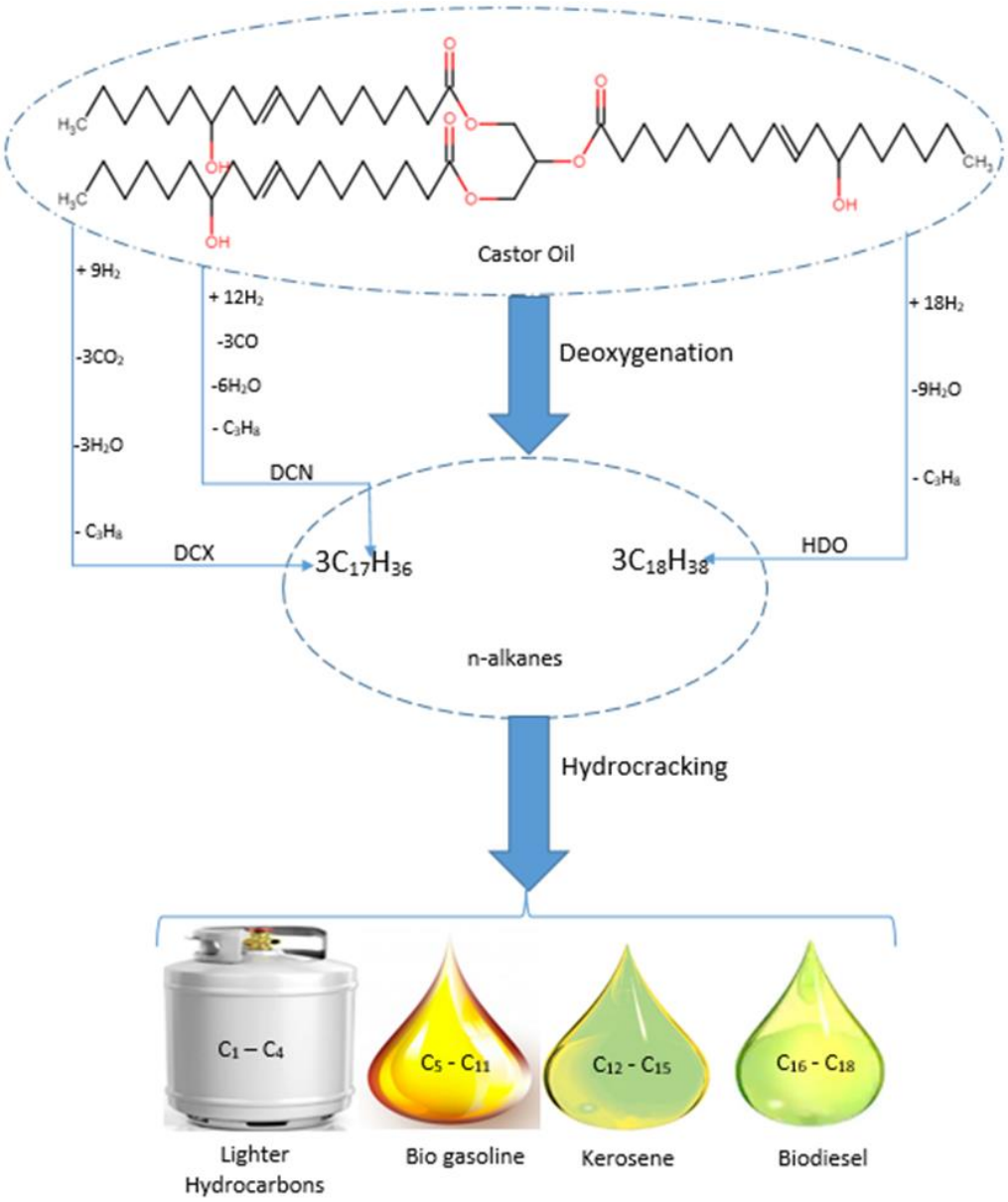


Figure 2.7: The Proposed Biodiesel Synthesis Strategy

The strategy is economically viable for industrial application if catalyzed by non-noble, highly active catalysts such as Ni-based bimetallic catalysts on appropriate supports, and deoxygenation is carried out under H_2 modest conditions. While a single step hydrodeoxygenation-hydrocracking process is viable, it not preferable because of the following reasons: the CO generated via decarbonylation tends to poison the metal component of the catalyst, thereby inducing a considerable disproportion between the metal and acid functions in hydrocracking reaction (Kim *et al.*, 2017); leading to overcracking of the hydrocarbons and premature catalyst deactivation as

a result of a considerable formation of aromatic species and coke (Oh *et al.*, 2018). In essence, the final product yield is largely influenced by the hydrocracking step since excessive cracking may result in substantial short-chain gaseous hydrocarbons production (Kim *et al.*, 2017). Other valuable liquid fuels that can be produced from this process are bio-gasoline as well as biojet fuels, depending on the reaction conditions.

2.4 Conclusions

The current commercially produced biodiesel in the form of Fatty Acid Alkyl Esters is not entirely favorable for the current diesel engine metallurgy because of the presence of oxygen in its composition, and this stifles its usage as a pure fuel as well as blending proportions with petroleum diesel. Biodiesel properties are imprinted by the feedstock properties and its synthesis strategy. Deoxygenation is a viable process for the production of renewable diesel from vegetal oils though either or a combination of hydrodeoxygenation, decarbonylation, and decarboxylation pathways, depending on the reaction conditions. Deoxygenation in a hydrogen environment favors the hydrodeoxygenation pathway and is expensive, however, it retains catalyst activity for longer periods than in hydrogen-free environments. The decarbonylation and decarboxylation pathways dominate hydrogen-free deoxygenation environments and they produce n-alkanes/n-alkenes with lower numbers of carbon atoms due to the C–C bond scission that accompanies them, nevertheless, they suffer from rapid catalyst deactivation which diminishes the resultant renewable diesel yield. Lower temperatures favor the hydrogenation reactions whereas higher temperatures facilitates the cracking reactions; excessively high temperatures promote aromatization and coke formation reactions which exacerbates catalyst deactivation and yields hydrocarbons of lower calorific value. The development of a two-step biodiesel synthesis strategy which employs separate deoxygenation and hydrocracking processes to minimize catalyst deactivation, is crucial for industrial scale production of engine-friendly biodiesel, due to the absence of oxygen in its composition and superior cold flow properties.

Chapter 3: Catalyst Synthesis and Selection

3.1 Introduction

The catalysts used in this project were bimetallic catalysts of Nickel and Cobalt, which were supported on alumina ($NiCo/Al_2O_3$). The motivation for the selection of these materials was reports in literature that suggest that Ni bimetallic catalysts have better deoxygenation catalytic activity than their monometallic counterparts, and have comparable catalytic activity to that of the best-performing expensive noble metals (Pt and Pd). Alumina support was selected for its relatively mild acidity since the primary objective was oxygen removal, i.e. the cracking of the carbon chains was to be minimized during the deoxygenation reactions, in order to keep the product selectivity within the middle distillates range. Also, a similar catalyst exhibited 78.2% conversion and 79% selectivity for diesel in the hydrotreatment of Jatropha FAME without the need for sulphidation in the preceding studies by Hari and Yaakob, (2015). In this Chapter the procedures followed in synthesizing and characterizing the $NiCo/Al_2O_3$ catalysts for this project are outlined; the characterization results are also presented and discussed, leading to the selection of the catalyst with the most suited physiochemical properties for the deoxygenation of seed oil.

3.2 Experimental Procedure

3.2.1 Catalyst Synthesis

The materials used for synthesizing the catalysts are Nickel (II) Chloride Hexahydrate (Sigma-Aldrich) and Cobaltous Nitrate Hexahydrate (Ace) as metal precursors, and Aluminium Oxide 90; 70-230 mesh ASTM (Merck) for the catalyst support. The $NiCo/Al_2O_3$ catalysts were synthesized through the co-impregnation method using aqueous solutions containing both metal precursors, $NiCl_2 \cdot 6H_2O$ and $Co(NO_3)_2 \cdot 6H_2O$, at varying ratios. The metal precursors were dissolved in 400ml distilled water at five different ratios shown in Table 3.1 to make five different solutions. To each aqueous solution was added 20g Al_2O_3 support slowly under constant stirring. The total metal loading of all the catalysts was maintained at 20 wt.%.The catalysts were then dried overnight at 90°C and subsequently calcined in air for 4 hours at 500°C.

Table 3.4: Catalyst Active Metal Loading to 20g Alumina

Catalyst	1Ni:4Co	2Ni:3Co	1Ni:1Co	3Ni:2Co	4Ni:1Co
Ni (g)	0.8	1.6	2.0	2.4	3.2
Co (g)	3.2	2.4	2.0	1.6	0.8

The notation of the catalysts in this report is presented interchangeably as either *x*Ni:*y*Co/Al_2O_3 or *x*Ni:*y*Co, where *x* and *y* are the ratios of the metal composition in the respective catalysts, however, all the catalysts were supported on alumina, regardless of the notation.

3.2.2 Catalyst characterization

The characteristic properties of the synthesized catalysts were investigated using the following characterization techniques: AAS, XRD, BET, TEM, SEM and FT-IR. Each of the techniques focused on a unique characteristic attribute although in some cases they would overlap, in which case would improve the quality of the results.

3.2.2.1 Atomic Absorption Spectrometry (AAS)

The elemental concentrations of the active metals in the catalysts i.e. Ni and Co, were confirmed using the AAS (Agilent Technologies 200 Series AA). The objective of this characterization was to have an understanding of the actual active metal compositions that constituted the synthesized catalysts. Sample preparation for analysis was done by dissolving 1g of each sample in an Aqua Regia solution comprising of 10ml Nitric Acid (55 vol.%) and 3ml Hydrochloric Acid (32 vol.%). The samples were then digested in a microwave digester (Auton Paar, Microwave Digestion System, Multiwave GO) at 175°C for 45 minutes. The liquid digestate was then allowed to cool to ambient temperature before being subjected to the AAS analysis. Each sample was analyzed 3 times so that the average concentrations were recorded, this was done for better accuracy.

3.2.2.2 Fourier Transform Infrared (FTIR) Spectrometry

The functional groups present in the catalysts were determined using the Bruker Tensor 27 FT-IR spectrometer in the wavenumber range of 400-4000cm^{-1}. Small quantities of catalyst samples were separately loaded and transmittance scans performed by the instrument's analyzer to generate an IR spectrum per sample. The present functional groups in the catalysts were identified by the peaks

they formed corresponding to specific wavenumbers on the generated IR spectra. It is also important to note that the transmittance scans were preceded by the background scan on the spectrometer for background correction.

3.2.2.3 X-Ray Diffractometry (XRD)

The phases present in the synthesized catalysts were examined by the D2 Phaser Burker X-ray diffractometer with Cu-Kα radiation in the range of $2\theta = 5 – 90°$ at a scanning speed of 1.52 per minute for 30 minutes per sample. The objective of this analysis was to investigate the influence of varying the active metal composition ratios on the phases formed in the catalysts.

3.2.2.4 Scanning Electron Microscopy (SEM)

The surface morphology of the catalysts and pre-impregnated alumina support were investigated using the FEI Quanta 200 ESEM. Sample preparation entailed mounting small amounts of the respective samples onto carbon resins, this was achieved through smearing and flattening material to be analysed onto the sample holders. This was followed by gold and palladium coating in order to prevent the samples from charging by the electrons emitted by the SEM during the analysis, which would resultantly distort the analysis. To estimate the dispersion of the active metals on the catalyst support surface, the Electron-Dispersive X-ray Spectroscopy (EDS or EDX) was employed on the samples. The EDS analysis was used as a qualitative measure of the catalyst samples, and the semi-quantitative properties of EDS were used only to compare the catalysts synthesised within this study; the obtained data are not meant to be compared with values from literature.

3.2.2.5 Transmission Electron Microscopy (TEM)

The intrinsic morphological properties of the synthesized catalysts were analysed using a FEI Tecnai T12 TEM. Sample preparation involved dispersing small sample amounts in ethanol then dropping the resultant homogeneous suspension on a copper grid 26 (Structure Probe, Inc. (SPI) carbon copper grid (200 mesh), and allowed to dry at room temperature. The grid was then mounted onto sample holder and placed into the instrument’s chamber for analysis.

3.2.2.6 Brunauer-Emmet-Teller (BET)

The specific surface area and pore size distribution of the catalysts were calculated through the Brunauer–Emmett–Teller (BET) and Barrett–Joyner–Halenda (BJH) methods by measuring N_2 adsorption–desorption isotherms at 77.3 K using a Micromeritics Tristar 3000 surface area and porosity analyser (V6.05). Catalyst samples of 0.50 g were degassed at 150 °C for 6 hours under a stream of nitrogen gas where N_2 adsorption-desorption occurred.

3.3 Results and Discussion

The characterization results of the five catalysts are presented in this section as a basis for the discussion on the influence of the catalyst composition on their physiochemical properties, hence catalytic behavior. The catalysts were synthesized using the co-impregnation method at varying concentrations of Ni and Co on Al_2O_3 support. To confirm the elemental concentration of Ni and Co in the catalysts, the Atomic Absorption Spectrometry (AAS) was employed, and the results are presented in Table 3.2 below.

Table 3.5: Catalyst Active Metal Composition Profiles

Catalyst	**Design Concentration (conc.%)**		**AAS Concentration (conc.%)**	
	Ni	**Co**	**Ni**	**Co**
1Ni:4Co	20	80	24	76
2Ni:3Co	40	60	45	55
1Ni:1Co	50	50	55	45
3Ni:2Co	60	40	65	35
4Ni:1Co	80	20	83	17

An increasing concentration trend of nickel against a decreasing concentration trend of cobalt is observed and congruent to expectation. The highest synergy in the catalytic activity of the active metals is likely to be realized for catalyst 1Ni:1Co relative to the other catalysts. Similarly, the individual dominance of Ni and Co on the overall catalytic activity and selectivity were to be realized for catalysts 4Ni:1Co and 1Ni:4Co, respectively. However, the actual concentration ratios did not accurately match the design ratios. This could be due to the difficulty in controlling the

dispersion of the metals across the catalyst support matrix, which is one of the limitations of the impregnation method. A similar phenomenon was reported by Trisunaryanti *et al.*, (2019) to be caused by mass loading during the impregnation process of Ni and Mo on an alumina support. Nonetheless, the impregnation method is one of the quick and simple methods of increasing the catalysts' active sites through metal loading on the catalyst support material.

3.3.1 Catalyst Functional Groups

The investigation of the functional groups present in the catalysts was conducted using the Bruker Tensor 27 FT-IR spectrometer and the resultant spectra are presented in Figure 3.1 below.

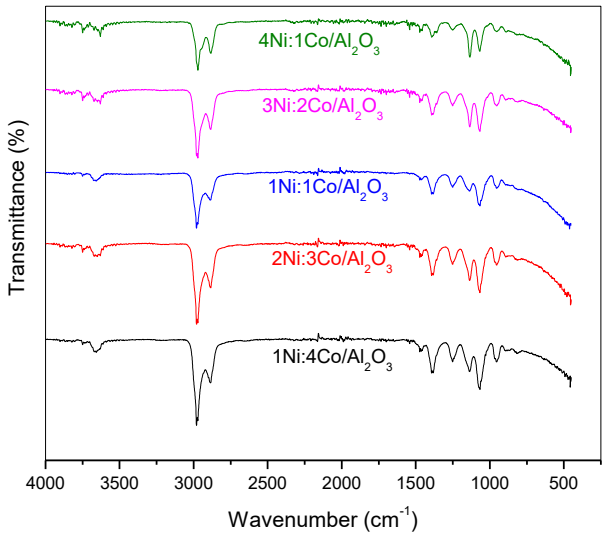


Figure 3.1: FTIR spectra for the catalysts

The five catalysts of different active metal loading ratios showed almost identical IR spectra. Major peaks were noted within the wavenumber ranges of 450cm^{-1}, 800-1500cm^{-1}, 2600-3050cm^{-1}, and 3600-3700cm^{-1}. Of particular importance to the catalysts were the active metal related functional groups, and these were observed in the region of 450-600cm^{-1}, which correspond to metal oxides vibration bonds. As such, the expanded view of the spectra in Figure 3.1 reveals that catalysts 1Ni:4Co and 4Ni:1Co had the most pronounced peaks within the metal oxides vibration range at 450-465cm^{-1}. Catalysts 2Ni:3Co and 3Ni:2Co also exhibited similar peaks but with lower intensity, especially for catalyst 2Ni:3Co. As for catalyst 1Ni:1Co, the peak was virtually absent, however, it showed a peak at 465-475cm^{-1} which was absent for the other catalysts. Other smaller

peaks in this vibration bond were observed up to 525cm^{-1}.This observation of increasing peak intensity with an increase in dominance of either Ni or Co in the ratio suggests that the two metals form similar oxides when they are the main constituent of the catalyst, and validates the assumption that the transmittance of a functional group is proportional to its relative abundance within a material. The peak at 1420 cm^{-1} is related to the adsorbed water whereas the one at 3388 cm^{-1} corresponds to the -OH, functional group (Sajjadi, Haghighi and Rahmani, 2015). Furthermore, depicted bonds in 1525 cm^{-1} corresponds to N–O as a result of atmospheric nitrogen in the lab, residual nitrate compounds such as cobalt nitrate that was employed for the catalyst synthesis. The observed reduction in intensity of the peak with reducing Co concentration in the catalyst confirms the source of the nitrogen to be largely the $Co(NO_3)_2 \cdot 6H_2O$ metal precursor.

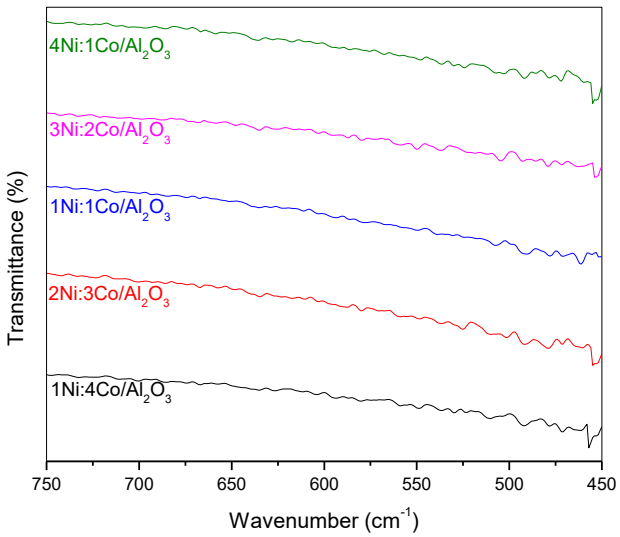


Figure 3.2: Expanded view of the FTIR spectra

3.3.2 Catalyst Phases

The phases formed by the synthesized catalysts of varying Ni/Co ratios on Al_2O_3 support were identified using the D2 Phaser Burker X-ray diffractometer, the obtained diffractograms are depicted in Figure 3.3 below.

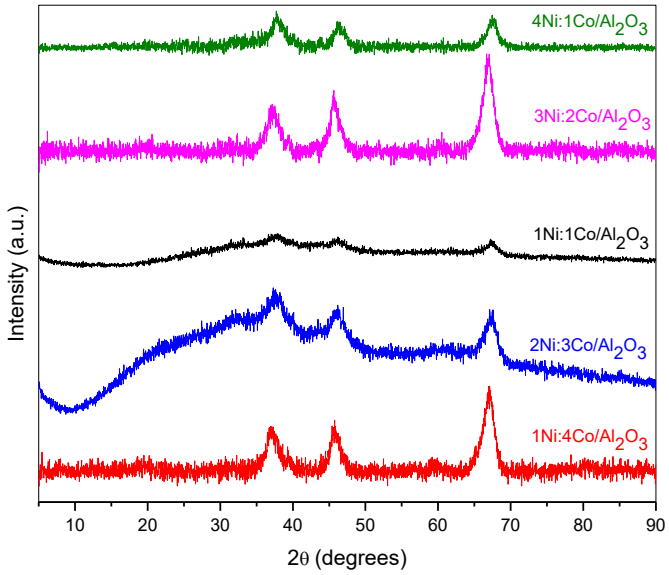


Figure 3.3: X-ray diffractograms of the catalysts

The five catalysts showed almost identical diffraction peaks, with the differences only being in the intensity of the peaks. This suggests that the catalysts had essentially the same phases although in varying degrees, owing to the differences in active metal ratios in the catalyst composition. The characteristic diffraction peaks of the alumina support were observed at $2\theta = 37.0°; 46.8°; 68.5°$, which correspond to Miller indices (311), (400), and (440), respectively. Unfortunately the contribution of Ni and Co was not visible, probably due to their low concentrations on the support. However, catalyst 1Ni:1Co/Al_2O_3 exhibited diffraction peaks with low intensity relative to the other catalysts. This may suggest that the active metal particles were well dispersed on the catalyst support, which may have led to the formation of the bimetallic phase. Also, it can be inferred that catalyst 1Ni:1Co has a different morphology, and is highly likely to be amorphous, unlike the other catalysts with sharp peaks.

3.3.3 Catalyst Morphology

The effects of metal impregnation and composition ratios on the alumina support surface morphology was determined using the SEM analysis. The Scanning Electron Micrographs of the alumina support and the five catalysts of varying Ni:Co ratios on alumina support are presented in Figure 3.4 below.

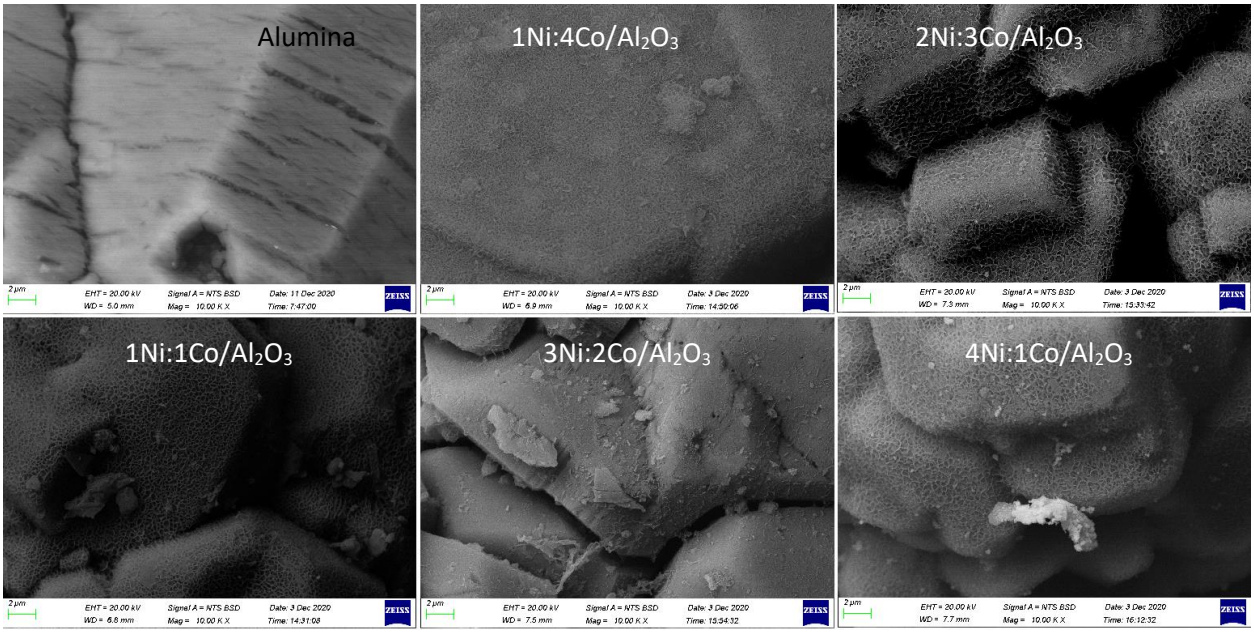


Figure 3.4: Scanning Electron Micrographs of the catalysts

The alumina support generally appears to be made up of irregularly-shaped clusters with diameters ranging from 36.69-113.6µm as shown in Figure A1 in the appendices. A closer look at the clusters reveals Al_2O_3 before impregnation to be having a relatively smooth surface with some parallel crevices cutting across its surface. On the other hand, the metal impregnated alumina, i.e. the catalysts, were characterized by rough surfaces without the aforementioned crevices. This observation confirms the impregnation of the active metals, Ni and Co, on the surface and crevices of Al_2O_3, as affirmed by the presence of their associated phases in the XRD analysis of the catalysts. The rough surfaces consisted of thread-like networks of depositions, which were especially visible for catalysts 1Ni:1Co and 2Ni:3Co. Additionally, some aggregates were observed for catalysts 1Ni:1Co, 3Ni:2Co, and 4Ni:1Co, and these could either be some agglomerates of the Ni oxides present in the catalysts, or some fragments of the alumina support that could have been generated by attrition during stirring, or both.

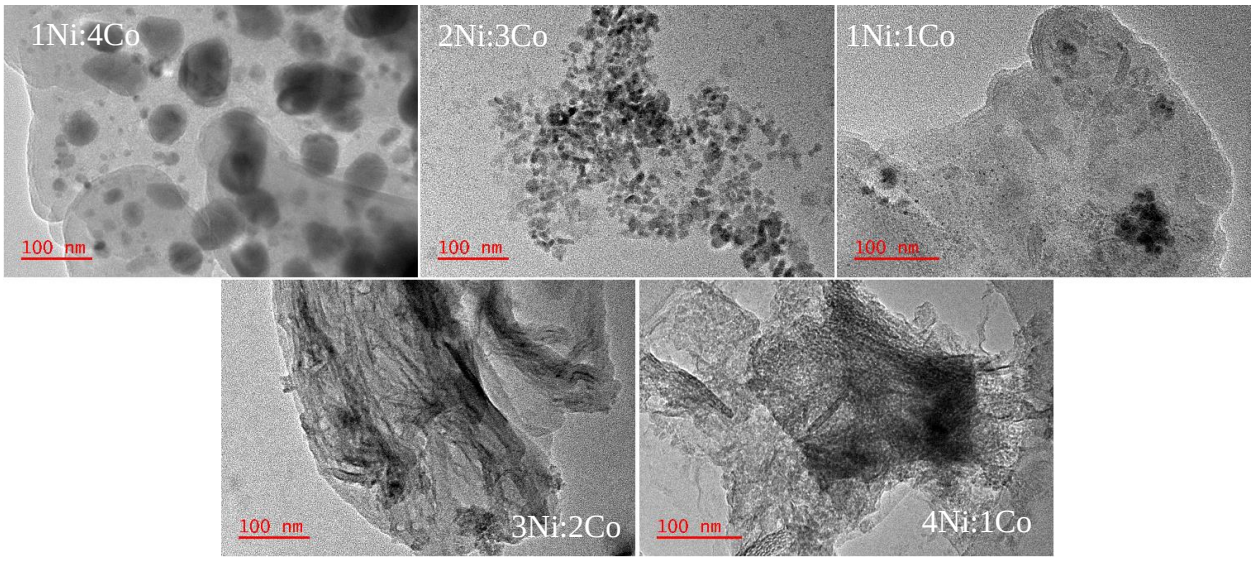


Figure 3.5: Transmission Electron Micrographs of the catalysts

The Transmission Electron Micrographs obtained from the characterization of the intrinsic morphological properties of the catalysts are presented in Figure 3.5 above. The catalysts show well dispersed small particles on the Al_2O_3 support. The particles however exhibited to be more agglomerative with increasing Co dominance in the catalyst composition ratio, as can be seen from the increasing size of the dispersed particles on the alumina support. This suggests that Co is more coagulative than Ni, thus Ni is likely to have more surface area hence more contact with the reactants compared to Co. As such, the influence of the Ni component of the catalyst was probably realized more than that of Co. On the other hand, dark cloud-like appearances that seemed to be increasing in size, with increasing Ni loading were observed. This could have been the ash that was generated during the calcination process, probably due to the relatively small agglomerates formed by Ni. If so is the case, then the effects of the Ni component in the catalyst was limited, especially for the higher Ni loadings. Despite the varying agglomeration sizes with varying Ni/Co ratios, all the catalysts do exhibit the same morphology. It is expected therefore, for the highest influence of the catalyst to have been realized for catalyst 1Ni:1Co since it had the least observable coagulation and ash content, which resembled some form of thermal decomposition of the catalyst.

3.3.4 Catalyst Surface Properties

As aforementioned, nitrogen adsorption-desorption was employed to investigate the specific surface area, pore volume, and the pore-size distribution of the five catalysts at 77.3K using a

Micromeritics Tristar 3000 surface area and porosity analyser (V6.05). The obtained adsorption-desorption isotherms for the catalysts are illustrated in Figure 3.6 below.

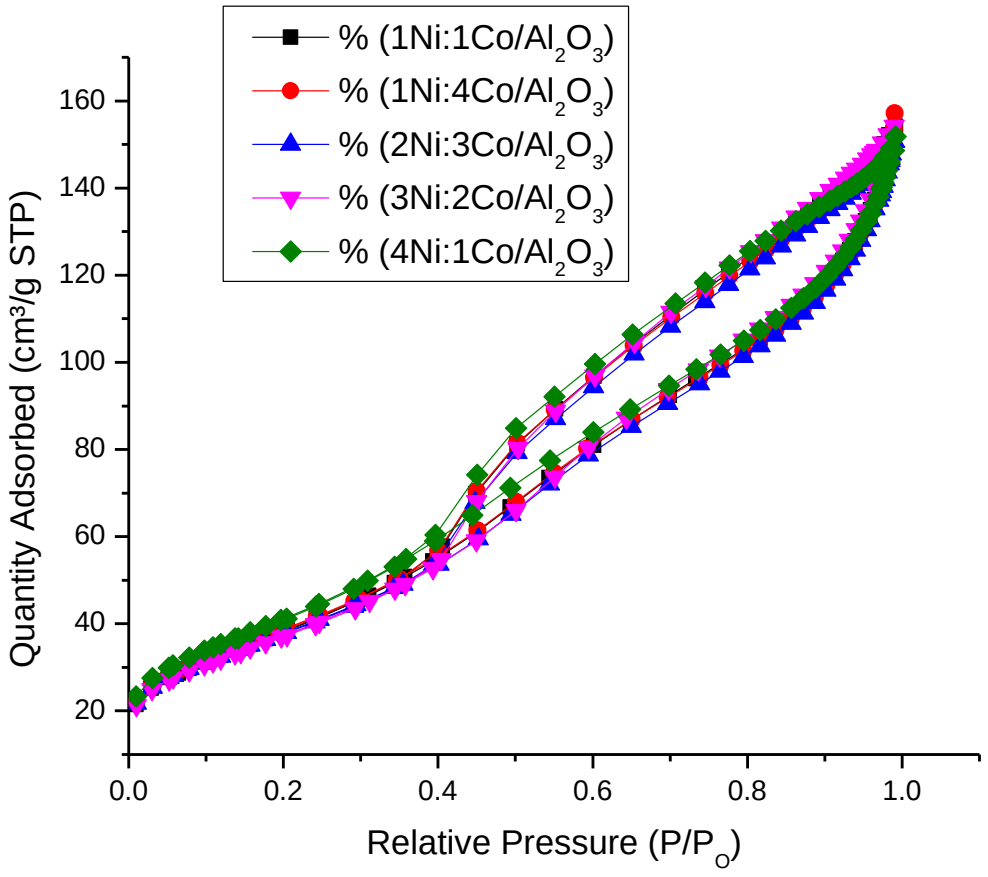


Figure 3.6: N_2 adsorption–desorption isotherms of $NiCo/Al_2O_3$ catalysts

Generally all the five catalysts exhibited type IV adsorption-desorption isotherms with H4 hysteresis loop within the same Relative Pressure (P/P_o) range (0.4-1.0); this is characteristic of mesoporous structures. This observation is consistent with that of Hari and Yaakob, (2015) as reported in literature for their 10 wt.% Ni and 10 wt.% Co bimetallic catalyst on γ-Al_2O_3 support. Pure Al_2O_3 is also reported to follow the type IV isotherm with a hysteresis loop, according to the International Union of Pure and Applied Chemistry (IUPAC) classification scheme for mesoporous material (Trisunaryanti *et al.*, 2019). Based on this observation, it can be assumed that the variable active metal loading ratios had negligible effects, if any at all, on the structure of the

Al_2O_3 support. This assumption can be cemented by the pore diameter distribution relative to the pore area and pore volume as analyzed by the *Barrett-Joyner-Halenda* (BJH) model depicted in Figures 3.7 and 3.8, respectively. The high and narrow peaks formed around 5nm are indicative of a largely homogeneous pore diameter distribution for the five catalysts, as would be expected for a pure material.

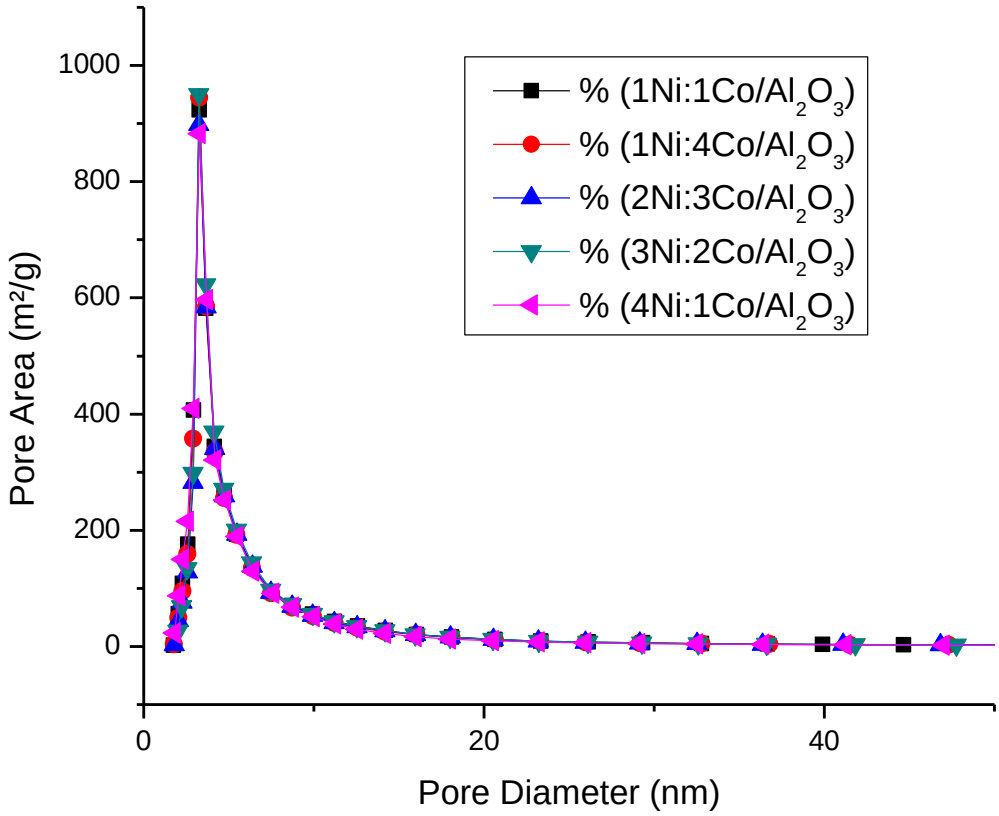


Figure 3.7: BJH Desorption dA/dlog(D) Pore Area

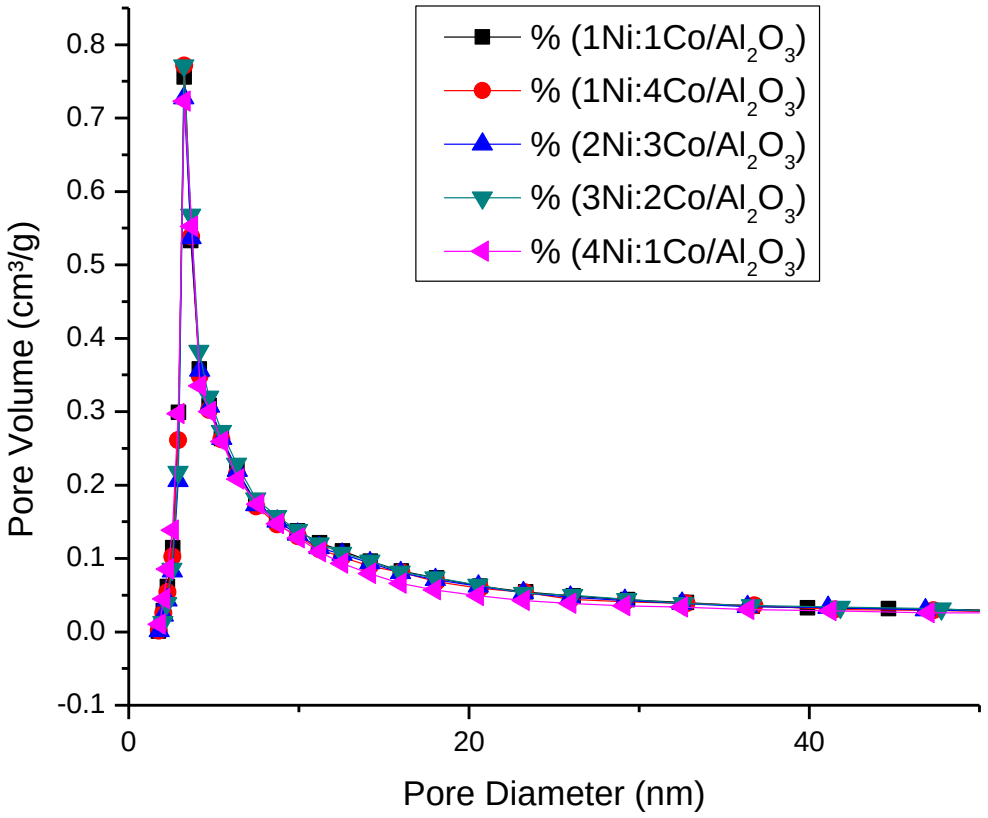


Figure 3.8: BJH Desorption dV/dlog(D) Pore Volume

Catalytic activity is also enhanced by increasing the surface area of a catalyst, this is due to the increment in contact area with the reactants that comes with increasing surface area. The average surface area and pore size distribution of the catalysts presented in Table 3.3 is a further testament to the absence of an observable influence of the catalyst loading ratios on its physical properties. This therefore suggests that the differences that may exist in the deoxygenation catalytic activity of the catalysts may be due to reasons other than their surface areas and pore size distribution.

Table 3.6: Surface area, pore volume and pore size of the $NiCo/Al_2O_3$ catalysts

Catalyst	**BET Surface Area (m^2/g)**	**Pore Volume (cm^3/g)**	**Pore Size (nm)**
1Ni:1Co/Al_2O_3	140.6	0.24	5.1
1Ni:4Co/Al_2O_3	141.8	0.25	5.2

2Ni:3Co/Al_2O_3	138.1	0.23	5.1
3Ni/2Co/Al_2O_3	136.8	0.24	5.1
4Ni/1Co/Al_2O_3	151.2	0.24	4.8

3.4 Conclusions and Recommendations

The co-impregnation method is a quick and simple method of loading the active metals onto the catalyst support material, however it has limitations in the control of the dispersion of the metals across the catalyst support matrix. Similar functional groups and phases were observed for the catalysts of different metal loading ratios, nevertheless the peak intensities are proportional to the relative abundance of the respective active metals. Ni and Co phases were not visible on the diffractograms obtained, probably due to their low concentrations on the support. The variable metal loading ratios had negligible effect on the surface area and pore size of the catalyst support, therefore the differences that may exist in the deoxygenation catalytic activity of the catalysts may be due to reasons other than their surface areas and pore size distribution.

Chapter 4: Deoxygenation of Waste Cooking Oil for Bio-Energy Production

4.1 Introduction

This chapter entails the deoxygenation and characterization procedures for the waste cooking oil followed in this project, the results are presented and discussed on the influence of catalyst metal composition ratios, catalyst loading, reaction temperature and duration on DO activity. Design Expert® also, was employed in the designing of the deoxygenation experiments and analysis of the results in order to pave way for its optimization function which is discussed in chapter 5. Conclusions and recommendations are given at the end of this chapter based on the discussion of the presented results, relative to previous similar studies in literature.

4.2 Experimental Procedure

This section outlines the steps taken in the deoxygenation of the waste cooking oil as well as the characterization of the products thereof. It also sheds light on how the level of deoxygenation was ascertained in the DO products.

4.2.1 Deoxygenation (DO)

A semi-batch reactor configuration presented diagrammatically in Figure 4.1 and pictorially in Figures C1 and C2 in the appendices as used for all the DO reactions in this work. A typical DO run entailed the following procedure: i. 100ml of the WCO was added into the reaction vessel; ii. The catalyst was then added into the oil while already stirring at level 6 setting on the magnetic stirrer *(to prevent the catalyst from settling at the bottom of the flask)*; iii. The reactor was sealed using parafilm to prevent atmospheric air ingress and the escape the gaseous reaction products and unreacted hydrogen gas; iv. Nitrogen purging then followed in order to create an inert environment in the reactor while raising the temperature from ambient to 5°C above the desired reaction temperature *(to cater for heat lost to the air from the reaction vessel)*; v. Upon reaching the desired reaction temperature, N_2 was stopped and H_2 was switched on; vi. The reaction duration lasted from the time H_2 input was started to the desired reaction time under constant reaction conditions;

vii. The heating would be stopped upon attaining the desired reaction time while maintaining stirring and H_2 input *(to quicken the cooling of the deoxygenated oil)*; viii. N_2 switch-over from H_2 upon cooling down to 100°C *(to purge the unreacted hydrogen while fast tracking cooling to room temperature)*; ix. The deoxygenated oil was unloaded from the reaction vessel and filtratered for removal of suspended particles; x. A sample of the deoxygenated oil was diluted with n-Hexane (Sigma Aldrich) for viscosity reduction to ease its GC-MS characterization. Important to note also is that the inlet pressure of the gases into the reaction vessel was always kept at 200kPa.

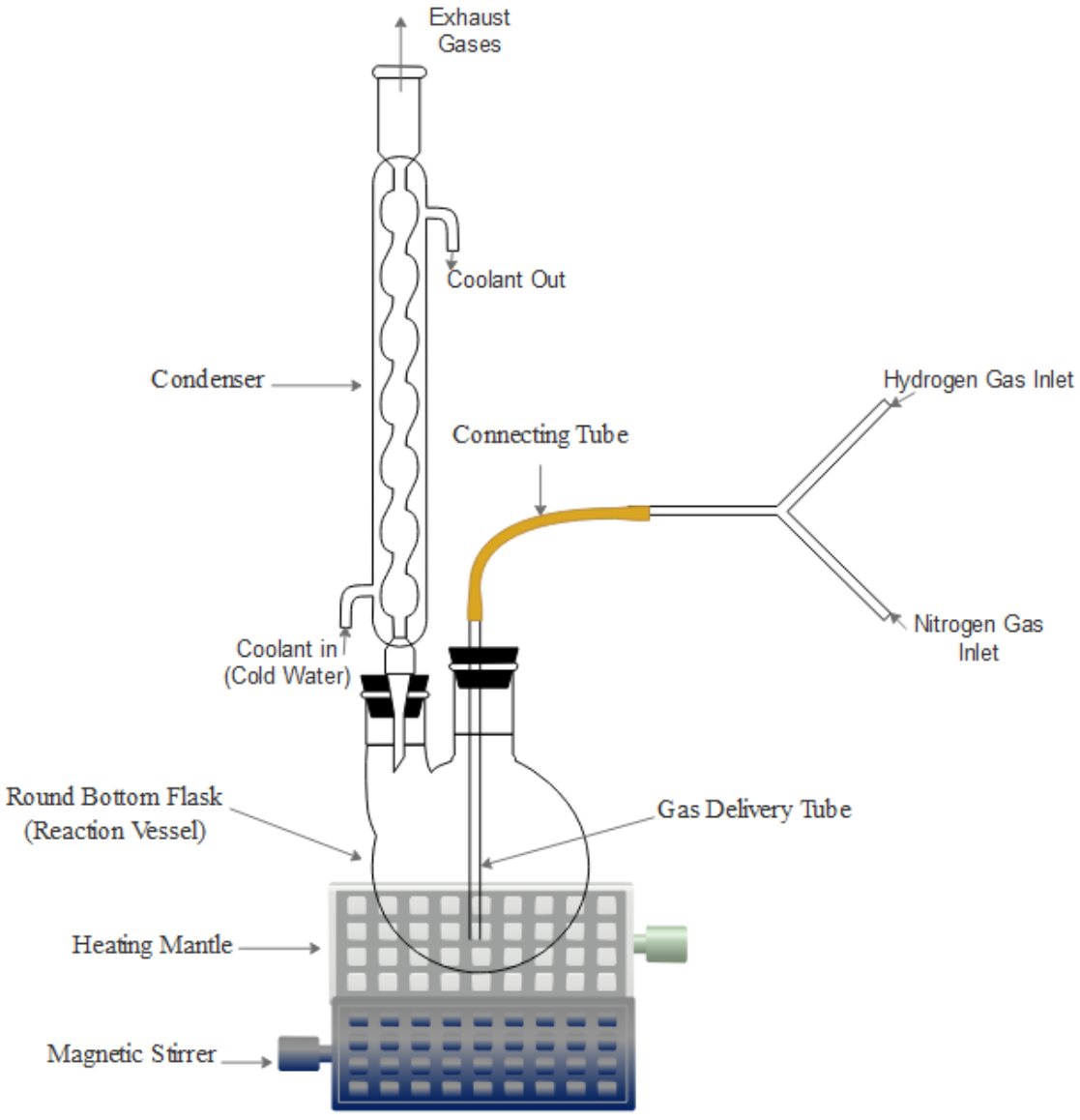


Figure 4.1: Deoxygenation apparatus setup

The above procedure was employed for the deoxygenation of used waste cooking oil obtained from Sizzlers Restaurant at the Matrix building within the University of the Witwatersrand, Braamfontein Campus, under the parameters presented in Table 4.1 below.

Table 4.1: Waste cooking oil deoxygenation parameters

Run	Catalyst	Temperature (°C)	Time (hours)	Catalyst Loading (wt.%)
1	1Ni:4Co	300	2.5	1
2	2Ni:3Co	300	2.5	1
3	1Ni:1Co	300	2.5	1
4	3Ni:2Co	300	2.5	1
5	4Ni:1Co	300	2.5	1
6	1Ni:1Co	300	3	1
7	3Ni:2Co	300	3	1
8	1Ni:1Co	300	3.5	1
9	3Ni:2Co	300	3.5	1
10	1Ni:1Co	300	4	1
11	3Ni:2Co	300	4	1
12	1Ni:1Co	300	4.5	1
13	3Ni:2Co	300	4.5	1
14	1Ni:1Co	300	5	1
15	3Ni:2Co	300	5	1
16	1Ni:1Co	278.4	4	1.25
17	1Ni:1Co	244.4	5.5	1
18	1Ni:1Co	240	4	0.5
19	1Ni:1Co	273.6	2.5	0.75
20	1Ni:1Co	320	5.5	1.25
21	1Ni:1Co	271.2	4	0.75
22	1Ni:1Co	240	2.5	1.25
23	1Ni:1Co	274.8	5.5	1.25
24	1Ni:1Co	297.2	3.25	1
25	1Ni:1Co	316.8	4	0.75

26	1Ni:1Co	320	2.5	1.25
27	1Ni:1Co	240	4	1
28	1Ni:1Co	292	5.5	0.5
29	1Ni:1Co	250	5.5	0.5
30	1Ni:1Co	320	2.5	0.5
31	1Ni:1Co	300	5	0.75
32	1Ni:1Co	300	5	1.25

Runs 1-5 were done to investigate the influence of the catalyst active metal ratios on their deoxygenation selectivity, as a follow-up to findings in Chapter 3. As will be discussed in the results and discussion section, runs 6-15 were further screening runs for catalysts 1Ni:1Co and 3Ni:2Co since they had initially exhibited comparable DO selectivities, albeit this gave useful data for the investigation of the influence of reaction time on WCO deoxygenation. Runs 16-30 were designed by Design Expert® which varied the three reaction parameters concurrently, i.e. the reaction temperature, duration and amount of catalyst in the reaction vessel per run. Finally, runs 31 and 32 were done to cement the investigation of the influence of catalyst loading/amount on the deoxygenation of the waste cooking oil.

4.2.2 Characterization of the DO Products

The deoxygenated oil was characterized by a GC-MS/FID (QP2010 Ultra, Shimadzu Corporation, Kyoto, Japan) equipped with an autosampler AOC-20i (Shimadzu). Separations were accomplished using a Rtx®-5MS Restek fused silica capillary column of 30m length × 0.25mm internal diameter, 0.25mm film thickness, at a constant helium (99.999%) flow rate of 1.2 ml/minute. Sample injection volumes of 0.5 µl were employed, with a split ratio of 1:10. The oven temperature was programmed from 50°C (isothermal for 1.5 minutes), with an increase of 4°C/minute, to 200°C, then 10°C/minute to 250°C, ending with a 5 minutes isothermal at 250°C. The MS and FID data were simultaneously acquired employing a Detector Splitting System; the split flow ratio was 4:1 (MS:FID). A 0.62 m length x 0.15 mm internal diameter restrictor tube (capillary column) was used to connect the splitter to the MS detector; a 0.74 m length x 0.22 mm internal diameter restrictor tube was used to connect the splitter to the FID detector. The MS data (total ion chromatogram, TIC) were acquired in the full scan mode (m/z 40–350) at a scan rate of

0.3 scan/s using the electron ionization (EI) with an electron energy of 70 eV. The injector temperature was 250°C and the ion-source temperature was 250°C. The FID temperature was set to 250°C, and the gas supplies for the FID were hydrogen, air, and helium at flow rates of 30, 300, and 30 ml/minute, respectively. The deoxygenation extent in the oil and selectivity of its various constituents was derived from the GC-MS data. Equations 4.1 and 4.2 below were employed for calculating the oxygen content and the extent of deoxygenation, respectively, from the GC-MS data. Similar approaches have been used in literature by Oh *et al.*, (2017) and Pham *et al.*, (2019).

Equation 4.6

$$Total\ Oxygen\ Content = \sum \left(\frac{15.999n}{M} \times Percentage\ Composition \right)$$

Where n is the total number of oxygen atoms per oil constituent; and M is the molar mass of the oil constituent.

Equation 4.7

$$Deoxygenation\ (\%) = \frac{O_2\%\ in\ original\ oil - O_2\%\ in\ deoxygenated\ oil}{O_2\%\ in\ original\ oil} \times 100\%$$

4.3 Results and Discussion

In this section the results from the deoxygenation of WCO are presented and discussed. The influence of the parameters that were varied during the deoxygenation experimental studies is extrapolated from the results in the discussion while drawing comparisons from preceding studies in literature. The waste cooking oil before deoxygenation consisted largely of triglycerides and a significant portion of free fatty acids. The fatty acids distribution in the WCO is presented in Table 4.2. The deoxygenation reactions yielded two main categories of organic liquid products, i.e. hydrocarbons and oxygenates, the latter being made up of reaction intermediates such as fatty alcohols, acids and esters, as well as ketones and aldehydes.

Table 4:2: Fatty Acids Distribution of Waste Cooking Oil

Fatty Acid	Chemical Formula	Concentration (%)
Oleic Acid (C18:1)	$C_{18}H_{34}O_2$	39.4
Linoleic Acid (18:2)	$C_{18}H_{32}O_2$	44.6
Palmitic Acid (C16:0)	$C_{16}H_{32}O_2$	8.9

Stearic Acid (C18:0)	$C_{18}H_{36}O_2$	7.1

4.3.1 Influence of catalyst metal loading on DO activity

Catalyst performance is a function of its composition, preparation procedure, and the reaction conditions (Sahu *et al.*, 2015). The five catalysts of varying Ni/Co ratios were used to catalyze the deoxygenation of waste cooking oil under similar conditions i.e. 2.5 hours reaction time, 1 wt.% loading, at 300°C, under 200kPa H_2; for investigating the influence of catalyst composition on its DO catalytic activity. As can be seen in Figure 4.2 below, catalyst 1Ni:1Co demonstrated the highest deoxygenation catalytic activity (58.5%) compared to the other four catalysts. The lowest deoxygenation activity (14.6%) on the other hand was realized for catalyst 2Ni:3Co, and this may have suggested it to be having the least deoxygenation selectivity amongst the five catalysts.

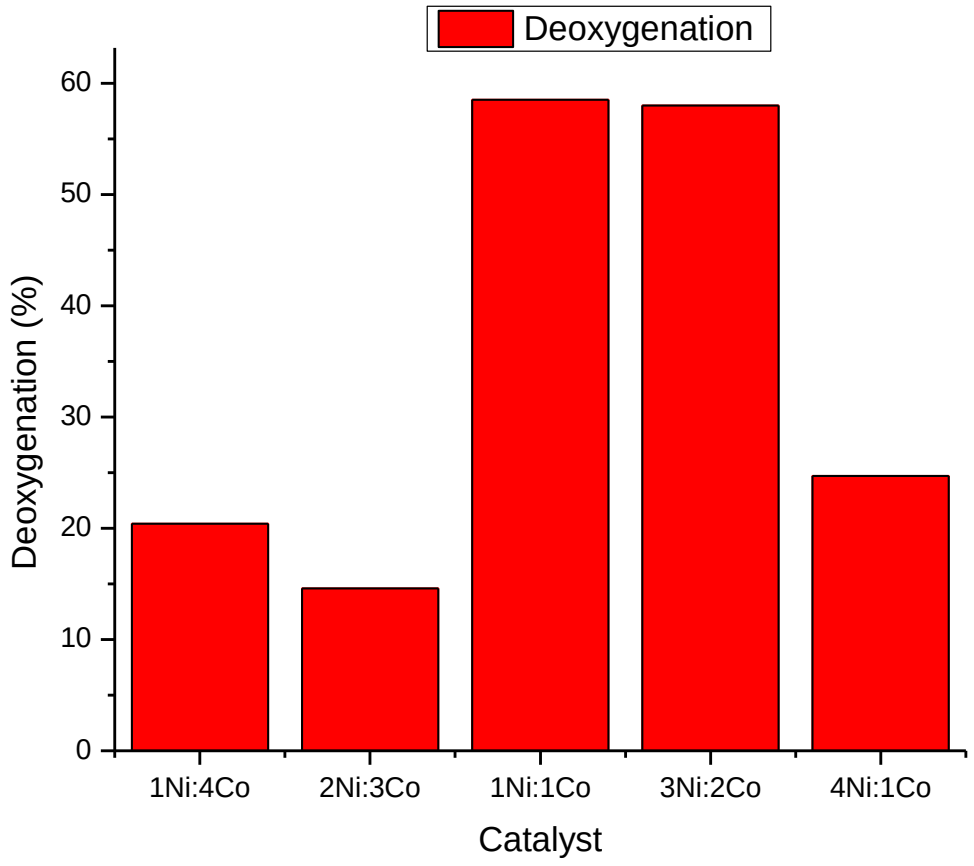


Figure 4.2: Deoxygenation with respect to catalyst composition

It is noted that the highest deoxygenation of the WCO was realized for the catalyst with equivalent proportions of Ni and Co. This observation insinuates some form of synergy in catalytic activity of the active metals, Ni and Co, which is higher than when there is a large margin between the proportions of either metals. This is consistent with the suggestions in literature that Ni bimetallic catalysts have more catalytic activity for deoxygenation than its monometallic catalysts on a suitable support (Rogers and Zheng, 2016). Catalyst 3Ni:2Co realized a competitive oxygen reduction (58%) to the highest realized under similar conditions, it can be assumed therefore that the optimum catalyst composition ratio for Ni and Co under the deoxygenation conditions used is between 1Ni:1Co and 3Ni:2Co. Furthermore, it was observed that the catalysts whose composition was dominated by Ni relative to Co generally exhibited greater deoxygenation catalytic activity compared to the Co-dominated ones. Based on this observation, it may then be assumed that Ni has better deoxygenation catalytic activity than that of Co under the reaction conditions used. Zhang, Lin and Zheng, (2014) investigated the inherent influence of unsupported nickel and cobalt on the main deoxygenation routes and discovered that Ni-promoted catalyst have higher selectivity for the hydrodeoxygenation reaction over the other pathways, whereas the Co-promoted catalyst exhibited hydrodecarbonylation preference. This therefore suggests that HDO was the prevalent mechanism through which the deoxygenation of WCO occurred, and is congruent with expectation, since the hydrogen atmosphere in which the reaction underwent favors HDO and is inhibitory to the DCX pathway. The DCN pathway is reported in literature to be accompanying HDO as a complementary pathway, whereby the aldehydes and ketones aldehydes deoxygenation intermediates are further deoxygenated by the scission of the C–C bond, to liberate CO (Rogers and Zheng, 2016).

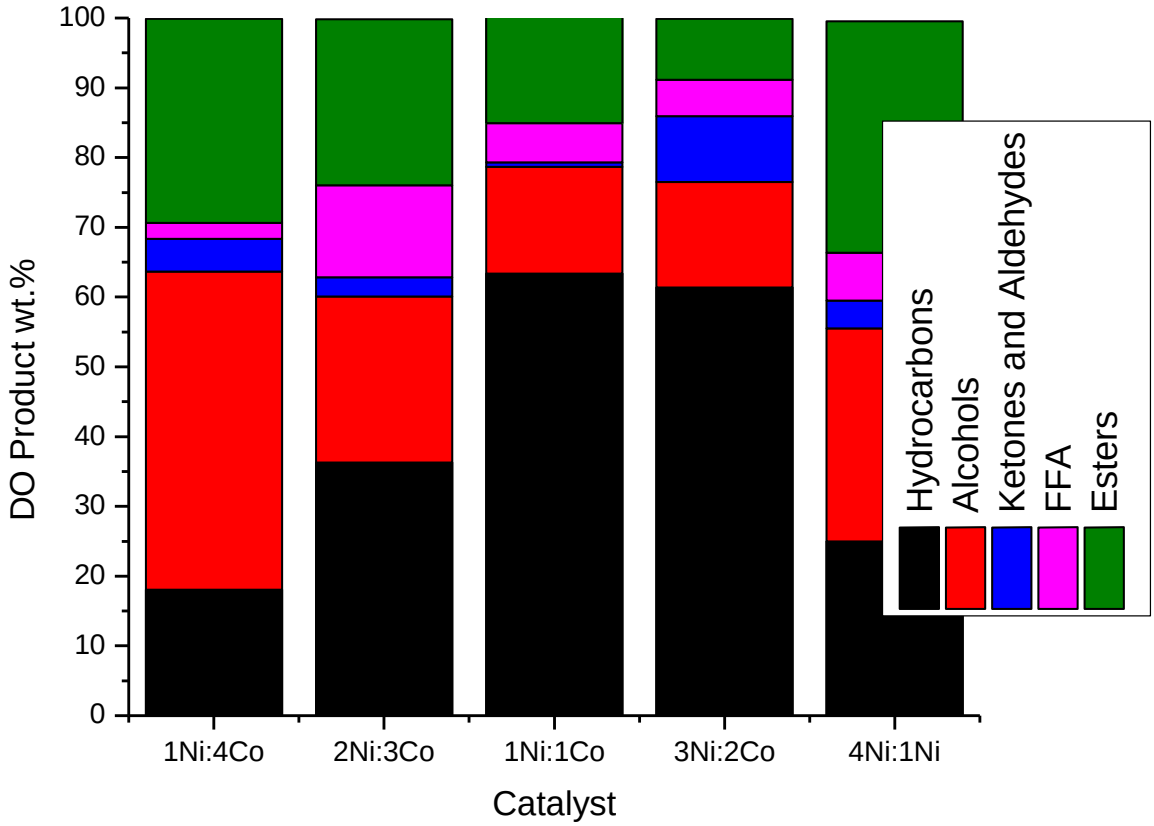


Figure 4 3: Functional group selectivity with respect to catalyst composition

The selectivity of the ultimate deoxygenation products, i.e. hydrocarbons (Figure 4.3), followed a similar trend to that of deoxygenation except that catalyst 2Ni:3Co realized higher hydrocarbons selectivity than those of catalysts 4Ni:1Co and 1Ni:4Co, notwithstanding that its DO catalytic activity was the least of the five catalysts. This observation is validated by the higher selectivity of fatty alcohols for the catalysts 4Ni:1Co and 1Ni:4Co than that of catalyst 2Ni:3Co, and supports the submissions in literature by Kubic, (2010), that fatty alcohols are intermediate products of the deoxygenation of triglycerides. The formation of alcohols, ketones and aldehydes as intermediate products may have been preceded by the formation of fatty acids from the triglycerides and followed by the formation of the hydrocarbons. According to Rogers and Zheng, (2016), the complete decomposition of triglycerides into fatty acids requires hydrogen, this insinuates that hydrogenolysis was inevitably involved in the dissociation of the triglycerides in the WCO into fatty acids, producing propane as a byproduct. The general dominance of fatty alcohols over other

intermediate products with C=O bonds across all the catalysts and lack of an observable trend of the catalysts' selectivity for fatty acids suggest a strong hydrogenation function of the catalyst support. Since the role of the catalyst support is to dissociate the hydrogen molecules into free radicals, the resultant abundance of hydrogen free radicals due to the catalyst support may have easily skewed the reaction selectivity towards hydrogenation (Pattanaik and Misra, 2017; Nekhavhambe, Mukaya and Nkazi, 2019). This assumption concurs with reports in literature that the Lewis acid sites on Al_2O_3 support increases its selectivity for the hydrogenation and dehydration reactions, which resultantly enhances the HDO pathway (Zhang, Lin and Zheng, 2014; Hari and Yaakob, 2015). It can then be deduced that the formation of the fatty alcohols from fatty acids occurred through hydrogenolysis to produce water as a by-product, and this is a characteristic of the HDO pathway. It is also a possibility that the hydrogenation of fatty acids occurred through the hydrogenation of the hydroxyl group, to produce water, aldehydes, and ketones, which may have followed indirect decarbonylation in the event of a C–C bond scission to produce hydrocarbons with one less carbon atom than the initial fatty acid (Rogers and Zheng, 2016; Ng *et al.*, 2017). However, the minimum presence of aldehydes and ketones relative to other deoxygenation intermediates across all the five catalysts maintains that HDO was the main DO pathway through which the deoxygenation of seed oil was achieved. The successive formation of the hydrocarbons could then have been realized by either the decarbonylation or hydrodeoxygenation of the intermediate products through the cleavage of the C–C bond or C–O, respectively. Since Oleic and Linoleic acids are the dominant constituents of the waste cooking oil, as presented in Table 4.2, the proposed DO mechanisms are given based on their respective triglycerides in Figure 4.4 below.

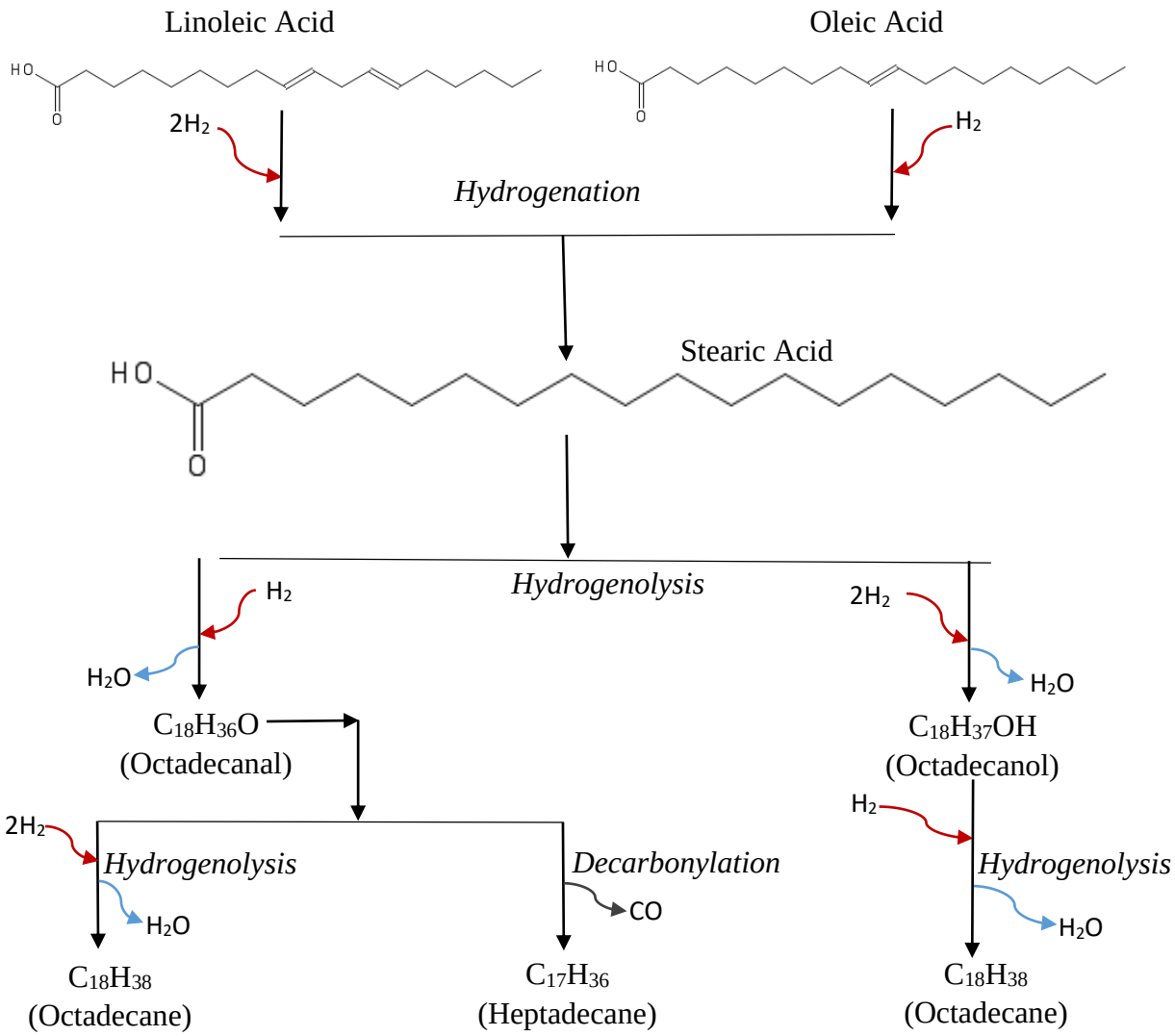


Figure 4 4: Proposed DO mechanisms of Linoleic Acid and Oleic Acid

The mechanisms propose that the deoxygenation of triglycerides occurred through a series of hydrogenation and hydrogenolysis reactions, which was also accompanied indirect decarbonylation. Similar mechanisms are also reported in literature (Fu, Lu and Savage, 2011; Ayodele, 2017; Janampelli and Darbha, 2019). On the other hand, the presence of alkyl esters in the products implies that esterification side reactions between the deoxygenation intermediates, fatty acids and fatty alcohols, could have occurred during the deoxygenation of the WCO. The likelihood of the occurrence of esterification reactions is high given the conditions under which the deoxygenation reactions were conducted, the temperature used (300°C) is above the supercritical temperature of most alcohols, and this is conducive for the occurrence of supercritical

non-catalytic esterification (Mujeeb, Vedamurthy and T, 2016; Stephen and Periyasamy, 2018). Esterification reactions between fatty acids and alcohols are also reported in literature as competing with deoxygenation reactions during the deoxygenation of rapeseed oil over a sulphided $NiMo/Al_2O_3$ catalyst (Kubic, 2010). Accordingly, the observed general increase in the oil viscosity after deoxygenation for all the catalysts may have been induced by the presence of alkyl esters in the deoxygenated oil. If the assumption for the occurrence of esterification side reactions is true during the deoxygenation process, the higher fatty acid alkyl esters' selectivity exhibited by catalysts 1Ni:4Co and 4Ni:1Co relative to that of hydrocarbons could suggest that the esterification reactions were more pronounced for them than the other catalysts. Be that as it may, a drop in ester constitution and an increase in hydrocarbons composition was noted for all the five catalysts relative to the original waste cooking oil composition, this is testament that the DO reactions were occurring faster than esterification.

The high and comparable catalytic activity for DO of catalysts 1Ni:1Co and 3Ni:2Co prompted further catalyst screening runs, with the intention of continuing with the best performing catalyst for the optimization of the deoxygenation of WCO. Reaction temperature and catalyst loading was kept constant at 300°C and 1wt.%, respectively, while varying the reaction duration up to 5 hours, at 30 minute intervals. The attained results are presented in appendix C3. Catalyst 1Ni:1Co exhibited superior overall deoxygenation catalytic behavior compared to catalyst 3Ni:2Co. Moreover, catalyst 1Ni:1Co had higher hydrocarbons selectivity while catalyst 3Ni:2Co showed higher selectivity for the DO intermediates, i.e. the ketones, alcohols, aldehydes, FFA and esters. This may suggest that, in the case of higher esters selectivity, esterification reactions between the fatty acids and alcohols may have been happening faster than the deoxygenation reactions of the DO intermediates for catalyst 3Ni:2Co.

4.3.2 Influence of reaction time on DO activity

The determination of the relationship between reaction time and deoxygenation was done using the results from the screening runs of catalysts 1Ni:1Co and 3Ni:2Co as well as the design expert analysis. During the screening runs, reaction time was varied from 2.5 to 5 hours for the same catalyst loading (1 wt.%), reaction temperature (300°C) and hydrogen pressure (200kPa), however, since catalyst 1Ni:1Co proved to be the better catalyst, its results were used for this investigation. Figures 4.5 and 4.6 depict the design expert curve for catalyst 1Ni:1Co runs, with

respect to reaction time, and the deoxygenation response to the varying reaction durations during the catalyst screening, respectively.

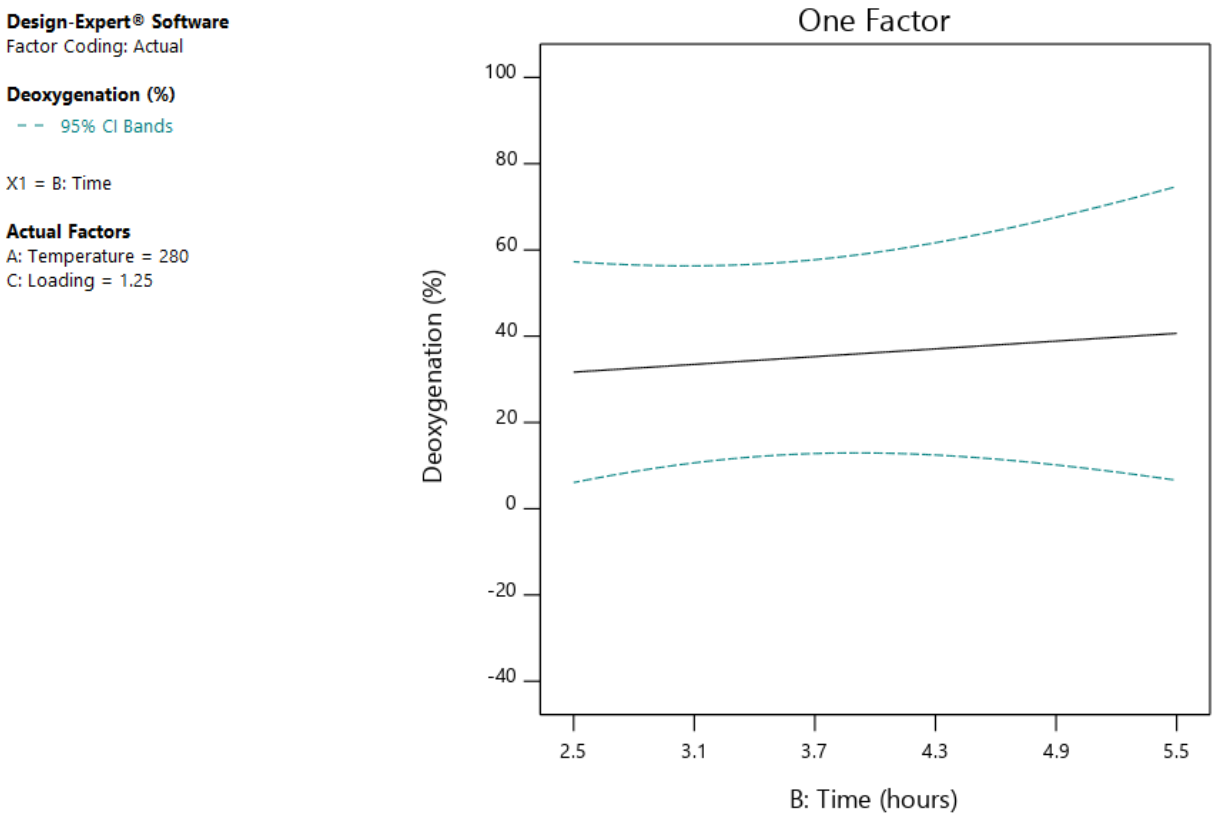


Figure 4.5: Deoxygenation response to reaction time

A general increment in DO activity was noted with longer reaction duration for the screening runs. This is in agreement with the analysis from design expert which also registers a steady increase in DO with time, the linear relationship being the response to the first order optimization model used, as will be explained in Chapter 5. Generally, higher hydrocarbon yields were realized with increased DO time, in other words, deoxygenation increases with reaction time (Meller *et al.*, 2014; Pham *et al.*, 2019). This could be because the large sizes fatty acid chains and the presence of C=O bonds in the WCO requires large amounts of energy for their scission in order to eliminate the oxygen.

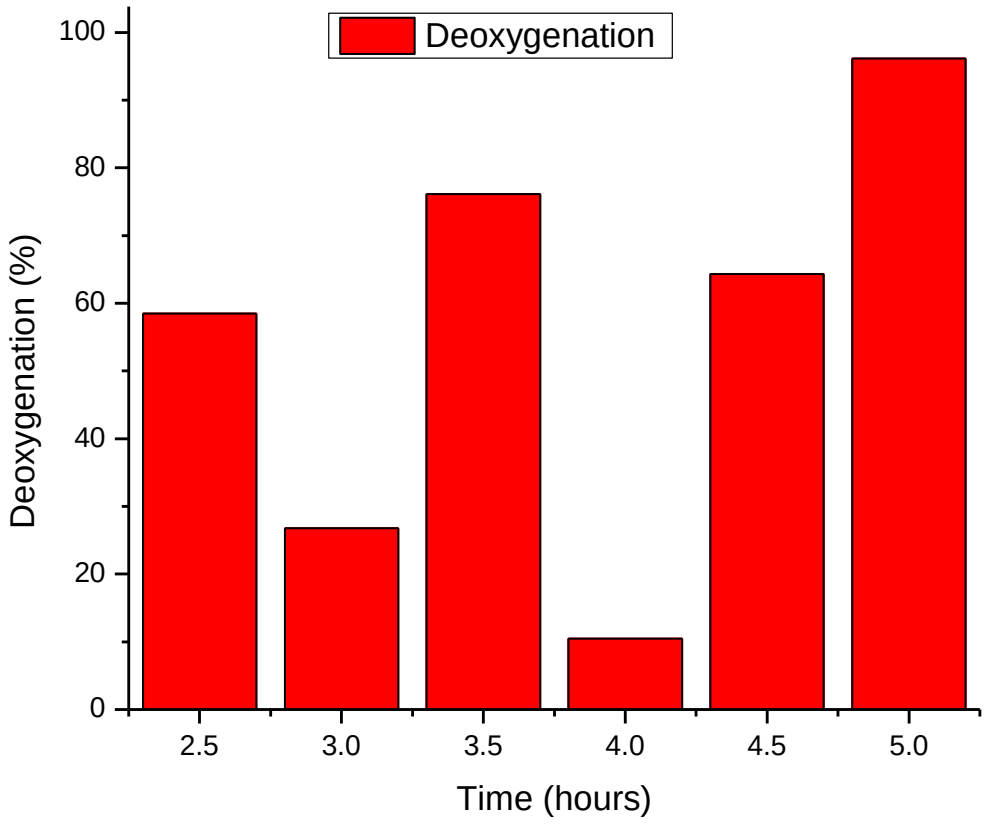


Figure 4.6: Deoxygenation relationship with reaction time

According to Figure 4.6, the catalyst remained active for up to 5 hours without observable deactivation under the reaction conditions used. A similar catalyst, $NiCo/Al_2O_3$ also exhibited constant activity during the hydrotreatment of Jatropha FAME to produce diesel range hydrocarbons, for up to 5 hours in a continuous-flow reaction set up (Hari and Yaakob, 2015). This makes impeccable sense given the reports in literature that H_2 maintains catalyst activity by inhibiting catalyst deactivation (Nguyen *et al.*, 2016; Munir, Irfan and Usman, 2018). Moreover, the production of coke was minimized, since HDO was the dominant reaction pathway through which the deoxygenation of WCO was realized. Also, CO and CO_2 are very unstable in the presence of H_2 as they tend to undergo the methanation reaction, especially given that the reaction conditions and the catalyst used are conducive for the reaction (Kumar *et al.*, 2014; Online *et al.*, 2015). It was also observed that the response of deoxygenation to time was undulating in nature, this is an anomaly whose cause calls for further investigation. Edeh, Overton and Bowra, (2019)

experienced a similar phenomenon during the hydrothermal deoxygenation of palmitic acid in the presence of Pd/C catalyst.

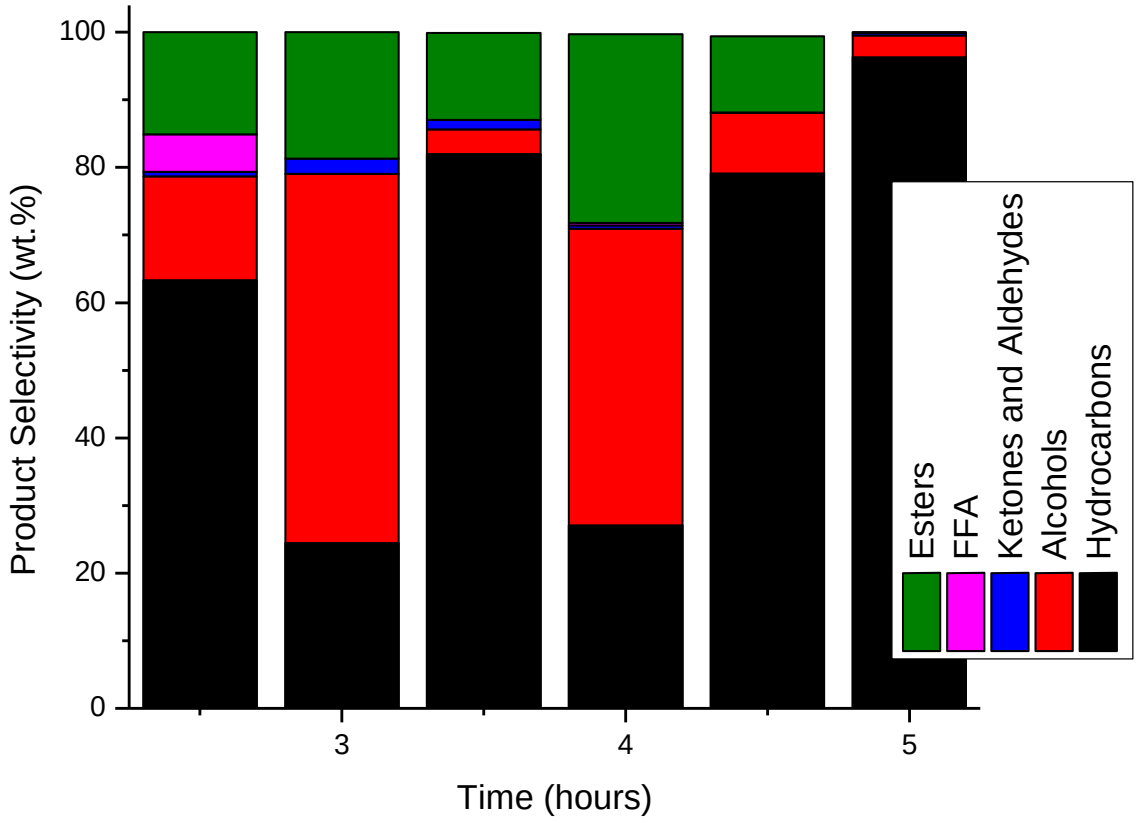


Figure 4.7: Functional group selectivity with respect to reaction time

The selectivity of hydrocarbons followed a closely similar trend to that of deoxygenation as expected (Figure 4.7). It can be noted that the complete conversion of the waste cooking oil into saturated hydrocarbons under the reaction conditions used required slightly more than 5 hours. However, the hydrocarbons yield for the 3-hour-long reaction was lower than that of the 4-hour reaction notwithstanding that the DO for the former was 16.34% more than that of the later. This may be explained by the realization that the higher deoxygenation that was attained at 3 hours produced more of alcohols, which are DO intermediate products, compared to the 4 hour reaction which produced more of the DO final products, hydrocarbons. The relatively high ester selectivity for the 3- and 4-hour reactions could be suggestive of a pronounced occurrence of the esterification

side reactions, as such, it can be assumed that at some point during the progression of the deoxygenation process there exists some equilibrium of some sort between the deoxygenation and the side reactions, which may in effect slow down the oxygen removal process. This if true, suggests that the catalyst's selectivity for DO may have been to a limited extend, as a result of the limited interaction of the catalyst with the reactants as will be discussed in the next section, and that the catalyst was not reduced in H_2 prior to the DO process. Also, the presence of C=C bonds in the fatty acids constituents could have promoted their oxidation with the oxygen released from the dissociation of the water molecule during the water gas shift reaction that has been reported to be one of the side reactions that accompany the deoxygenation of fatty acids (Hermida, Abdullah and Mohamed, 2015). This can be used to explain the observed undulating nature of the deoxygenation trend with time.

4.3.3 Influence of catalyst loading

The investigation of the influence of catalyst loading on the deoxygenation of WCO was done at varying loading levels whilst keeping all the other DO variables constant, i.e. at 300°C, 200kPa H_2 pressure, and 5 hours reaction time. Findings from this investigation (Figure 4.8) and those of the design expert analysis of all the DO runs (Figure 4.9) for catalyst 1Ni:1Co were used to explain the relationship between catalyst loading and deoxygenation.

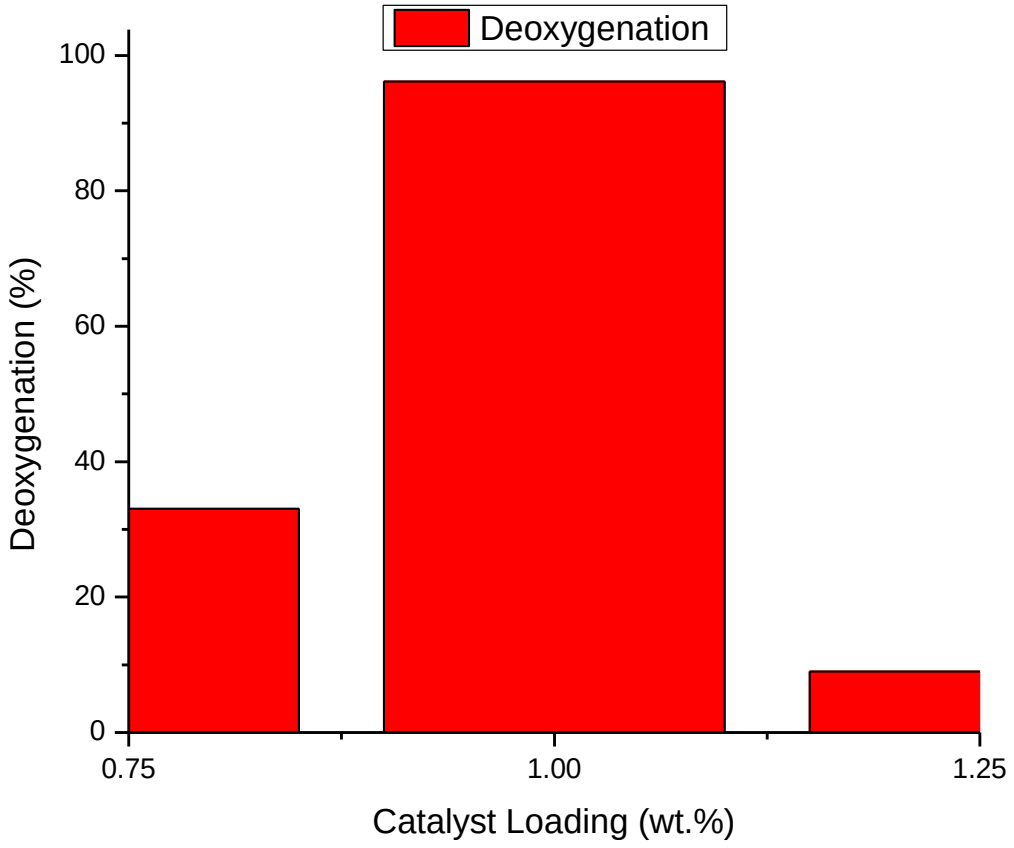


Figure 4 8: Effect of catalyst loading on deoxygenation

The optimum catalyst loading is 1wt.% for the conditions used, this is because the highest deoxygenation was realized at this loading. At catalyst loading of 0.5wt.% the deoxygenation could not be ascertained as the oil repeatedly formed a gel that could not dissolve in n-Hexane for the GCMS analysis, before reaching 5 hours reaction time. This reveals that low catalyst loadings suppress the hydrogenation of the oil constituents and their products, which in turn results in high yield of olefins, and these are susceptible to polymerization. However, the design expert analysis exhibited a constant positive deoxygenation for all the catalyst loading levels. This observation is against expectation, the level of deoxygenation would have been expected to increase with catalyst loading as the rate of hydrogen dissociation and hydrogenation is also dependent on the catalyst loading. Nonetheless, regardless of the continuous stirring during the deoxygenation process, most of the catalyst would settle at the bottom of the reaction vessel, and this suggests limited interaction of the catalyst with the reactants. This observation could be a vindication to the observed constant

deoxygenation response to the catalyst loading variations. The reasons for the settling of the catalyst at the bottom of the reaction vessel could include but are not limited to the following: i. The relatively large catalyst support particles (70-230 mesh) could not be efficiently dispersed in the undiluted oil, as would have been the case with nanoparticles; ii. The stirring may have generated some form of electrical charges on the catalyst particles which may have consequently led to their coagulation at the bottom of the flask.

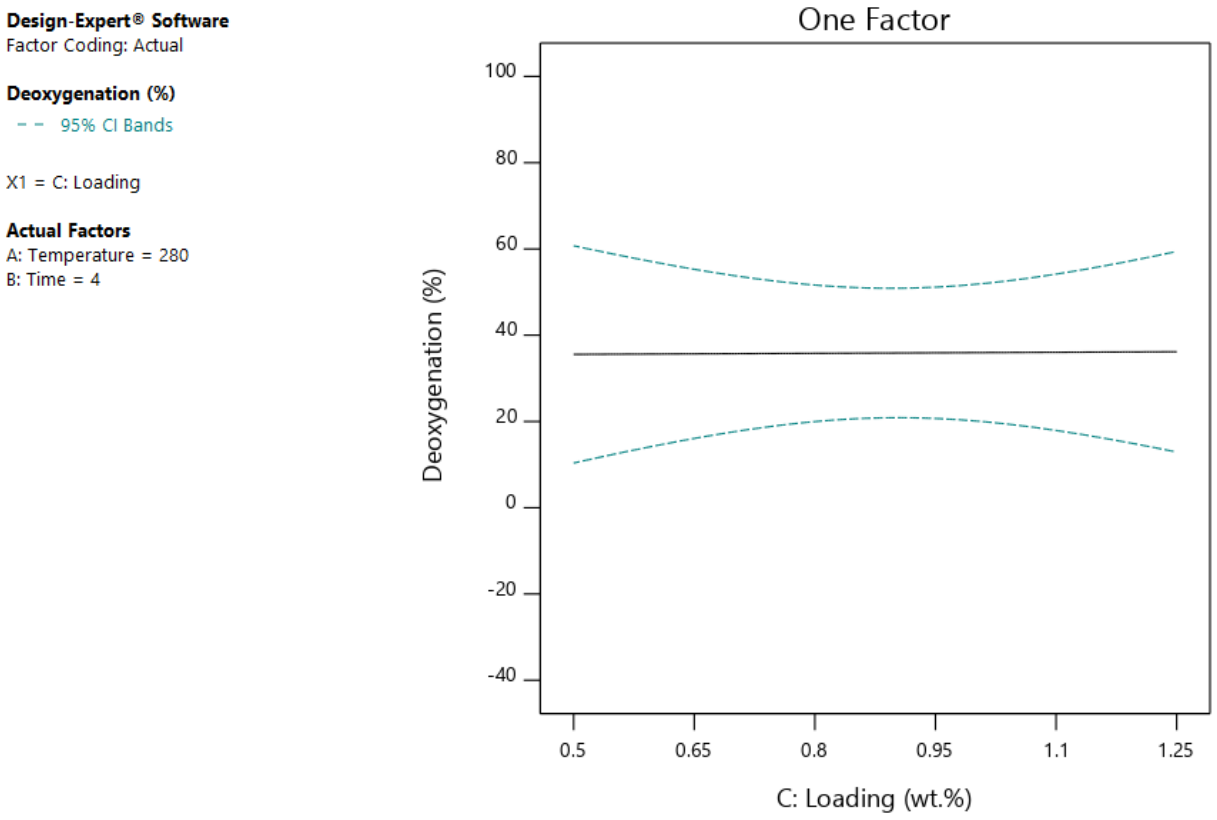


Figure 4 9: Relationship between catalyst loading and deoxygenation

Dilution of the waste cooking oil with a solvent could have improved on the dispersion of the catalyst in the oil by reducing its viscosity, thereby increasing the surface area for the interaction of the reactants with the catalyst. Solvent dilution of the oil has been reported several times in literature (Hari and Yaakob, 2015; Yoosuk *et al.*, 2019). However, since the reaction was carried out at atmospheric pressure, the use of the solvent would be futile because the boiling temperature for most solvents such as n-Heptane are very much below the reaction temperatures (plus or minus 300°C). Employing the catalyst thus in the form of nanoparticles could have greatly increased the reaction surface area through improved dispersion in the oil as well as the inherently large surface

area of nanoparticles relative to microparticles. The phenomenon of the generation of charges in the catalyst particles was also observed during the SEM analysis, and this necessitated the coating of the samples for proper analysis. The attrition of surfaces also, generally generates some static charges between the surfaces, and these could have been the cause for the coagulation at the bottom of the reaction vessel.

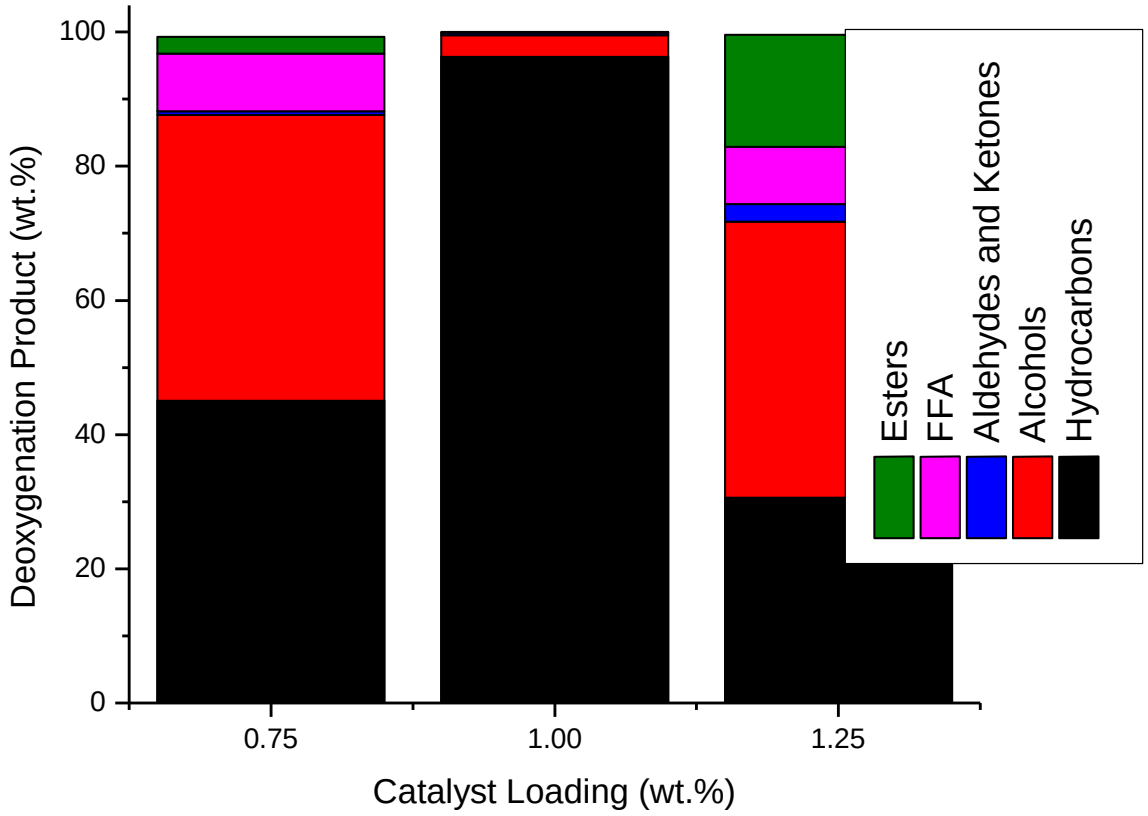


Figure 4 10: Functional group selectivity with catalyst loading

With regards to the product distribution as presented in Figure 4.10, a higher yield for fatty acids alkyl esters at 1.25wt.% than at 0.75wt.% could be suggestive of a significantly higher esterification rate at 1.25wt.% loading than the later. It can then be inferred that the excessive use of the catalysts promotes side reactions which may slow down the oxygen elimination reactions, or maybe reach an equilibrium with the deoxygenation reactions as discussed in the previous section.

4.3.4 Influence of reaction temperature

The reaction temperature is the primary means of controlling catalytic activity and product selectivity during the deoxygenation process (Dawes *et al.*, 2015). The relationship between temperature and deoxygenation was derived solely from the design expert analysis, this is because temperature, of all the other factors was varied as a continuous variable while others were treated as discrete variables. Also, temperature is the only model factor on the design expert model whose p-value is less than 0.05, as will be discussed in Chapter 5, meaning that there are minute chances of this analysis with respect to temperature to be inaccurate.

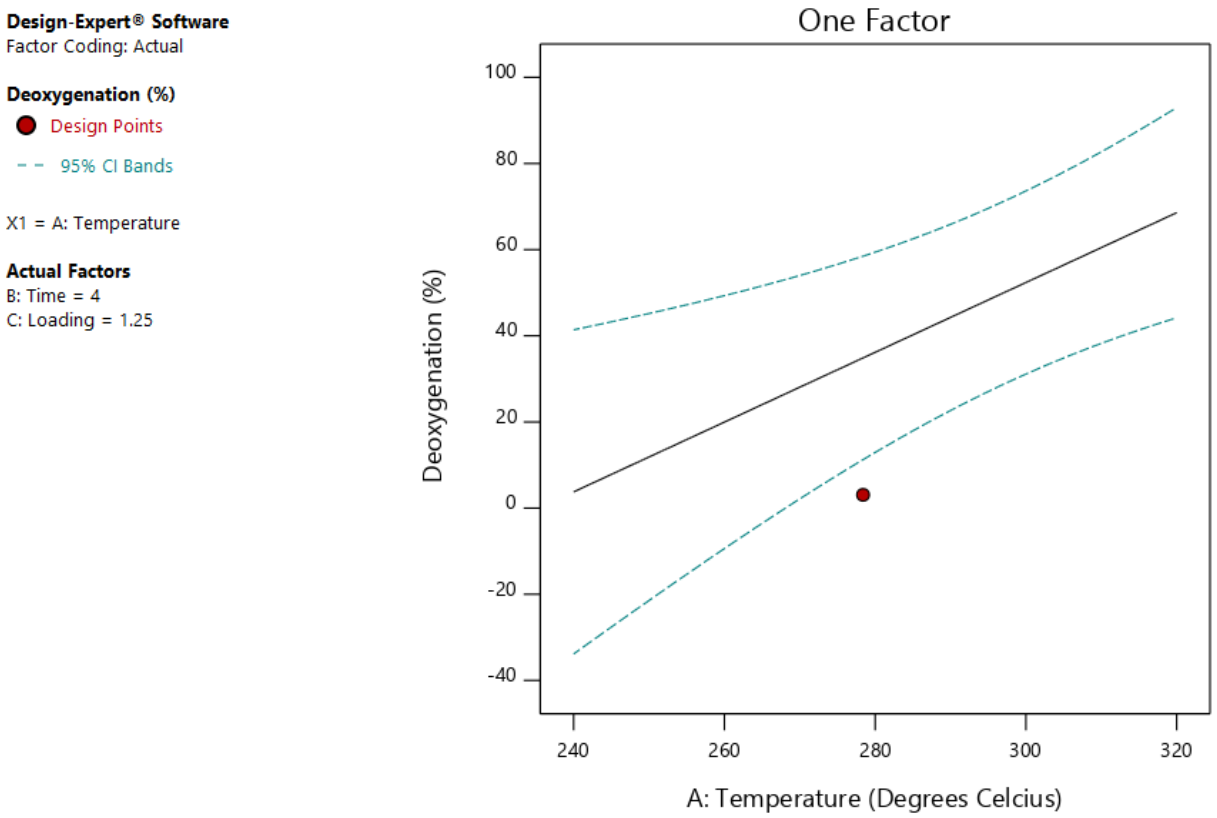


Figure 4 11: The relationship between deoxygenation and reaction temperature

It can be seen in Figure 4.11 that deoxygenation increases with reaction temperature, the linear relationship is in response to the linear model that was used for the analysis of the response with respect to the reaction variables under investigation. This observation of the increment of the hydrocarbon fraction, hence deoxygenation, with reaction temperature concurs with observations in literature for hydrotreatment processes of different oils (Meller *et al.*, 2014; Hari and Yaakob,

2015; Pham *et al.*, 2019). The observed phenomenon can be explained by the increase in the energy available for the cleavage of bonds with reaction temperature, which is also the reason for the increase in shorter hydrocarbon chains yields at higher reaction temperatures. Accordingly, the deoxygenation reactions at higher reaction temperatures will largely be aided by the thermal cracking reactions (which also become more pronounced at higher temperatures), hence the higher deoxygenation. Also, the higher oxygen reduction with higher temperatures could have been realized due the inverse variation of oil viscosity with temperature i.e., higher interaction surface area of the oil, catalyst and hydrogen gas would be realized due to the oil viscosity decay that accompanies higher temperatures (Cai *et al.*, 2015; Marx, 2016; Verma, Sharma and Dwivedi, 2016). However, with increasing temperatures higher olefinic and aromatic hydrocarbons were realized, this suggests a significant reduction of the hydrogenation function with increasing temperatures. This assumption is logical given the exothermic nature of the hydrogenation reaction, exothermic reactions are suppressed by the increment in temperature. The increase in the aromatic hydrocarbons yield is indicative of the promotion of side reactions such as cyclization and aromatization, with reaction temperature and these are undesirable since they reduce the calorific value of the resultant fuels. Excessively high reaction temperatures also, have been reported to upsetting the products selectivity due to the uncontrolled thermal cracking that accompanies them (Nguyen et al., 2016; Munir, Irfan and Usman, 2018). Moreover, longer reaction times at high temperatures resulted in gel formation in the oil, and this can be attributed to the polymerization side reactions that have been reported to be pronounced at high reaction temperatures (Wang et al., no date). Although high temperatures proved to be favorable for the deoxygenation reactions, the quality and chain-lengths of hydrocarbons produced was also of paramount importance since the deoxygenation process in this project is meant to be a pretreatment of the hydrocracking process for the production of better quality liquid fuels on a large scale. This maintains the importance of controlling the reaction temperature so that deoxygenation occurs at the fastest rate while also preserving the saturation and the lengths of the resultant hydrocarbon chains.

4.3.5 Kinetic Analysis of the Deoxygenation of Waste Cooking Oil

The kinetic analyses of chemical reactions are conducted in order to find out the reaction rate and activation energy required for the attainment of equilibrium. However, the deoxygenation of

triglycerides and fatty acids is a multi-step chemical reaction, this makes the kinetic modelling complex and time consuming, consequently requiring sophisticated analytical equipment facilities. The deoxygenation of WCO in this work did not follow any of the kinetic models due to the damping motion of the rate of deoxygenation observed, with respect to reaction temperature. This calls for more investigation on the cause of this observed damping motion so that if the cause is arrested, then can DO follow a proper kinetic model. At best, the only reasonable kinetic model that was followed by the DO in this work is the fifth order model shown in Equation 4.1 below.

Equation 4.8:

$$y = 215.05x^5 - 4050.3x^4 + 30066x^3 - 109899x^2 + 197709x - 139931$$

4.3.6 Hydrocracking of WCO

The main thrust of this project was oxygen removal from oil, however it was noted that the DO reactions were accompanied by carbon chain length reduction reactions (hydrocracking), yielding some considerable hydrocarbons amounts that falls within the useful liquid fuel range, i.e. biogasoline ($C_{5\text{-}11}$), biojet ($C_{12\text{-}15}$), and biodiesel ($C_{16\text{-}20}$) fuels. This is both advantageous and disadvantageous given that the deoxygenation process in this work is meant to be a pretreatment of the final product selectivity defining process, hydrocracking. The motivation for separating the two processes as aforementioned in Chapter 1, is the rapid catalyst deactivation that may occur when both processes are to be achieved in situ on industrial scale oil volumes, thereby upsetting final product selectivity (Kim, Kim and Lee, 2017; Oh *et al.*, 2018). Cracking reactions have also been reported by Pham *et al.*, (2019) to be side reactions that accompany deoxygenation. The advantage of yielding hydrocarbons that are within the useful liquid fuel range during the deoxygenation step is that it reduces the energy and catalyst requirements for the subsequent hydrocracking step in order to produce desired liquid fuels. Conversely, subjecting the useful liquid fuel range hydrocarbons fraction to a hydrocracking process may result in further hydrocarbon chain lengths reduction, which may bias the final product selectivity towards gaseous hydrocarbon fuels; unless of course if the deoxygenated oil is subjected to a separation process of the liquid fuels before the hydrocracking process. A discussion on the relationship between hydrocarbons selectivity and the deoxygenation variables investigated in this chapter is contained in this section, based on the obtained experimental results and submissions in literature.

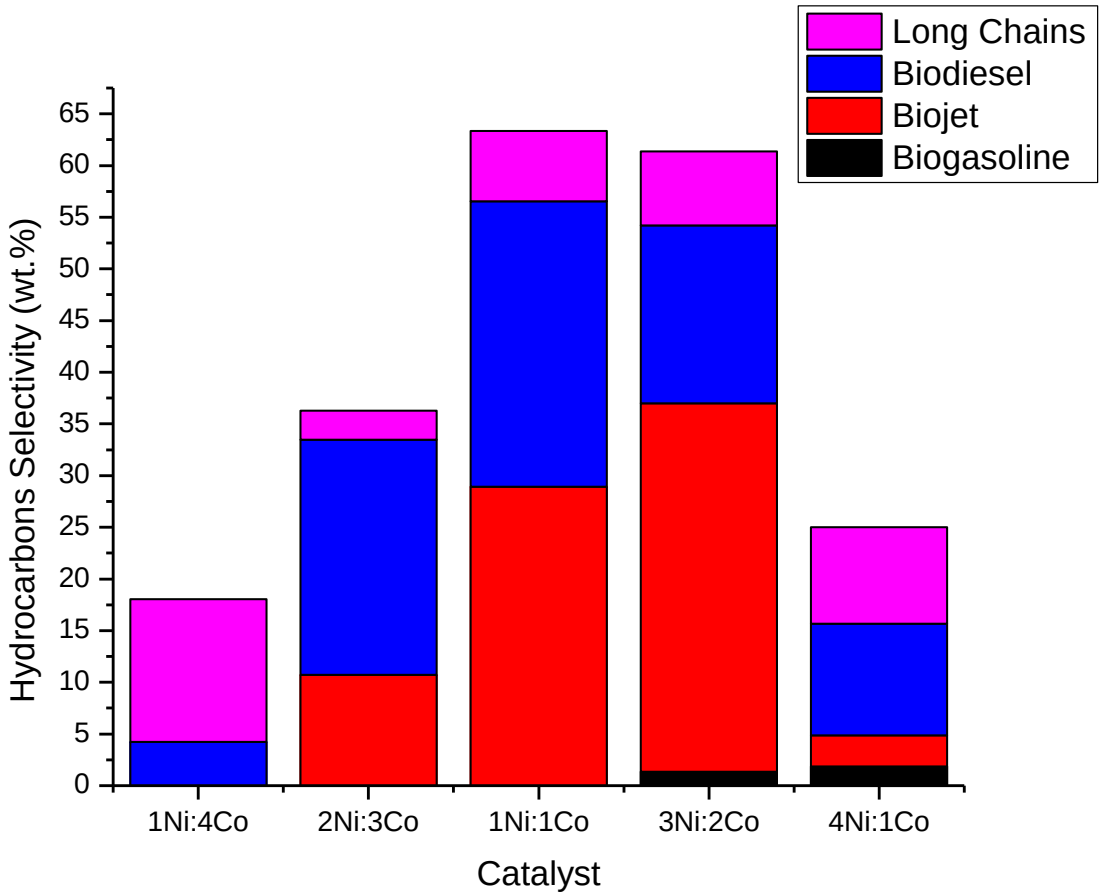


Figure 4.12: Hydrocarbons selectivity with respect to catalyst composition

The hydrocarbons selectivity as depicted in Figure 4.12 for the different catalyst metal composition ratios reveals a selectivity bias for hydrocarbons in the ranges of biojet (C_{12}-C_{15}) and biodiesel fuels, a considerable fraction of long-chain hydrocarbons (C_{20+}), and light traces of biogasoline (C_5-C_{11}). Lighter hydrocarbons could have been lost as gases during the progression of the reactions owing to the semi-batch nature of the reactor used. The highest selectivities for biojet and biodiesel fuels were realized for catalyst 3Ni:2Co (35.06 wt.%) and catalyst 1Ni:1Co (24.56 wt.%), respectively. A decline in selectivity for both fuels was observed as the as the metallic ratios of the catalysts became skewed towards one metal, especially Co. This suggests that the optimum catalytic synergy of Ni and Co on an alumina support has high selectivity for middle distillates. Hari and Yaakob, (2015) reported a diesel selectivity of 79 wt.% during the hydrotreatment of Jatropha FAME with a similar catalyst. Traces of biogasoline were increasingly visible with increasing dominance of Ni in the metal composition ratio of the catalysts. It can be inferred thus

that Ni has a higher cracking function than Co. This difference can be attributed, most probably, to differences in electronic properties of these catalysts (Kubic, 2010). The significant presence of long chain hydrocarbons is expected, as it represents a limited cracking function due to the lower acidity of the alumina catalyst support used (Agudelo *et al.*, 2015). Meanwhile the presence of olefinic and cyclic hydrocarbons in the deoxygenated WCO is indicative of a certain degree of limitation with regards to the hydrogenation activity. This concurs with observations in the previous sections of insufficient interaction of the catalysts with the reactants during the reaction which culminated in low catalytic activity.

The hydrocarbons selectivity responded to the other deoxygenation variable parameters in more or less the same way as did the level of deoxygenation (appendices C3 and C4); higher levels of oxygen content reduction in the WCO yielded higher volumes of shorter hydrocarbon chains. Generally, the hydrocarbons selectivity for all the deoxygenation of WCO parameters used in this project was inclined towards the C_{14}-C_{18} range n-alkanes. Accordingly, the highest level of deoxygenation realized the highest biojet fuel yield (61.06 wt.% $C_{14}H_{30}$) and the lowest long chain hydrocarbons (2.38 wt.% C_{20+}). This is indicative of some significantly high hydrocracking activity during the deoxygenation of the seed oil. The highest selectivity for biodiesel (C_{16}-C_{20}), 53.17wt.%, was realized at (3.5hrs reaction time, 300°C, and 1wt.% catalyst loading) and was largely dominated by $C_{16}H_{34}$ (42.76 wt.%). On the other hand, the highest selectivity for long chain hydrocarbons realized was 34.65wt.%, and this was largely $C_{43}H_{88}$ at (3hrs reaction time, 300°C, and 1wt.% catalyst loading). The overall highest middle distillates selectivity was realized for the highest deoxygenation which yielded 61.06wt.% $C_{14}H_{30}$ and 32.8wt.% $C_{18}H_{38}$. Based on this overall distribution of products, it can be concluded that the deoxygenation of WCO proceeded through a combination of the hydrodeoxygenation and indirect decarbonylation/decarboxylation pathways, as well as the hydrocracking route. This confirms the observations of Hari and Yaakob, 2015 in the hydrotreatment of Jatropha FAME. The even numbered n-alkanes i.e. C_{16} and C_{18}, are the main products of hydrodeoxygenation, whereas the odd numbered n-alkanes (C_{15} and C_{17}) are the major hydrodecarbonylation/ hydrodecarboxylation products (Hari and Yaakob, 2015). The smaller hydrocarbon chains (C_{-15}), on the other hand are largely products of hydrocracking.

4.4 Conclusions and Recommendations

Waste cooking oil deoxygenation was achieved through a combination of the hydrodeoxygenation, hydrodecarbonylation/hydrodecarboxylation, and hydrocracking reactions. The optimum conditions for the deoxygenation of 100ml waste cooking oil under 200kPa H_2 in the semi-batch reactor configuration used are: 1:1 composition of Ni and Co at 10wt.% loading each on the alumina support, for the catalyst; 1wt.% catalyst loading; 300°C reaction temperature; and 5 hours reaction time. The highest deoxygenation (96.12%) coincided with the highest combined middle distillates selectivity, i.e. 61.06 wt.% $C_{14}H_{30}$ plus 32.8wt.% $C_{18}H_{38}$, under the optimum conditions. Nickel favors the hydrodeoxygenation pathway whereas Cobalt favors the decarbonylation pathway, however hydrodeoxygenation was the main pathway the deoxygenation ensued as evidenced by the dominance of straight chain even numbered n-alkanes in the product distribution. Reaction time affected the deoxygenation of WCO positively although the damping motion observed needs further investigations. The influence of catalyst loading was suppressed by the limited interaction of the catalyst with reactants, this could be averted by reducing the catalyst to nanoparticles and solvent dilution of the oil, in the future work. Catalyst reduction in H_2 prior to the DO reaction should also be considered in the future work so as to improve and perpetuate catalytic activity. Higher reaction temperatures increases the rate of deoxygenation, and this is attributed to the thermal cracking reactions which intensify at excessively high reaction temperatures. However, high reaction temperatures increases the selectivity of shorter hydrocarbons, as well as facilitating undesirable side reactions such as cyclization and aromatization. A combination of high reaction temperature and low catalyst loading promoted the polymerization reactions in the oil during the deoxygenation process, and this invariably resulted in gel formation. The main improvement in this work, relative to erstwhile research works is the realization of a high deoxygenation under relatively low pressure, and also with a catalyst that had not been reduced/activated in a hydrogen prior to the reaction.

Chapter 5: Optimization of the Deoxygenation of Waste Cooking Oil

5.1 Introduction

Optimization of the deoxygenation reactions in this research work was attained through the Design-Expert ® Software (Version 11.1.2.0). The design of experiments feature of the software was also employed in designing the experiments for investigating the influence of reaction time, temperature, and catalyst loading on the deoxygenation of waste cooking oil, to pave way for the optimization function. This chapter outlines the procedure followed on design expert from the design of experiments to the outcomes of the optimization process.

5.2 Design of Experiments

Subsequent to the catalyst screening, the best performing catalyst, 1Ni:1Co/Al_2O_3, was selected for the investigation of the other reaction parameters' influence on deoxygenation activity. The design of the experiments for the investigation was done using design expert with the factors/variables being reaction temperature, duration and catalyst loading, and the response being the level of deoxygenation. This was done to generate an appropriate sample size for the optimization the DO parameters. Table 5.1 presents the information on the factors used in the design of the experiments.

Table 5 1: Design of Experiments Specifications

Name	Units	Change	Type	Levels	L[1]	L[2]	L[3]	L[4]	L[5]
Temperature	°C	Easy	Continuous	N/A	240	320			
Time	hours	Easy	Discrete	5	2.5	3.25	4	4.75	5.5
Catalyst Loading	wt.%	Easy	Discrete	4	0.5	0.75	1	1.25	

All the variables were programmed as easy to change because they could all be set independently from each other. The outcome of the design of experiments was a prescription of experiments to

run concurrently varying the factors (Table 4.1) so that the analysis of the results would enable the optimization of the process.

5.3 Analysis

The results from the initial catalyst screening runs using catalyst 1Ni:1Co were then combined with the results from the design of experiments for the analysis of the interaction of variables (Response Surface Study) as well as optimization of the deoxygenation using the historical data design type of Design Expert®. The resultant attributes of the factors and those of the response are presented in Tables 5.2 and 5.3 below.

Table 5.2: Factors Summary

Factor	Name	Units	Type	Coded Low	Coded High	Mean	Std. Dev.
A	Temperature	°C	Numeric	240.0	320.0	292.31	24.67
B	Time	hours	Numeric	2.50	5.50	3.69	1.04
C	Loading	wt.%	Numeric	0.50	1.25	0.9265	0.2617

Table 5 3: Response Summary

Response	Name	Units	Analysis	Min.	Max.	Mean	Std. Dev.	Ratio	Transform	Model
R1	Deoxygenation	%	Polynomial	3.07	96.12	44.95	30.01	31.31	None	Linear

The model summary statistics shown in Table 5.4, provides an insight on the fitness of various models on the analysis of deoxygenation, with respect to the factors, using the R^2 values. The R^2 values are a measure of the extent to which the obtained data fit into a model. The linear model turned out to be the most preferable model, and was employed for the analysis of the response, i.e. deoxygenation, because it maximized the adjusted and predicted R^2, it also was the only significant model. The seemingly low R^2 values may have been induced by the undulating response of deoxygenation to reaction duration as was discussed in Chapter 4. There also was some reasonable coherence between the predicted and the adjusted R^2 for the linear model, with the difference

between the two being less than 0.2. Additionally, the measure of the signal to noise ratio (Adeq Precision) of 6.289 is indicative of an adequate signal for analysis from the linear model, since a ratio greater than 4 is desirable (Yunardi, 2014).

Table 5 4: Model Summary Statistics

Source	Std. Dev.	R^2	Adjusted R^2	Predicted R^2	PRESS	
Linear	**24.19**	**0.4722**	**0.3503**	**0.1958**	**11586.55**	**Suggested**
2FI	26.87	0.4988	0.1981	-0.9969	28771.03	
Quadratic	22.18	0.7609	0.4536	-0.4470	20848.35	
Cubic	36.65	0.8135	-0.4917		*	Aliased

Accordingly, the final Equation in terms of coded variables is illustrated in Equation 5.1. This Equation is useful for identifying the relative impact of the factors by comparing the factor coefficients, which represent the expected change in response per unit change in factor value when all remaining factors are held constant. It can be inferred therefore from the Equation, that all the reaction variable parameters used in this project have direct proportionality with the deoxygenation of waste cooking oil. Also, the reaction temperature had the highest influence on deoxygenation, followed by the reaction duration, and lastly the catalyst loading. The intercept is the overall average deoxygenation for all the runs from where the coefficients are derived, as adjustments around that average, with respect to the individual factor settings.

Equation 5.9

$$Deoxygenation = 35.86 + 32.4A + 4.49B + 0.3044C$$

The analysis of variance (ANOVA) results for the model and its terms are presented in Table 5.5. The statistical significance of Equation terms was estimated based on p-values. A model term is significant when its p-value is less than 0.0500, whereas a p-values which is greater than 0.1000 indicate that the model term is insignificant. In this case reaction temperature is a significant model term. The model F-value of 3.88 which represents its Lack of Fit confirms that the linear model is significant, there is only a 3.51% chance that an F-value this large could occur due to noise.

Table 5 5: ANOVA of the optimization model

Source	Sum of Squares	df	Mean Square	F-value	p-value	
Model	6802.62	3	2267.54	3.88	0.0351	significant
A-Temperature	6169.64	1	6169.64	10.55	0.0064	
B-Time	150.08	1	150.08	0.2566	0.6210	
C-Loading	0.7013	1	0.7013	0.0012	0.9729	
Residual	7604.97	13	585.00			
Cor Total	14407.59	16				

The resultant linear surface response from the first order optimization model used is shown in Figure 5.1 below. A response surface is a geometrical representation of a response variable plotted as a function of the independent variables.

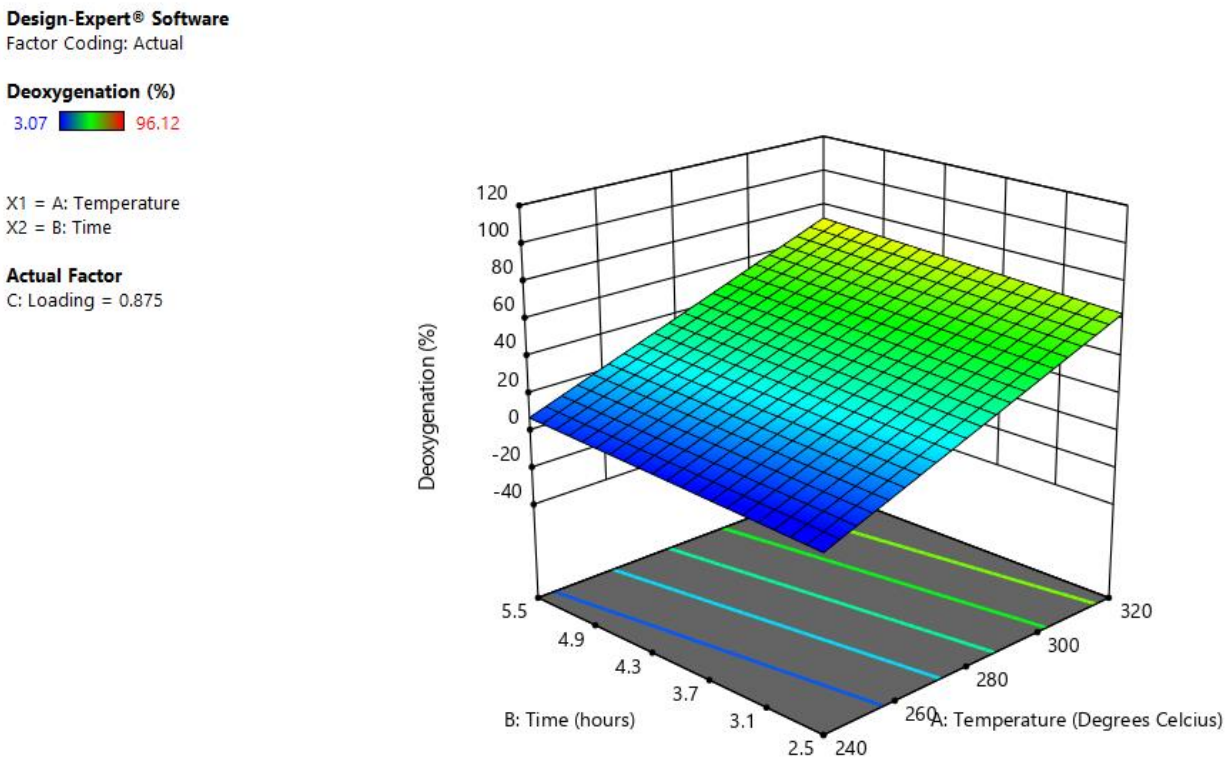


Figure 5.1: Surface Response from the optimization model

5.4 Optimization

The optimization of the deoxygenation process was achieved with the objective of maximizing the response within the set range of the factors. The criteria used gave the level of deoxygenation the highest scale of importance and within the limits of 50% and 100%. The optimization constraints are summarized in Table 5.6 below.

Table 5 6: The Optimization Constraints

Name	**Goal**	**Lower Limit**	**Upper Limit**	**Lower Weight**	**Upper Weight**	**Importance**
A:Temperature	is in range	240	320	1	1	3
B:Time	is in range	2.5	5.5	1	1	3
C:Loading	is in range	0.5	1.25	1	1	3
Deoxygenation	maximize	50	100	1	1	5

The optimization process yielded 88 solutions as shown in appendix D2, and the selected solution for experimental verification in the laboratory had the highest desirability (0.461) and deoxygenation estimate (73.06%) at the maximum values of the factors. Figure 5.2 below depicts the graphical representation of the selected optimization solution. The optimization solution essentially prescribed the use of factors in their upper limits, i.e. 320°C reaction temperature, 5.5 hours reaction time, and 1.25wt.% catalyst loading. The experimental examination of the optimum conditions yielded a 77.97% deoxygenation, and this validated the model used.

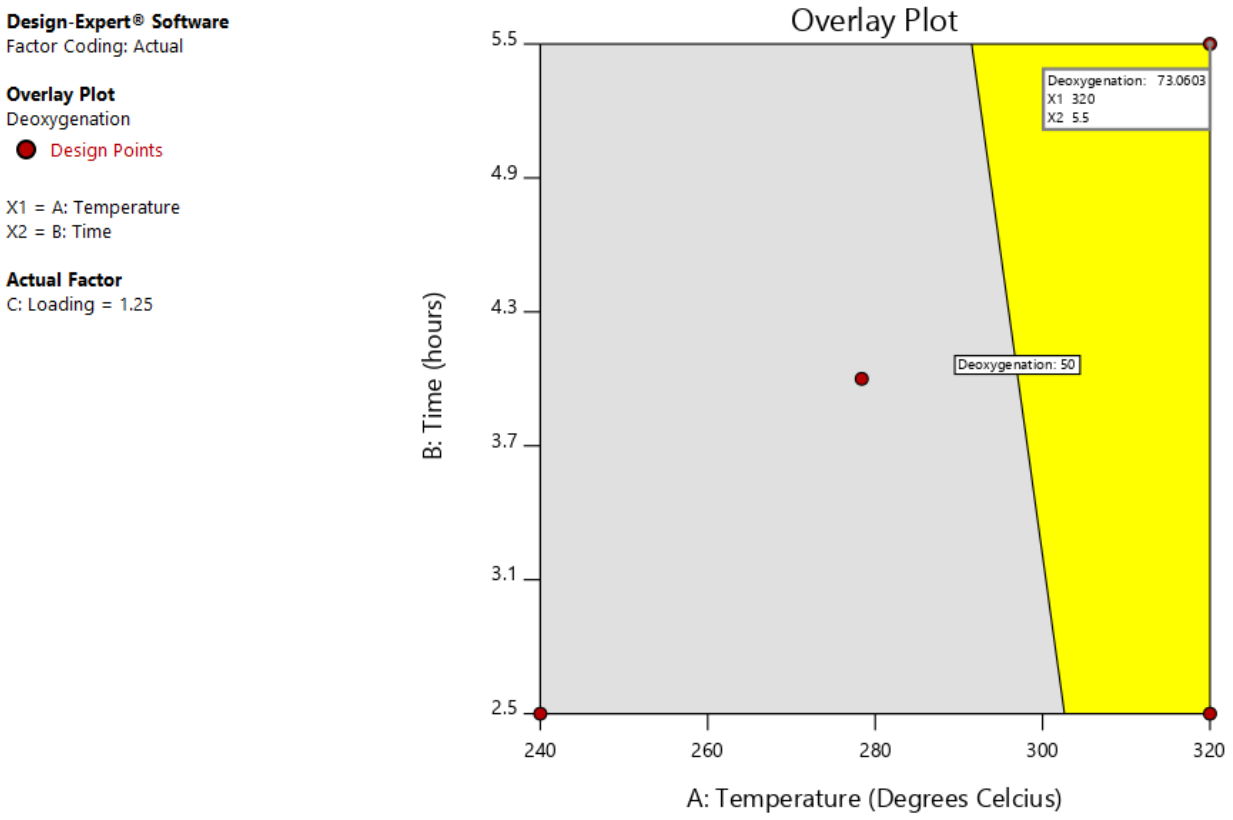


Figure 5 2: The Optimization Model

5.5 Conclusions and Recommendations

A linear optimization model was employed for the deoxygenation of waste cooking oil reaction parameters for the maximization of the level of deoxygenation. The optimum deoxygenation parameters were found to be the upper limits of the factors, i.e. 320°C reaction temperature, 5.5 hours reaction time, and 1.25wt.% catalyst loading. The experimental examination of the optimum conditions yielded a 77.97% deoxygenation against a design expert predicted 73.06%, and this validated the employed model. The model F-value of 3.88 which represents its 'lack of fit' confirms that the linear model is significant, there is only a 3.51% chance that an F-value this large could occur due to noise. Based on the optimization model Equation, the reaction temperature had the highest influence on deoxygenation, followed by the reaction duration, and lastly the catalyst loading. The recommendation is to employ design expert from the design stage to the optimization stage for smooth modelling.

Chapter 6: Strategic Method for the Deoxygenation of Seed Oil

6.1 Introduction

The optimum conditions for the deoxygenation of waste cooking oil were applied on castor oil to investigate the influence of oil composition on its deoxygenation behavior, following the same methodology as outlined in Chapter 4. As will be discussed in this chapter, the deoxygenation behavior of castor oil varied from that of WCO. This necessitated the development of a strategic method for the deoxygenation of seed oil which is outlined in this chapter. A mechanism also, for addressing the undulating deoxygenation response of waste cooking oil with time is postulated.

6.2 Deoxygenation of Castor Oil

Castor oil provided by PEEKAY industries, was deoxygenated under the conditions for which the highest deoxygenation was realized with WCO, i.e. 1wt.% catalyst loading, 300°C reaction temperature, 5 hours reaction time, and 200kPa hydrogen pressure. The resultant deoxygenation of castor oil realized was 37.4% against a 96.12% oxygen reduction from waste cooking oil for the same conditions. The Design Expert® predicted optimum conditions for the deoxygenation of WCO were also employed in the deoxygenation of the castor oil, however, the castor oil turned into a gel after 3.75 hours of reaction time. These observations suggested that the optimum deoxygenation conditions of the two oils of different compositions were unrelated. It is logical to assume that castor oil requires higher catalytic activity for its deoxygenation compared to WCO, this is because the main fatty acid of castor oil, ricinoleic acid, contains an excess of three oxygen atoms, compared to all the fatty acids constituting WCO, which have two oxygen atoms each. In fact, the initial oxygen composition of castor oil (10.53%) is almost twice that of the waste cooking oil used (5.79%). It can also be assumed that the deoxygenation of castor oil requires more reaction time than that of WCO, for the same reaction conditions, given that deoxygenation increases with reaction time, and that castor oil has more oxygen constitution than the latter. The gel formation under the Design Expert® conditions can be justified by the realization that the reaction temperature used (320°C) was above the boiling temperature of castor oil (313°C) under

atmospheric pressure, and this could have promoted the polymerization reactions. As such, it can be concluded that the seed oil composition plays a crucial role in determining its deoxygenation mechanisms and success, and that the catalyst used, $NiCo/Al_2O_3$, has more selectivity for WCO than castor oil. The hydrocarbons selectivity realized with castor oil were largely long chains and biojet fuel range cyclic hydrocarbons (24.02wt.% $C_{12}H_{22}$), this is indicative of a pronounced rate of the undesirable cyclization side reactions, probably due to limited surface area of the interaction of reactants with the catalyst as reported in chapter 4. Adequate interaction surface area between the reactants and the catalysts enhances hydrogen dissociation and the hydrogenation function in the reaction, thereby suppressing the aromatization and cyclization side reactions. An efficient hydrogenation function during the deoxygenation reactions also suppresses the cracking reactions as it promotes the stability of molecules by saturating them. However, some considerable traces of hexadecane (5.27wt.%) and heptadecane (3.43wt.%) were observed in the deoxygenated castor oil, these are suggestive of some significant hydrodeoxygenation and hydrodecarbonylation/ hydrodecarboxylation activity, respectively, during the deoxygenation reaction. Hydrocracking reactions also, are highly likely to have been accompanying the deoxygenation reactions hence the shorter hydrocarbon chains produced. Accordingly, the proposed deoxygenation mechanisms for castor oil with respect to hexadecane and heptadecane are illustrated in Figure 6.1 below.

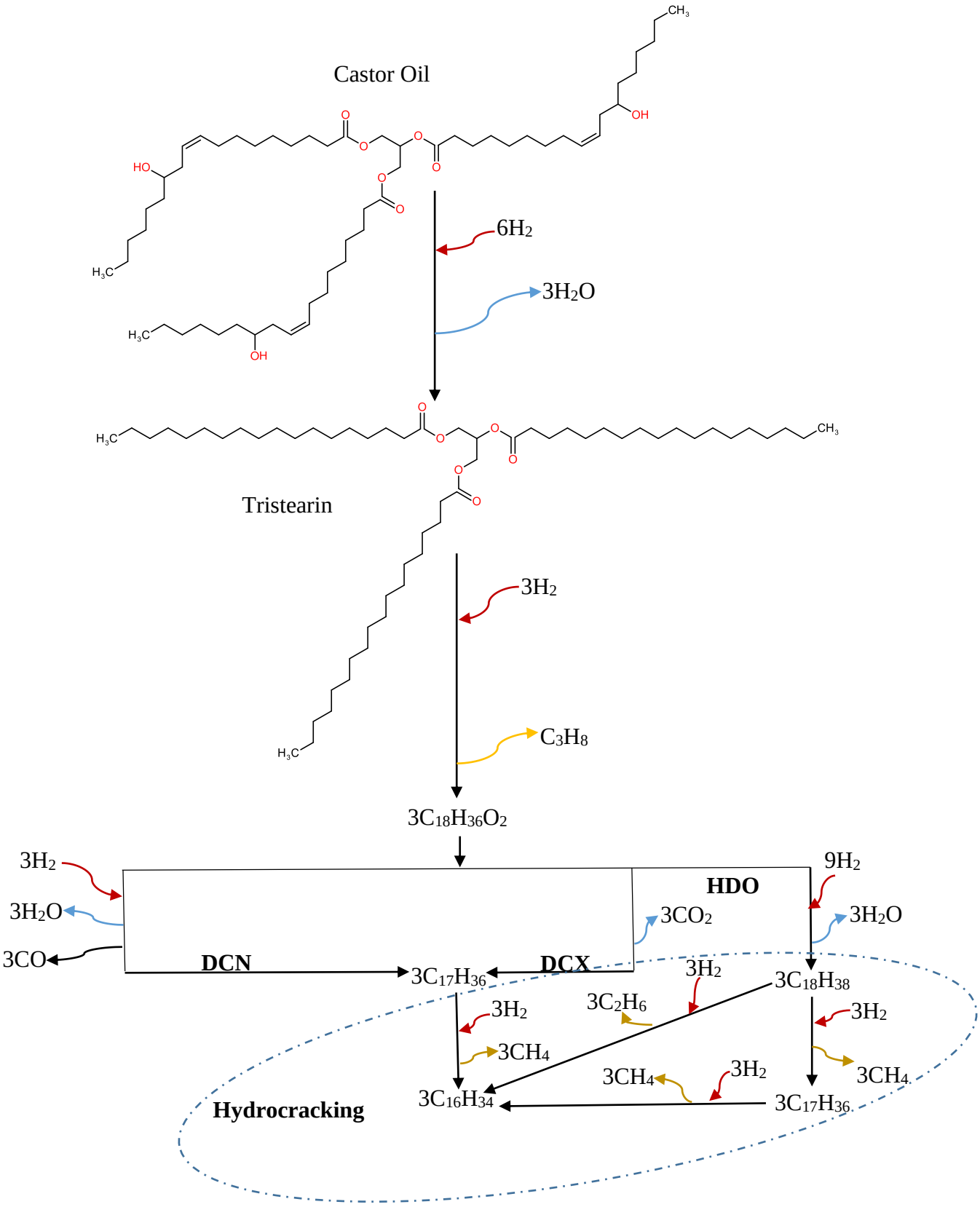


Figure 6.1: Proposed deoxygenation mechanisms of castor oil

The hydrotreatment of castor oil can be assumed to have followed the above mechanism in agreement with the report by Orozco *et al.*, 2017. The hydrogenation of castor oil yielded tristearin by saturating the C=C and eliminating the hydroxyl group from the castor oil through hydrogenolysis. Triglyceride decomposition, by virtue of its high dependability on hydrogen was achieved through hydrogenolysis, yielding stearic acid and propane. Stearic acid was then deoxygenated into $C_{18}H_{38}$ and $C_{17}H_{36}$ through the HDO and DCO_x pathways, respectively. The production of $C_{16}H_{34}$ could have been attained through the hydrocracking of either $C_{18}H_{38}$ to produce C_2H_6 as a byproduct, or $C_{17}H_{36}$ producing CH_4 as a byproduct. Other than the DCO_x reactions, $C_{17}H_{34}$ could also have been produced by the hydrocracking of $C_{18}H_{38}$, to produce CH_4 as a byproduct. The seemingly higher selectivity for the hydrocracking reactions against the deoxygenation reactions in the deoxygenation of castor oil is a clear indication also of variable catalytic behavior with different oil compositions. The varying catalytic behavior could have been induced by the relatively limited surface area of interaction of the reactants with the catalyst owing to the higher viscosity of castor oil over that of seed oil. If so is the case, it may then suggest that the higher selectivity for the cracking reactions may have been due to the thermal decomposition of the carbon chains. The dominance of the thermal cracking reactions is a clear indicator of the suppression of the hydrogenation function in the reaction, the hydrogenation reactions which are effected by the catalyst. This may then be a plausible explanation to the high cyclic hydrocarbons concentration in the deoxygenated castor oil.

6.3 Development of a Strategic Method for Seed Oil Deoxygenation

6.3.1 Method Development

Catalytic behavior varies with reaction conditions, thus it is important to understand the catalytic mechanism of a catalyst when optimizing the deoxygenation conditions (Li et al., 2018). The variable reaction conditions in this context can also be extended to mean the different oil compositions, and the differences could be due to seed type, nurturing, and oil extraction method differences. It is against that background therefore, and the revelation in the previous section that oil composition plays a critical role in determining the deoxygenation mechanisms and success, that the methodology in Figure 6.2 was developed.

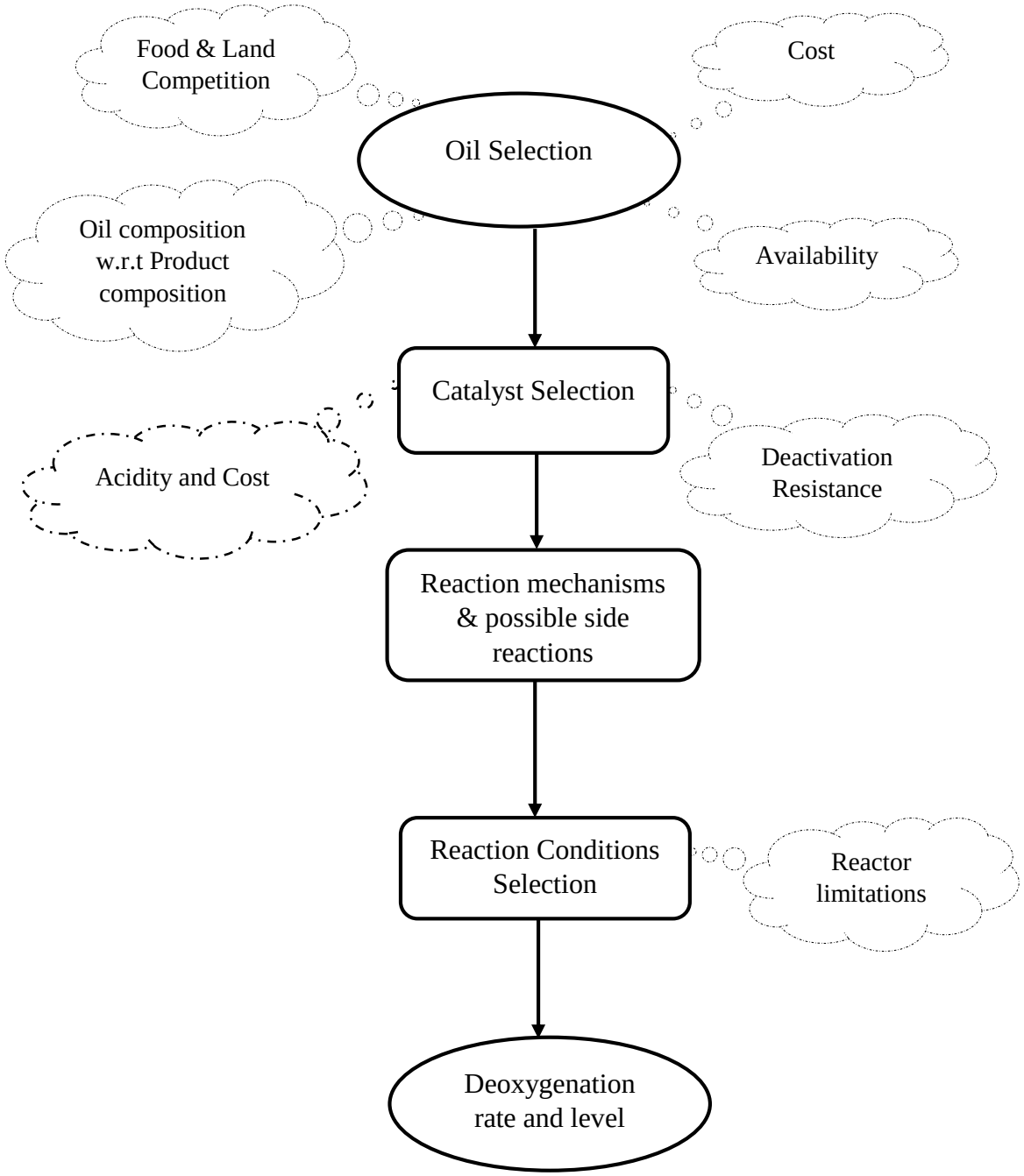


Figure 6 2: Strategic method for seed oil deoxygenation

The proposed methodology is meant to simplify the optimization process for the deoxygenation of the different seed oils by factoring in the raised considerations during the design stage of the deoxygenation process. Initially the selection of the feedstock oil is influenced by a number of factors which include cost, availability, food and land competition, and its composition with respect to the desired product composition and structure. Invariably the compositional characteristic features of a fuel are imprinted onto it by its parent oil, which also is a function of

its nurturing, strain, etc. As has been revealed in this section, that catalytic activity differs with oil composition, the selection of the catalyst should be done based on the oil composition and the desired reaction mechanisms, as well as the possible side reactions, such as coking, polymerization, cyclization, esterification etc. The cost and resistance to deactivation are also other important factors to consider when selecting the catalyst. Finally, the selection of the reaction conditions should be done so as to maximize catalytic activity while suppressing the undesired side reactions, which may be competing with or reversing the deoxygenation reactions. However, the reaction conditions are influenced by the limitations of the reactor. Successful optimization should enable the realization of the highest catalytic activity hence product selectivity at the lowest running costs.

6.3.2 Proposed Deoxygenation Mechanism for Addressing the Damping Behavior of Deoxygenation

The undulating response of deoxygenation to reaction time makes it difficult to do the reaction kinetics of the deoxygenation reactions. This could be induced by the various degrees of unsaturation within the substrate carbon chains or the multiple reaction stages that are involved in the deoxygenation of oil, or even the occurrence of side reactions such as cyclization, esterification and polymerization, at different reaction stages and conditions as competitors to the main deoxygenation reactions. As such, a mechanism for addressing the damping behavior/motion is proposed. It involves the initial saturation of all the olefinic bonds before any oxygen removal is to occur, this is to prevent the regaining of the removed oxygen from other reaction intermediates through reactions such as the hydrolysis of the unsaturated chains. The saturation of olefins also suppresses the polymerization reactions during the deoxygenation process. Since deoxygenation generally increases with time, it is given that the triglycerides and fatty acids are not all deoxygenated at the same time, this therefore leaves the possibility of the regaining of the lost oxygen from other intermediates through the unsaturated bonds.

6.4 Conclusions and Recommendations

Seed oil composition plays a crucial role in determining its deoxygenation mechanisms and success. The optimum deoxygenation conditions of seed oils of different compositions are unrelated; the $NiCo/Al_2O_3$ catalyst used in this project has more selectivity for the deoxygenation of waste cooking oil than castor oil. Castor oil requires higher catalytic activity for its deoxygenation compared to WCO because of its higher oxygen constitution than the latter. The selection of the catalyst should be done based on the oil composition and the desired reaction mechanisms, as well as the possible side reactions, such as coking, polymerization, cyclization, esterification etc. Other reaction parameters should be designed so as to maximize catalytic activity while suppressing the undesired side reactions, which may be competing with or reversing the deoxygenation reactions. Polymerization and cyclization reactions are more pronounced at higher deoxygenation temperatures due to the dominance of the thermal cracking reactions and suppression of the hydrogenation reactions at higher temperature conditions. A deoxygenation mechanism with a high hydrogenation selectivity is likely to have a stable deoxygenation response to reaction parameters than was realized in this project due to the suppression of the undesirable side reactions which compete with, or reverses the deoxygenation reactions.

Chapter 7: General Conclusions

7.1 Introduction

This project entailed the investigation of the relationships between reaction parameters namely reaction temperature, duration, catalyst loading, and catalyst active metal composition ratios with the deoxygenation of waste cooking oil for the establishment of the optimum deoxygenation conditions. It also extended to the investigation of the influence seed oil composition on its deoxygenation success. The conclusions drawn from the investigations are presented in this chapter and the recommendations for future work are postulated.

7.2 Conclusions and Recommendations

The co-impregnation method is a quick and simple method of loading the active metals onto the catalyst support material, however it has limitations in the control of the dispersion of the metals across the catalyst support matrix. Similar functional groups and phases were observed for the catalysts of different metal loading ratios, nevertheless the peak intensities are proportional to the relative abundance of the respective active metals. Ni and Co phases were not visible on the diffractograms obtained, probably due to their low concentrations on the support. The variable metal loading ratios had negligible effect on the surface area and pore size of the catalyst support, therefore the differences that may exist in the deoxygenation catalytic activity of the catalysts may be due to reasons other than their surface areas and pore size distribution.

Waste cooking oil deoxygenation was achieved through a combination of the hydrodeoxygenation, hydrodecarbonylation/hydrodecarboxylation, and hydrocracking reactions. The optimum conditions for the deoxygenation of 100 ml waste cooking oil under 200kPa H_2 in the semi-batch reactor configuration used are: 1:1 composition of Ni and Co at 10 wt.% loading each on the alumina support, for the catalyst; 1wt.% catalyst loading; 300°C reaction temperature; and 5 hours reaction time. The highest deoxygenation (96.12%) coincided with the highest combined middle distillates selectivity, i.e. 61.06 wt.% $C_{14}H_{30}$ plus 32.8wt.% $C_{18}H_{38}$, under the optimum conditions. Nickel favors the hydrodeoxygenation pathway whereas Cobalt favors the decarbonylation pathway, however hydrodeoxygenation was the main pathway the deoxygenation ensued as

evidenced by the dominance of straight chain even numbered n-alkanes in the product distribution. Reaction time affected the deoxygenation of WCO positively although the damping motion observed needs further investigations. The influence of catalyst loading was suppressed by the limited interaction of the catalyst with reactants, this could be averted by reducing the catalyst to nanoparticles and solvent dilution of the oil, in the future work. Catalyst reduction in H_2 prior to the DO reaction should also be considered in the future work so as to improve and perpetuate catalytic activity. Higher reaction temperatures increases the rate of deoxygenation, and this is attributed to the thermal cracking reactions which intensify at excessively high reaction temperatures. However, high reaction temperatures increases the selectivity of shorter hydrocarbons, as well as facilitating undesirable side reactions such as cyclization and aromatization. A combination of high reaction temperature and low catalyst loading promoted the polymerization reactions in the oil during the deoxygenation process, and this invariably resulted in gel formation. The main improvement in this work, relative to erstwhile research works is the realization of a high deoxygenation under relatively low pressure, and also with a catalyst that had not been reduced/activated in a hydrogen prior to the reaction.

A linear optimization model was employed for the deoxygenation of waste cooking oil reaction parameters for the maximization of the level of deoxygenation. The Design Expert® optimum deoxygenation parameters were found to be the upper limits of the factors, i.e. 320°C reaction temperature, 5.5 hours reaction time, and 1.25wt.% catalyst loading. The experimental examination of the optimum conditions yielded a 77.97% deoxygenation against a design expert predicted 73.06%, and this validated the employed model. The model F-value of 3.88 which represents its 'lack of fit' confirms that the linear model is significant, there is only a 3.51% chance that an F-value this large could occur due to noise. Based on the optimization model Equation, the reaction temperature had the highest influence on deoxygenation, followed by the reaction duration, and lastly the catalyst loading. The recommendation is to employ design expert from the design stage to the optimization stage for smooth modelling.

Seed oil composition plays a crucial role in determining its deoxygenation mechanisms and success. The optimum deoxygenation conditions of seed oils of different compositions are unrelated; the $NiCo/Al_2O_3$ catalyst used in this project has more selectivity for the deoxygenation of waste cooking oil than castor oil. Castor oil requires higher catalytic activity for its

deoxygenation compared to WCO because of its higher oxygen constitution than the latter. The selection of the catalyst should be done based on the oil composition and the desired reaction mechanisms, as well as the possible side reactions, such as coking, polymerization, cyclization, esterification etc. Other reaction parameters should be designed so as to maximize catalytic activity while suppressing the undesired side reactions, which may be competing with or reversing the deoxygenation reactions. Polymerization and cyclization reactions are more pronounced at higher deoxygenation temperatures due to the dominance of the thermal cracking reactions and suppression of the hydrogenation reactions at higher temperature conditions. A deoxygenation mechanism with a high hydrogenation selectivity is likely to have a stable deoxygenation response to reaction parameters than was realized in this project due to the suppression of the undesirable side reactions which compete with, or reverses the deoxygenation reactions.

References

Abd-Alla, M. H. *et al.* (2015) 'Improvement of fungal lipids esterification process by bacterial lipase for biodiesel synthesis', *Fuel*. Elsevier Ltd, 160, pp. 196–204. doi: 10.1016/j.fuel.2015.07.080.

Agudelo, J. L. *et al.* (2015) 'Influence of steam-calcination and acid leaching treatment on the VGO hydrocracking performance of faujasite zeolite', *Fuel Processing Technology*. Elsevier B.V., 133, pp. 89–96. doi: 10.1016/j.fuproc.2015.01.011.

Aguieiras, E. C. G., Cavalcanti-Oliveira, E. D. and Freire, D. M. G. (2015) 'Current status and new developments of biodiesel production using fungal lipases', *Fuel*. Elsevier Ltd, 159, pp. 52–67. doi: 10.1016/j.fuel.2015.06.064.

Alaba, P. A., Sani, Y. M. and Ashri Wan Daud, W. M. (2016) 'Efficient biodiesel production: Via solid superacid catalysis: A critical review on recent breakthrough', *RSC Advances*. Royal Society of Chemistry, 6(82), pp. 78351–78368. doi: 10.1039/c6ra08399d.

Aldhaidhawi, M., Chiriac, R. and Badescu, V. (2017) 'Ignition delay, combustion and emission characteristics of Diesel engine fueled with rapeseed biodiesel – A literature review', *Renewable and Sustainable Energy Reviews*. Elsevier Ltd, 73(November 2015), pp. 178–186. doi: 10.1016/j.rser.2017.01.129.

Ali, O. M. *et al.* (2015) 'Analysis of blended fuel properties and engine performance with palm biodiesel-diesel blended fuel', *Renewable Energy*. Elsevier Ltd, 86, pp. 59–67. doi: 10.1016/j.renene.2015.07.103.

Altaie, M. A. H. *et al.* (2015) 'Cold flow and fuel properties of methyl oleate and palm-oil methyl ester blends', *Fuel*. Elsevier Ltd, 160, pp. 238–244. doi: 10.1016/j.fuel.2015.07.084.

Amin, A. *et al.* (2016) 'Experimental and empirical study of diesel and castor biodiesel blending effect, on kinematic viscosity, density and calorific value', *Egyptian Journal of Petroleum*. Egyptian Petroleum Research Institute, 25(4), pp. 509–514. doi: 10.1016/j.ejpe.2015.11.002.

Ayodele, O. B. (2017) 'Influence of oxalate ligand functionalization on Co / ZSM-5 activity in Fischer Tropsch synthesis and hydrodeoxygenation of oleic acid into hydrocarbon fuels',

Scientific Reports. Springer US, (July), pp. 1–14. doi: 10.1038/s41598-017-09706-z.

Bagchi, S. K., Rao, P. S. and Mallick, N. (2015) 'Development of an oven drying protocol to improve biodiesel production for an indigenous chlorophycean microalga Scenedesmus sp.', *Bioresource Technology*. Elsevier Ltd, 180, pp. 207–213. doi: 10.1016/j.biortech.2014.12.092.

Banković-Ilić, I. B. *et al.* (2017) 'Application of nano CaO–based catalysts in biodiesel synthesis', *Renewable and Sustainable Energy Reviews*, 72(January), pp. 746–760. doi: 10.1016/j.rser.2017.01.076.

Bhatia, S. K. *et al.* (2015) 'Development of semi-synthetic microbial consortia of Streptomyces coelicolor for increased production of biodiesel (fatty acid methyl esters)', *Fuel*. Elsevier Ltd, 159, pp. 189–196. doi: 10.1016/j.fuel.2015.06.084.

Ca, R. E. P. U. B. L. I. C. O. F. S. O. U. T. H. A. F. R. I. (2020) 'Government Gazette Staatskoerant'.

Cai, Z. Z. *et al.* (2015) 'A two-step biodiesel production process from waste cooking oil via recycling crude glycerol esterification catalyzed by alkali catalyst', *Fuel Processing Technology*. Elsevier B.V., 137, pp. 186–193. doi: 10.1016/j.fuproc.2015.04.017.

Campanelli, P., Banchero, M. and Manna, L. (2010) 'Synthesis of biodiesel from edible, non-edible and waste cooking oils via supercritical methyl acetate transesterification', *Fuel*. Elsevier Ltd, 89(12), pp. 3675–3682. doi: 10.1016/j.fuel.2010.07.033.

César, A. da S. *et al.* (2017) 'The potential of waste cooking oil as supply for the Brazilian biodiesel chain', *Renewable and Sustainable Energy Reviews*. Elsevier Ltd, 72(November 2016), pp. 246–253. doi: 10.1016/j.rser.2016.11.240.

Collection, E. D. (2016) *Overview of the Petrol and Diesel Market in South Africa between 2007 and 2016*.

Damanik, N. *et al.* (2018) 'A review on the engine performance and exhaust emission characteristics of diesel engines fueled with biodiesel blends', *Environmental Science and Pollution Research*. Environmental Science and Pollution Research, 25(16), pp. 15307–15325. doi: 10.1007/s11356-018-2098-8.

Daramola, M. O., Nkazi, D. and Mtshali, K. (2015) 'Synthesis and evaluation of catalytic activity of calcined sodium silicate for transesterification of waste cooking oil to biodiesel', *International Journal of Renewable Energy Research*, 5(2), pp. 517–523. doi: 10.20508/ijrer.19184.

Dawes, G. J. S. *et al.* (2015) 'Deoxygenation of biobased molecules by decarboxylation and decarbonylation - A review on the role of heterogeneous, homogeneous and bio-catalysis', *Green Chemistry*. Royal Society of Chemistry, 17(6), pp. 3231–3250. doi: 10.1039/c5gc00023h.

van Dyk, S. *et al.* (2019) 'Potential synergies of drop-in biofuel production with further co-processing at oil refineries', *Biofuels, Bioproducts and Biorefining*, 13(3), pp. 760–775. doi: 10.1002/bbb.1974.

Edeh, I., Overton, T. and Bowra, S. (2019) 'Catalytic hydrothermal deoxygenation of fatty acids over palladium on activated carbon catalyst (Pd / C) for renewable diesel production activated carbon catalyst (Pd / C) for renewable diesel production', *Biofuels*. Taylor & Francis, 0(0), pp. 1–8. doi: 10.1080/17597269.2019.1580971.

Fu, J., Lu, X. and Savage, P. E. (2011) 'Hydrothermal Decarboxylation and Hydrogenation of Fatty Acids over Pt / C', 310027, pp. 481–486. doi: 10.1002/cssc.201000370.

Gharehghani, A., Mirsalim, M. and Hosseini, R. (2017) 'Effects of waste fish oil biodiesel on diesel engine combustion characteristics and emission', *Renewable Energy*. Elsevier Ltd, 101(2017), pp. 930–936. doi: 10.1016/j.renene.2016.09.045.

Go, A. W. *et al.* (2016) 'Developments in in-situ (trans) esterification for biodiesel production: A critical review', *Renewable and Sustainable Energy Reviews*, 60, pp. 284–305. doi: 10.1016/j.rser.2016.01.070.

Goede, S. De *et al.* (2015) 'A Comparison of the Stability Performance of Blends of Paraffinic Diesel and Petroleum-Derived Diesel , with RME Biodiesel Using Laboratory Stability Measurement Techniques', 2015.

Gomes, M. G. *et al.* (2015) 'Purification of biodiesel by dry washing, employing starch and cellulose as natural adsorbents', *Fuel*. Elsevier Ltd, 155, pp. 1–6. doi: 10.1016/j.fuel.2015.04.012.

Hachemi, I. *et al.* (2017) 'Sulfur-free Ni catalyst for production of green diesel by hydrodeoxygenation', *Journal of Catalysis*. Elsevier Inc., 347, pp. 205–221. doi: 10.1016/j.jcat.2016.12.009.

Hajjari, M. *et al.* (2017) 'A review on the prospects of sustainable biodiesel production: A global scenario with an emphasis on waste-oil biodiesel utilization', *Renewable and Sustainable Energy Reviews*. Elsevier Ltd, 72(November 2016), pp. 445–464. doi: 10.1016/j.rser.2017.01.034.

Han, M. *et al.* (2016) 'Efficient confinement of ionic liquids in MIL-100(Fe) frameworks by the "impregnation-reaction-encapsulation" strategy for biodiesel production', *RSC Advances*. Royal Society of Chemistry, 6(43), pp. 37110–37117. doi: 10.1039/c6ra00579a.

Hari, T. K. and Yaakob, Z. (2015) 'Production of diesel fuel by the hydrotreatment of jatropha oil derived fatty acid methyl esters over', *Reaction Kinetics, Mechanisms and Catalysis*. Springer Netherlands, pp. 131–145. doi: 10.1007/s11144-015-0874-8.

Hassan, Abbas *et al.* (2017) 'System and process for hydrocracking', 2(12). Available at: https://patents.google.com/patent/US9669381B2/en.

He, B. *et al.* (2015) 'Biodiesel production from soybean oil by guanidinylated chitosan', *Fuel*. Elsevier Ltd, 159, pp. 33–39. doi: 10.1016/j.fuel.2015.06.038.

Hegde, K. *et al.* (2015) 'Genetic Engineering Strategies for Enhanced Biodiesel Production', *Molecular Biotechnology*. Springer US, 57(7), pp. 606–624. doi: 10.1007/s12033-015-9869-y.

Herbert, W. *et al.* (2019) 'Biofuels technology development in Southern Africa Biofuels technology development in Southern Africa'. Taylor & Francis, 3637. doi: 10.1080/0376835X.2018.1481732.

Hermida, L., Abdullah, A. Z. and Mohamed, A. R. (2015) 'Deoxygenation of fatty acid to produce diesel-like hydrocarbons: A review of process conditions, reaction kinetics and mechanism', *Renewable and Sustainable Energy Reviews*. Elsevier, 42, pp. 1223–1233. doi: 10.1016/j.rser.2014.10.099.

Hilbers, T. J., Sprakel, L. M. J. and Ham, L. G. J. Van Der (2015) 'Green Diesel from Hydrotreated Vegetable Oil Process Design Study', (4), pp. 651–657. doi: 10.1002/ceat.201400648.

Huang, J. *et al.* (2015) 'Biodiesel production from microalgae oil catalyzed by a recombinant lipase', *Bioresource Technology*. Elsevier Ltd, 180, pp. 47–53. doi: 10.1016/j.biortech.2014.12.072.

Ishak, Z. I. *et al.* (2017) 'A review of ionic liquids as catalysts for transesterification reactions of biodiesel and glycerol carbonate production', *Catalysis Reviews - Science and Engineering*. Taylor & Francis, 59(1), pp. 44–93. doi: 10.1080/01614940.2016.1268021.

Janampelli, S. and Darbha, S. (2019) 'Hydrodeoxygenation of Vegetable Oils and Fatty Acids over Different Group VIII Metal Catalysts for Producing Biofuels', *Catalysis Surveys from Asia*. Springer US, 23(2), pp. 90–101. doi: 10.1007/s10563-019-09266-4.

Jayakumar, S. *et al.* (2017) 'The prospect of microalgal biodiesel using agro-industrial and industrial wastes in Malaysia', *Renewable and Sustainable Energy Reviews*, 72(January), pp. 33–47. doi: 10.1016/j.rser.2017.01.002.

Karmee, S. K. (2016) 'Liquid biofuels from food waste: Current trends, prospect and limitation', *Renewable and Sustainable Energy Reviews*. Elsevier, 53, pp. 945–953. doi: 10.1016/j.rser.2015.09.041.

Katiyar, R. *et al.* (2017) 'Microalgae: An emerging source of energy based bio-products and a solution for environmental issues', *Renewable and Sustainable Energy Reviews*. Elsevier Ltd, 72(November 2016), pp. 1083–1093. doi: 10.1016/j.rser.2016.10.028.

Kesaano, M. *et al.* (2015) 'Dissolved inorganic carbon enhanced growth, nutrient uptake, and lipid accumulation in wastewater grown microalgal biofilms', *Bioresource Technology*. Elsevier Ltd, 180, pp. 7–15. doi: 10.1016/j.biortech.2014.12.082.

Kim, M. Y. *et al.* (2017) 'Maximizing Biojet Fuel Production from Triglyceride: Importance of the Hydrocracking Catalyst and Separate Deoxygenation/Hydrocracking Steps', *ACS Catalysis*, 7(9), pp. 6256–6267. doi: 10.1021/acscatal.7b01326.

Kim, S. H., Kim, K. D. and Lee, Y. K. (2017) 'Effects of dispersed MoS2 catalysts and reaction conditions on slurry phase hydrocracking of vacuum residue', *Journal of Catalysis*. Elsevier Inc., 347, pp. 127–137. doi: 10.1016/j.jcat.2016.11.015.

Kong, Z. *et al.* (2020) 'Heliyon Review article A review of thermal homogeneous catalytic

deoxygenation reactions for valuable products', *Heliyon*. Elsevier Ltd, 6(May 2019), p. e03446. doi: 10.1016/j.heliyon.2020.e03446.

Kubic, D. (2010) 'Applied Catalysis A : General Deoxygenation of vegetable oils over sulfided Ni , Mo and NiMo catalysts ˇ k Kaluz', 372, pp. 199–208. doi: 10.1016/j.apcata.2009.10.034.

Kumar, D. and Ali, A. (2015) 'Direct synthesis of fatty acid alkanolamides and fatty acid alkyl esters from high free fatty acid containing triglycerides as lubricity improvers using heterogeneous catalyst', *Fuel*. Elsevier Ltd, 159, pp. 845–853. doi: 10.1016/j.fuel.2015.07.046.

Kumar, D., Singh, B. and Korstad, J. (2017) 'Utilization of lignocellulosic biomass by oleaginous yeast and bacteria for production of biodiesel and renewable diesel', *Renewable and Sustainable Energy Reviews*. Elsevier Ltd, 73(October 2015), pp. 654–671. doi: 10.1016/j.rser.2017.01.022.

Kumar, M. and Sharma, M. P. (2016) 'Selection of potential oils for biodiesel production', *Renewable and Sustainable Energy Reviews*. Elsevier Ltd, 56, pp. 1129–1138. doi: 10.1016/j.rser.2015.12.032.

Kumar, P. *et al.* (2014) 'Kinetics of hydrodeoxygenation of stearic acid using supported nickel catalysts: Effects of supports', *Applied Catalysis A: General*. Elsevier B.V., 471, pp. 28–38. doi: 10.1016/j.apcata.2013.11.021.

Kumar, P. and Rehman, A. (2016) 'Bio-diesel in homogeneous charge compression ignition (HCCI) combustion', *Renewable and Sustainable Energy Reviews*. Elsevier Ltd, 56, pp. 536–550. doi: 10.1016/j.rser.2015.11.088.

Laesecke, J., Ellis, N. and Kirchen, P. (2017) 'Production, analysis and combustion characterization of biomass fast pyrolysis oil – Biodiesel blends for use in diesel engines', *Fuel*. Elsevier Ltd, 199, pp. 346–357. doi: 10.1016/j.fuel.2017.01.093.

Lam, S. S. *et al.* (2016) 'Progress in waste oil to sustainable energy, with emphasis on pyrolysis techniques', *Renewable and Sustainable Energy Reviews*. Elsevier, 53, pp. 741–753. doi: 10.1016/j.rser.2015.09.005.

Laviola, B. G. *et al.* (2017) 'Biometric and biotechnology strategies in Jatropha genetic breeding for biodiesel production', *Renewable and Sustainable Energy Reviews*. Elsevier Ltd,

76(January), pp. 894–904. doi: 10.1016/j.rser.2017.03.116.

Lee, J. *et al.* (2017) 'Establishing a green platform for biodiesel synthesis via strategic utilization of biochar and dimethyl carbonate', *Bioresource Technology*. Elsevier Ltd, 241, pp. 1178–1181. doi: 10.1016/j.biortech.2017.05.187.

Li, D. *et al.* (2015) 'Recent advances for the production of hydrocarbon biofuel via deoxygenation progress', *Science Bulletin*. Science China Press, 60(24), pp. 2096–2106. doi: 10.1007/s11434-015-0971-0.

Li, Q., Backes, F. and Wachtmeister, G. (2015) 'Application of canola oil operation in a diesel engine with common rail system', *Fuel*, 159, pp. 141–149. doi: 10.1016/j.fuel.2015.06.060.

Li, X. *et al.* (2018) 'Heterogeneous sulfur-free hydrodeoxygenation catalysts for selectively upgrading the renewable bio-oils to second generation biofuels', *Renewable and Sustainable Energy Reviews*. Elsevier Ltd, 82(September 2016), pp. 3762–3797. doi: 10.1016/j.rser.2017.10.091.

Li, X. and Luo, X. (2015) 'Preparation of Mesoporous Activated Carbon Supported Ni Catalyst for Deoxygenation of Stearic Acid into Hydrocarbons', 34(2). doi: 10.1002/ep.

Links, D. A. *et al.* (2012) 'Green Chemistry', (3), pp. 2499–2505. doi: 10.1039/c2gc35450k.

Liu, J. *et al.* (2012) 'Hydroprocessing of Jatropha oil over NiMoCe / Al 2 O 3 catalyst', *International Journal of Hydrogen Energy*. Elsevier Ltd, pp. 3–9. doi: 10.1016/j.ijhydene.2012.09.020.

Liu, J. *et al.* (2015) 'Hydroprocessing of Jatropha Oil for Production of Green Diesel over Non-sulfided Ni-PTA / Al 2 O 3 Catalyst', *Nature Publishing Group*. Nature Publishing Group, (July 2014), pp. 1–13. doi: 10.1038/srep11327.

Liu, S. *et al.* (2015) 'Bioresource Technology Bio-aviation fuel production from hydroprocessing castor oil promoted by the nickel-based bifunctional catalysts', *BIORESOURCE TECHNOLOGY*. Elsevier Ltd, 183, pp. 93–100. doi: 10.1016/j.biortech.2015.02.056.

Liu, T. *et al.* (2016) 'Development of a skeletal mechanism for biodiesel blend surrogates with varying fatty acid methyl esters proportion', *Applied Energy*. Elsevier Ltd, 162(x), pp. 278–288.

doi: 10.1016/j.apenergy.2015.10.090.

Lopez, G. *et al.* (2017) 'Thermochemical routes for the valorization of waste polyolefinic plastics to produce fuels and chemicals. A review', *Renewable and Sustainable Energy Reviews*. Elsevier Ltd, 73(January), pp. 346–368. doi: 10.1016/j.rser.2017.01.142.

Lotti, M. *et al.* (2018) 'Enzymatic Production of Biodiesel: Strategies to Overcome Methanol Inactivation', *Biotechnology Journal*, 13(5), pp. 1–10. doi: 10.1002/biot.201700155.

Mahmudul, H. M. *et al.* (2017) 'Production, characterization and performance of biodiesel as an alternative fuel in diesel engines – A review', *Renewable and Sustainable Energy Reviews*. Elsevier Ltd, 72(November 2016), pp. 497–509. doi: 10.1016/j.rser.2017.01.001.

Makar, Y. and Ganda, E. T. (2018) 'Bio-oil as a potential source of petroleum range fuels', 81(July 2017), pp. 69–75. doi: 10.1016/j.rser.2017.07.036.

Maroa, S. and Inambao, F. (2019) 'The effect of cetane number and oxygen content in the performance and emissions characteristics of a diesel engine using biodiesel blends', *Journal of Energy in Southern Africa*, 30(2), pp. 1–13. doi: 10.17159/2413-3051/2019/v30i2a5337.

Marx, S. (2016) 'Glycerol-free biodiesel production through transesterification: A review', *Fuel Processing Technology*. Elsevier B.V., 151, pp. 139–147. doi: 10.1016/j.fuproc.2016.05.033.

Mata, T. M. and Martins, A. A. (2015) 'Biodiesel Production Processes', (August).

Maymandi, M. G. and Rahimpour, F. (2015) 'Optimization of lipid productivity by Citrobacter youngae CECT 5335 and biodiesel preparation using ionic liquid catalyst', *Fuel*. Elsevier Ltd, 159, pp. 476–483. doi: 10.1016/j.fuel.2015.07.014.

Meller, E. *et al.* (2014) 'Catalytic deoxygenation of castor oil over Pd / C for the production of cost effective biofuel', *FUEL*. Elsevier Ltd, (May). doi: 10.1016/j.fuel.2014.04.094.

Micic, R. D. *et al.* (2015) 'Activation temperature imposed textural and surface synergism of CaO catalyst for sunflower oil transesterification', *Fuel*. Elsevier Ltd, 159, pp. 638–645. doi: 10.1016/j.fuel.2015.07.025.

Millo, F. *et al.* (2015) 'Effects of different biofuels blends on performance and emissions of an automotive diesel engine', *Fuel*. Elsevier Ltd, 159(x), pp. 614–627. doi:

10.1016/j.fuel.2015.06.096.

Moazeni, F., Chen, Y. C. and Zhang, G. (2019) 'Enzymatic transesterification for biodiesel production from used cooking oil, a review', *Journal of Cleaner Production*. Elsevier Ltd, 216, pp. 117–128. doi: 10.1016/j.jclepro.2019.01.181.

Mofijur, M. *et al.* (2016) 'Role of biofuel and their binary (diesel-biodiesel) and ternary (ethanol-biodiesel-diesel) blends on internal combustion engines emission reduction', *Renewable and Sustainable Energy Reviews*, 53, pp. 265–278. doi: 10.1016/j.rser.2015.08.046.

Moreno-Garcia, L. *et al.* (2017) 'Microalgae biomass production for a biorefinery system: Recent advances and the way towards sustainability', *Renewable and Sustainable Energy Reviews*, 76(May 2016), pp. 493–506. doi: 10.1016/j.rser.2017.03.024.

Mostafa, S. S. M. and El-Gendy, N. S. (2017) 'Evaluation of fuel properties for microalgae Spirulina platensis bio-diesel and its blends with Egyptian petro-diesel', *Arabian Journal of Chemistry*. King Saud University, 10, pp. S2040–S2050. doi: 10.1016/j.arabjc.2013.07.034.

Mujeeb, M. A., Vedamurthy, A. B. and T, S. C. (2016) 'Current strategies and prospects of biodiesel production: A review', *Pelagia Research Library Advances in Applied Science Research*, 7(1), pp. 120–133. Available at: www.pelagiaresearchlibrary.com.

Munir, D., Irfan, M. F. and Usman, M. R. (2018) 'Hydrocracking of virgin and waste plastics: A detailed review', *Renewable and Sustainable Energy Reviews*. Elsevier Ltd, 90(June 2016), pp. 490–515. doi: 10.1016/j.rser.2018.03.034.

Nanda, M. R. *et al.* (2016) 'Catalytic conversion of glycerol for sustainable production of solketal as a fuel additive: A review', *Renewable and Sustainable Energy Reviews*. Elsevier Ltd, 56(1), pp. 1022–1031. doi: 10.1016/j.rser.2015.12.008.

Nekhavhambe, E., Mukaya, H. E. and Nkazi, D. B. (2019) 'Development of castor oil–based polymers: A review', *Journal of Advanced Manufacturing and Processing*, 1(4), pp. 1–13. doi: 10.1002/amp2.10030.

Ng, A. *et al.* (2017) 'Applied Catalysis A , General A review on reaction mechanisms of metal-catalyzed deoxygenation process in bio-oil model compounds', *Applied Catalysis A, General*. Elsevier, 541(May), pp. 87–106. doi: 10.1016/j.apcata.2017.05.002.

Nguyen, M. T. *et al.* (2016) 'A review on the oil-soluble dispersed catalyst for slurry-phase hydrocracking of heavy oil', *Journal of Industrial and Engineering Chemistry*. The Korean Society of Industrial and Engineering Chemistry, 43, pp. 1–12. doi: 10.1016/j.jiec.2016.07.057.

Norjannah, B. *et al.* (2016) 'Enzymatic transesterification for biodiesel production: A comprehensive review', *RSC Advances*. Royal Society of Chemistry, 6(65), pp. 60034–60055. doi: 10.1039/c6ra08062f.

Nwokoagbara, E., Olaleye, A. K. and Wang, M. (2015) 'Biodiesel from microalgae: The use of multi-criteria decision analysis for strain selection', *Fuel*. Elsevier Ltd, 159, pp. 241–249. doi: 10.1016/j.fuel.2015.06.074.

Oh, S. *et al.* (2017) 'RSC Advances Evaluation of hydrodeoxygenation reactivity of pyrolysis bio-oil with various Ni-based catalysts for'. Royal Society of Chemistry, pp. 15116–15126. doi: 10.1039/c7ra01166k.

Oh, Y. K. *et al.* (2018) 'Recent developments and key barriers to advanced biofuels: A short review', *Bioresource Technology*. Elsevier, 257(December 2017), pp. 320–333. doi: 10.1016/j.biortech.2018.02.089.

Okoye, P. U. and Hameed, B. H. (2016) 'Review on recent progress in catalytic carboxylation and acetylation of glycerol as a byproduct of biodiesel production', *Renewable and Sustainable Energy Review*s. Elsevier, 53, pp. 558–574. doi: 10.1016/j.rser.2015.08.064.

Online, V. A. *et al.* (2015) 'Catalysis Science & Technology', pp. 2009–2015. doi: 10.1039/c3cy00139c.

Online, V. A. *et al.* (2017) 'RSC Advances Catalytic deoxygenation of triglycerides to green diesel over modi fi ed CaO-based catalysts †', pp. 46445–46460. doi: 10.1039/c7ra08061a.

Onoji, S. E. *et al.* (2016) 'Rubber seed oil: A potential renewable source of biodiesel for sustainable development in sub-Saharan Africa', *Energy Conversion and Management*. Elsevier Ltd, 110, pp. 125–134. doi: 10.1016/j.enconman.2015.12.002.

Orozco, L. M. *et al.* (2017) 'Second-generation green diesel from castor oil: development of a new and efficient continuous-production process', *Chemical Engineering Journal*. doi: 10.1016/j.cej.2017.04.027.

Palmer, J. D. and Brigham, C. J. (2016) ‘Feasibility of triacylglycerol production for biodiesel, utilizing Rhodococcus opacus as a biocatalyst and fishery waste as feedstock’, *Renewable and Sustainable Energy Reviews*. Elsevier Ltd, 56, pp. 922–928. doi: 10.1016/j.rser.2015.12.002.

Pattanaik, B. P. and Misra, R. D. (2017) ‘Effect of reaction pathway and operating parameters on the deoxygenation of vegetable oils to produce diesel range hydrocarbon fuels: A review’, *Renewable and Sustainable Energy Reviews*. Elsevier Ltd, 73(October 2015), pp. 545–557. doi: 10.1016/j.rser.2017.01.018.

Peng, C. *et al.* (2018) ‘Research and development of hydrocracking catalysts and technologies in China’, *Frontiers of Chemical Science and Engineering*, 12(4), pp. 867–877. doi: 10.1007/s11705-018-1768-x.

Pham, L. K. H. *et al.* (2019) ‘Formation and activity of activated carbon supported Ni2P catalysts for atmospheric deoxygenation of waste cooking oil’, *Fuel Processing Technology*. Elsevier, 185(November 2018), pp. 117–125. doi: 10.1016/j.fuproc.2018.12.009.

Rasyid, R. *et al.* (2015) ‘Hydrocracking of Calophyllum inophyllum oil with non-sulfide CoMo catalysts’, *Bulletin of Chemical Reaction Engineering & Catalysis*, 10(1), pp. 61–69. doi: 10.9767/bcrec.10.1.6597.61-69.

Rogers, K. A. and Zheng, Y. (2016) ‘Selective Deoxygenation of Biomass-Derived Bio-oils within Hydrogen-Modest Environments: A Review and New Insights’, *ChemSusChem*, 9(14), pp. 1750–1772. doi: 10.1002/cssc.201600144.

Romero, M. *et al.* (2015) ‘Preliminary experimental study on biofuel production by deoxygenation of Jatropha oil’, *Fuel Processing Technology*. Elsevier B.V., 137, pp. 31–37. doi: 10.1016/j.fuproc.2015.04.002.

Romero, M. J. A. *et al.* (2016) ‘Deoxygenation of waste cooking oil and non-edible oil for the production of liquid hydrocarbon biofuels’, *Waste Management*. Elsevier Ltd, 47, pp. 62–68. doi: 10.1016/j.wasman.2015.03.033.

Roy, M. M. *et al.* (2016) ‘Cold start idle emissions from a modern Tier-4 turbo-charged diesel engine fueled with diesel-biodiesel, diesel-biodiesel-ethanol, and diesel-biodiesel-diethyl ether blends’, *Applied Energy*. Elsevier Ltd, 180(x), pp. 52–65. doi: 10.1016/j.apenergy.2016.07.090.

Sahu, R. *et al.* (2015) 'A review of recent advances in catalytic hydrocracking of heavy residues', *Journal of Industrial and Engineering Chemistry*. The Korean Society of Industrial and Engineering Chemistry, 27, pp. 12–24. doi: 10.1016/j.jiec.2015.01.011.

Sajjadi, S. M., Haghighi, M. and Rahmani, F. (2015) 'Sol-gel synthesis of Ni-Co/Al2O3-MgO-ZrO2 nanocatalyst used in hydrogen production via reforming of CH4/CO2 greenhouse gases', *Journal of Natural Gas Science and Engineering*. Elsevier B.V, 22, pp. 9–21. doi: 10.1016/j.jngse.2014.11.014.

Salam, K. A., Velasquez-Orta, S. B. and Harvey, A. P. (2016) 'A sustainable integrated in situ transesterification of microalgae for biodiesel production and associated co-products - A review', *Renewable and Sustainable Energy Reviews*. Elsevier, 65, pp. 1179–1198. doi: 10.1016/j.rser.2016.07.068.

Sanli, H. *et al.* (2015) 'Effects of waste frying oil based methyl and ethyl ester biodiesel fuels on the performance, combustion and emission characteristics of a di diesel engine', *Fuel*. Elsevier Ltd, 159, pp. 179–187. doi: 10.1016/j.fuel.2015.06.081.

Schreiber, M. W. *et al.* (2016) 'Hydrodeoxygenation of fatty acid esters catalyzed by Ni on nano-sized MFI type zeolites', *Catalysis Science and Technology*. Royal Society of Chemistry, 6(22), pp. 7976–7984. doi: 10.1039/c6cy01598k.

Sehatpour, M. H., Kazemi, A. and Sehatpour, H. eddin (2017) 'Evaluation of alternative fuels for light-duty vehicles in Iran using a multi-criteria approach', *Renewable and Sustainable Energy Reviews*. Elsevier Ltd, 72(May 2016), pp. 295–310. doi: 10.1016/j.rser.2017.01.067.

Serqueira, D. S. *et al.* (2015) 'Tetrahydrocurcuminoids as potential antioxidants for biodiesels', *Fuel*. Elsevier Ltd, 160, pp. 490–494. doi: 10.1016/j.fuel.2015.07.104.

Shiu, P. *et al.* (2010) 'Bioresource Technology Biodiesel production from rice bran by a two-step in-situ process', *Bioresource Technology*. Elsevier Ltd, 101(3), pp. 984–989. doi: 10.1016/j.biortech.2009.09.011.

Sierra-Cantor, J. F. and Guerrero-Fajardo, C. A. (2017) 'Methods for improving the cold flow properties of biodiesel with high saturated fatty acids content: A review', *Renewable and Sustainable Energy Reviews*. Elsevier Ltd, 72(January), pp. 774–790. doi:

10.1016/j.rser.2017.01.077.

Silitonga, A. S. *et al.* (2018) 'Evaluation of the engine performance and exhaust emissions of biodiesel-bioethanol-diesel blends using kernel-based extreme learning machine', *Energy*. Elsevier Ltd, 159, pp. 1075–1087. doi: 10.1016/j.energy.2018.06.202.

Singh, S. and Patel, A. (2015) 'Mono lacunary phosphotungstate anchored to MCM-41 as recyclable catalyst for biodiesel production via transesterification of waste cooking oil', *Fuel*. Elsevier Ltd, 159, pp. 720–727. doi: 10.1016/j.fuel.2015.07.004.

Skorupskaite, V., Makareviciene, V. and Gumbyte, M. (2016) 'Opportunities for simultaneous oil extraction and transesterification during biodiesel fuel production from microalgae: A review', *Fuel Processing Technology*. Elsevier B.V., 150, pp. 78–87. doi: 10.1016/j.fuproc.2016.05.002.

Sodhi, A. K., Tripathi, S. and Kundu, K. (2017) 'Biodiesel production using waste cooking oil: a waste to energy conversion strategy', *Clean Technologies and Environmental Policy*. Springer Berlin Heidelberg, 19(6), pp. 1799–1807. doi: 10.1007/s10098-017-1357-6.

Spacino, K. R. *et al.* (2015) 'Determination of kinetic and thermodynamic parameters of the B100 biodiesel oxidation process in mixtures with natural antioxidants', *Fuel Processing Technology*. Elsevier B.V., 137, pp. 366–370. doi: 10.1016/j.fuproc.2015.05.006.

Stephen, J. L. and Periyasamy, B. (2018) 'Innovative developments in biofuels production from organic waste materials: A review', *Fuel*. Elsevier, 214(September 2017), pp. 623–633. doi: 10.1016/j.fuel.2017.11.042.

Strzalka, R., Schneider, D. and Eicker, U. (2017) 'Current status of bioenergy technologies in Germany', *Renewable and Sustainable Energy Reviews*. Elsevier Ltd, 72(January), pp. 801–820. doi: 10.1016/j.rser.2017.01.091.

Su, F. *et al.* (2015) 'Enhancing biodiesel production via a synergic effect between immobilized Rhizopus oryzae lipase and Novozym 435', *Fuel Processing Technology*. Elsevier B.V., 137, pp. 298–304. doi: 10.1016/j.fuproc.2015.03.013.

Tabatabaei, M. *et al.* (2015) 'Recent trends in biodiesel production', *Biofuel Research Journal*, 2(3), pp. 258–267. doi: 10.18331/BRJ2015.2.3.4.

Tapia, J. *et al.* (2017) 'NiMo-sul de supported on activated carbon to produce renewable diesel', 22(1), pp. 71–85. doi: 10.11144/Javeriana.SC22-1.nsoa.

Trisunaryanti, W. *et al.* (2019) 'Preparation of Ni- and Mo-based catalysts supported on γ -Al 2 O 3 for hydrocracking of Calophyllum inophyllum oil', *Biofuels*. Taylor & Francis, 0(0), pp. 1–6. doi: 10.1080/17597269.2019.1669871.

Veriansyah, B. *et al.* (2012) 'Production of renewable diesel by hydroprocessing of soybean oil : Effect of catalysts', *Fuel*. Elsevier Ltd, 94, pp. 578–585. doi: 10.1016/j.fuel.2011.10.057.

Verma, P. and Sharma, M. P. (2016) 'Review of process parameters for biodiesel production from different feedstocks', *Renewable and Sustainable Energy Reviews*. Elsevier, 62, pp. 1063–1071. doi: 10.1016/j.rser.2016.04.054.

Verma, P., Sharma, M. P. and Dwivedi, G. (2016) 'Impact of alcohol on biodiesel production and properties', *Renewable and Sustainable Energy Reviews*. Elsevier Ltd, 56, pp. 319–333. doi: 10.1016/j.rser.2015.11.048.

Viêgas, C. V. *et al.* (2015) 'A route to produce renewable diesel from algae: Synthesis and characterization of biodiesel via in situ transesterification of Chlorella alga and its catalytic deoxygenation to renewable diesel', *Fuel*, 155, pp. 144–154. doi: 10.1016/j.fuel.2015.03.064.

Wang, E. *et al.* (2015) 'Production of biodiesel with lithium glyceroxide', *Fuel*. Elsevier Ltd, 160, pp. 621–628. doi: 10.1016/j.fuel.2015.07.101.

Wang, F. *et al.* (2018) 'Hydrotreatment of vegetable oil for green diesel over activated carbon supported molybdenum carbide catalyst', *Fuel*. Elsevier, 216(November 2017), pp. 738–746. doi: 10.1016/j.fuel.2017.12.059.

Wang, H. *et al.* (no date) 'catalysts The E ff ects of Catalyst Support and Temperature on the Hydrotreating of Waste Cooking Oil (WCO) over CoMo Sulfided Catalysts', (2).

Wang, X. *et al.* (2015) 'Heavy metal chemical extraction from industrial and municipal mixed sludge by ultrasound-assisted citric acid', *Journal of Industrial and Engineering Chemistry*. The Korean Society of Industrial and Engineering Chemistry, 27, pp. 368–372. doi: 10.1016/j.jiec.2015.01.016.

Xu, W., Gao, L. and Xiao, G. (2015) 'Biodiesel production optimization using monolithic catalyst in a fixed-bed membrane reactor', *Fuel*. Elsevier Ltd, 159, pp. 484–490. doi: 10.1016/j.fuel.2015.07.017.

Yoosuk, B. *et al.* (2019) 'Hydrodeoxygenation of oleic acid and palmitic acid to hydrocarbon-like biofuel over unsupported Ni-Mo and Co-Mo sul fi de catalysts', *Renewable Energy*. Elsevier Ltd, 139, pp. 1391–1399. doi: 10.1016/j.renene.2019.03.030.

Yunardi, Y. (2014) 'Response Surface Methodology Approach to Optimizing Process Variables for the Densification of Rice Straw as a Rural Alternative Solid Fuel', (June). doi: 10.3923/jas.2011.1192.1198.

Zhang, H., Lin, H. and Zheng, Y. (2014) 'The role of cobalt and nickel in deoxygenation of vegetable oils', *Applied Catalysis B: Environmental*. Elsevier B.V., 160–161(1), pp. 415–422. doi: 10.1016/j.apcatb.2014.05.043.

Zhu, L. D., Li, Z. H. and Hiltunen, E. (2016) 'Strategies for Lipid Production Improvement in Microalgae as a Biodiesel Feedstock', *BioMed Research International*, 2016, pp. 7–9. doi: 10.1155/2016/8792548.

Zulkepli, S. *et al.* (2018) 'Modified mesoporous HMS supported Ni for deoxygenation of triolein into hydrocarbon-biofuel production', *Energy Conversion and Management*. Elsevier, 165(March), pp. 495–508. doi: 10.1016/j.enconman.2018.03.087.

Appendices

Appendix A: Literature Review

A1: Oil Yields for the common biodiesel feedstocks (Mofijur et al., 2016; Mujeeb, Vedamurthy and T, 2016; Hajjari et al., 2017; Jayakumar et al., 2017; Katiyar et al., 2017; Mahmudul et al., 2017)

Feedstocks	Oil Yield (L/ha year)	Global average water footprint (m^3/ton oil)	Seed oil Content (%oil by wt biomass)	Land use (m^2 year/kg biodiesel)	Capacity of land needed (mha)	Potential Sources
Calophyllum	4680		65			
Castor	1307-1413	24740	43.5-48	9		Brazil, Iran, Kenya
Coconuts	2689	4490	63-65		99	Indonesia, Philippines, Thailand
Corn	172	2575	44-48	66	1540	
Cotton Seed	325	3957	18-25			Brazil, Greece
Groundnuts	1059	7529	47.8			USA
Hemp	363		33	31		
Jatopha	741-1892	870	28-60	15	140	Australia, China, Cuba, India, Indonesia, Iran, Mali, Pakistan, Peru Thailand, Zimbabwe
Jojoba	1818		45-50			

Linseed	478	9415				Spain
Microalgae.7	136900	-	70	0.1	2	Iran
Microalgae.3	58700	-	30	0.2		
Microalgae.5	97800	-	50	0.1		
Moringa			40			Cuba
Mustard	572	5600				Canada
Olives	1212	14578	45-70			
Palm Oil	5366-5950	5186	30-60	2	45	Brazil, Ghana, Indonesia, Iran, Malaysia, Singapore, Thailand
Rapeseed	974- 1190	4301	38-46	12	223	Canada, China, France, Germany, India, Italy, Sweden, Turkey, UK
Rice Bran	828		15-23			
Safflower	779	16046				
Sesame	696	21793				
Soybean	446-636	4190	15-20	18	594	Argentina, Brazil, Canada, India, USA
Sunflower	952-1070	6792	25-40	11		France, India, Italy, Spain, Turkey

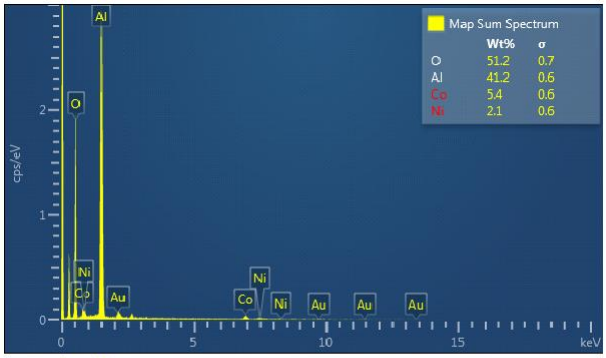
A2: ASTM D 6751 and EN 14214 specifications for biodiesel (Kumar and Ali, 2015; Sanli et al., 2015; Mofijur et al., 2016; Mujeeb, Vedamurthy and T, 2016; Hajjari et al., 2017; Mahmudul et al., 2017; Sierra-Cantor and Guerrero-Fajardo, 2017; Sodhi, Tripathi and Kundu, 2017)

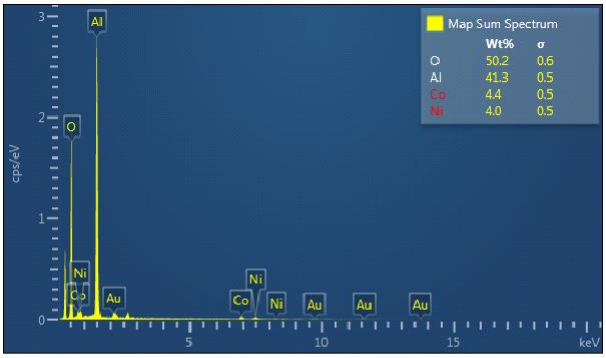
Properties	**ASTM D6751**		**EN14214**	
	Limit	**Method**	**Limit**	**Method**
Density at 15^{o}C	870-890 kg/m^3	ASTM D4052-91	860-900 kg/m^3	EN ISO 3675, EN ISO 12185
Flash Point	130°C minimum	ASTM D93	>101°C minimum	EN ISO 3679
Viscosity at 15^{o}C	1.9-6.0 mm^2/s	ASTM D445	3.5-5.0 mm^2/s	EN ISO 3140
Sulfated ash	0.02% m/m	ASTM D874	0.02% m/m maximum	EN ISO 3987
Cloud Point	Report to customer	ASTM D2500	Based on national specification	EN ISO 23015
Copper Strip Corrosion	Class 3 maximum	ASTM D130	Class 1 rating	EN ISO 2160
Cetane Number	47 minimum	ASTM D613	51 minimum	EN ISO 5165
Water Content and Sediment	0.05 (%v) maximum	ASTM 2709	500 mg/kg maximum	EN ISO 12937
Acid Number	0.5 mg KOH/g maximum	ASTM D664	0.5 mg KOH/g maximum	EN 14104
Free Glycerin	0.02% (m/m) maximum	ASTM D6584	0.02% (m/m) maximum	EN 1405/14016

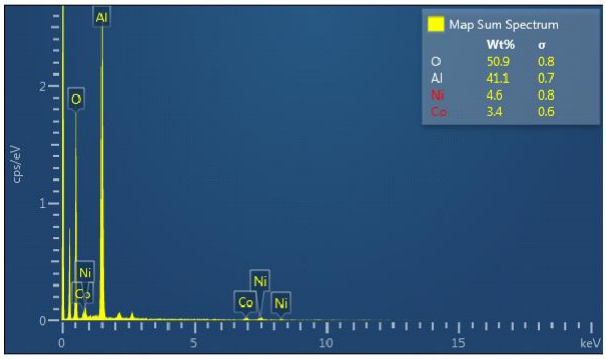
Total Glycerol	0.24% (m/m) maximum	ASTM D6548	0.25% (m/m)	EN 14105
Methanol Content	0.2% (m/m) maximum	EN14110	0.2% (m/m) maximum	EN14110
Phosphorus	10 mg/kg maximum	ASTM D4951	10 mg/kg maximum	EN 14107
Distillation Temperature	360°C	ASTM 1160	-	-
Sodium and Potassium	5ppm maximum	EN14538	5 mg/kg maximum	EN 14108/EN 14109
Oxidation Stability	3h minimum	EN ISO 14112	6h minimum	EN ISO 14112
Carbon Residue	0.05 wt.%	ASTM D4530	0.3% (m/m) maximum	EN ISO 10370
Calcium and Magnesium	5ppm maximum	EN14538	5ppm maximum	EN 14538
Iodine	-	-	120g/100g maximum	EN 14111

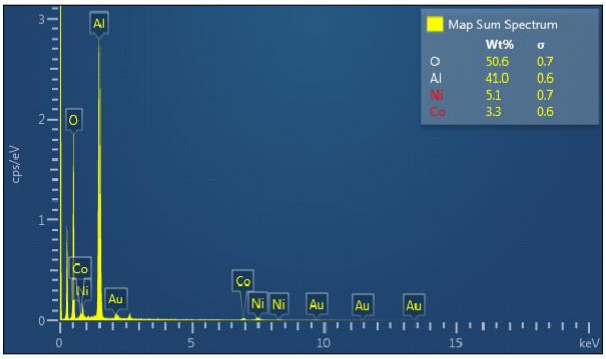
Appendix B: Catalyst Synthesis and Selection

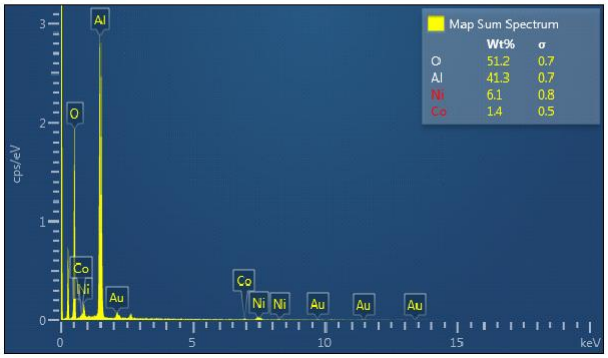
B1: EDX



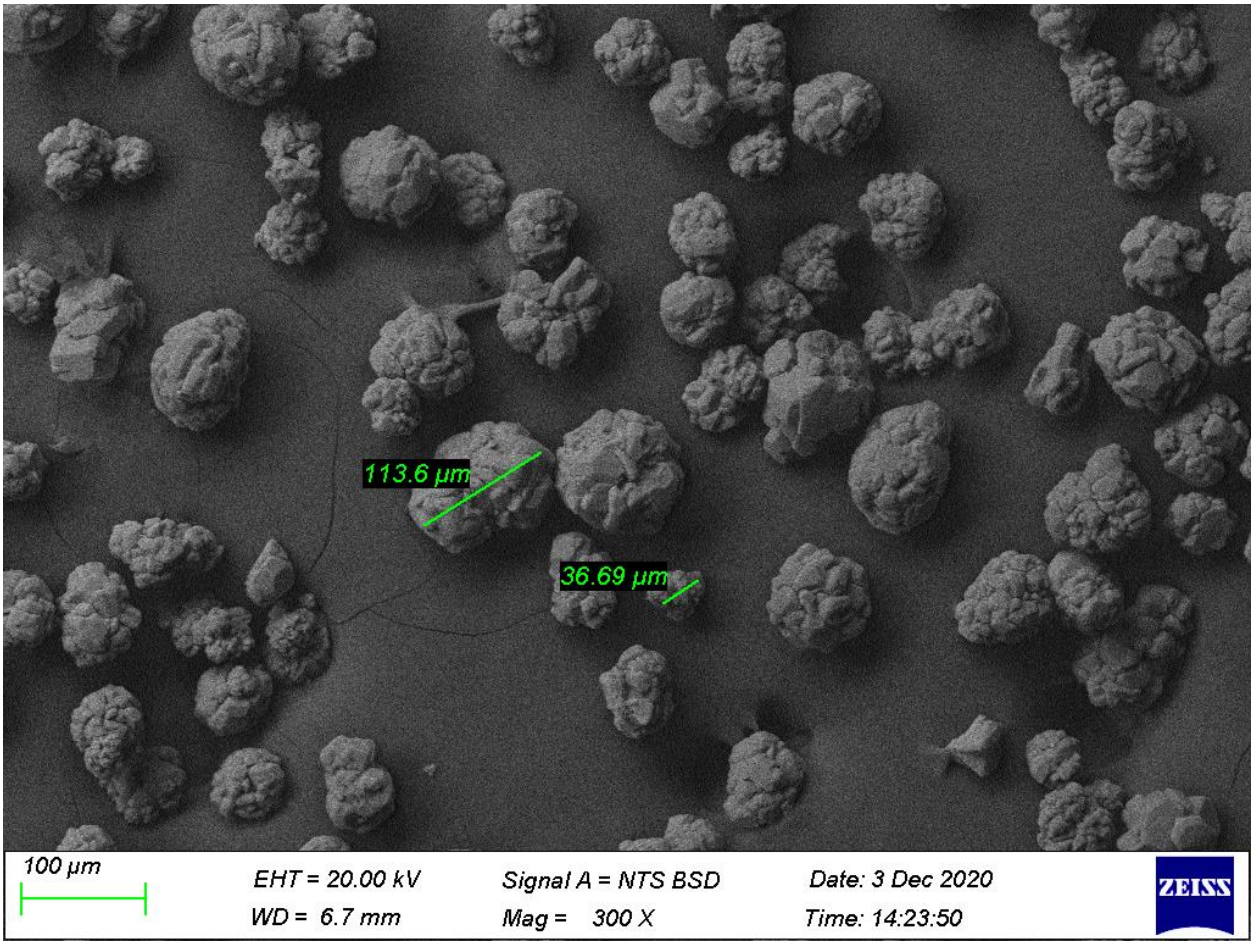




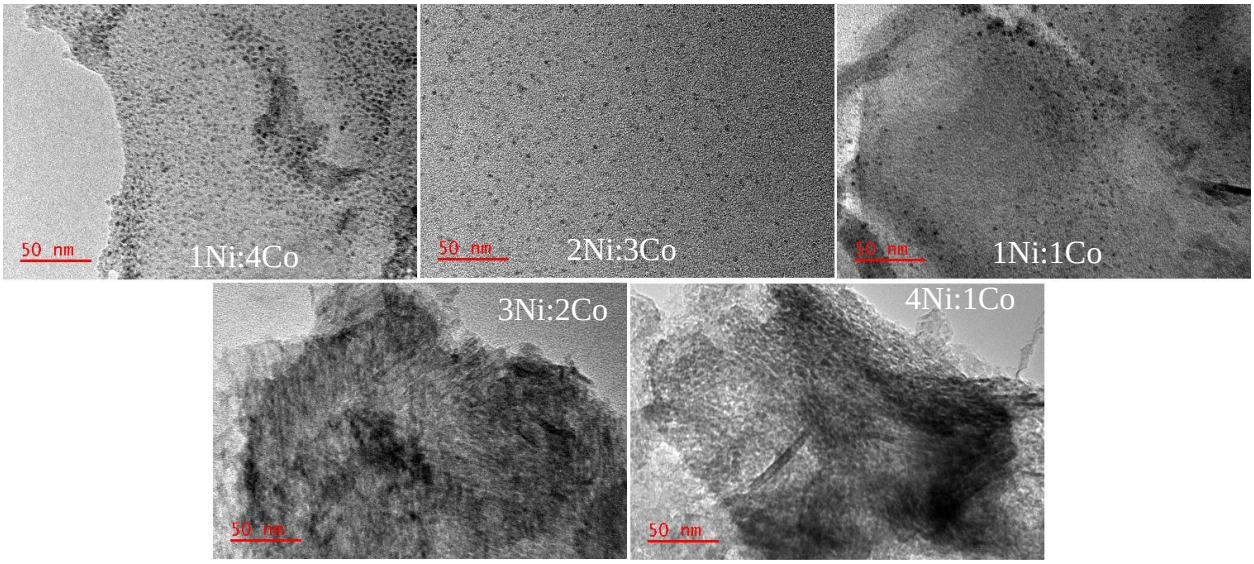




B2: Full map of the SEM of Al_2O_3



B3: 50 nm TEM micrographs of the catalysts



Appendix C: Deoxygenation of Waste Cooking Oil

C1: DO set up



C2: Closer view of the DO set up

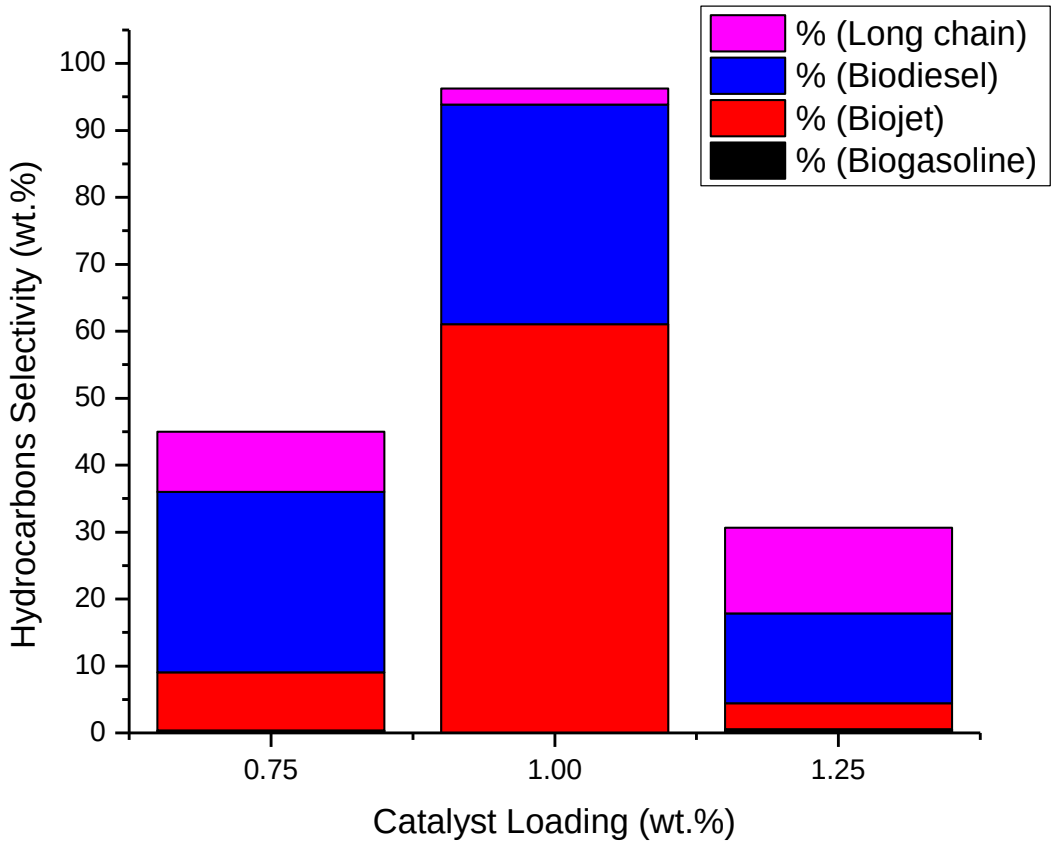


C3: Catalyst Screening Runs

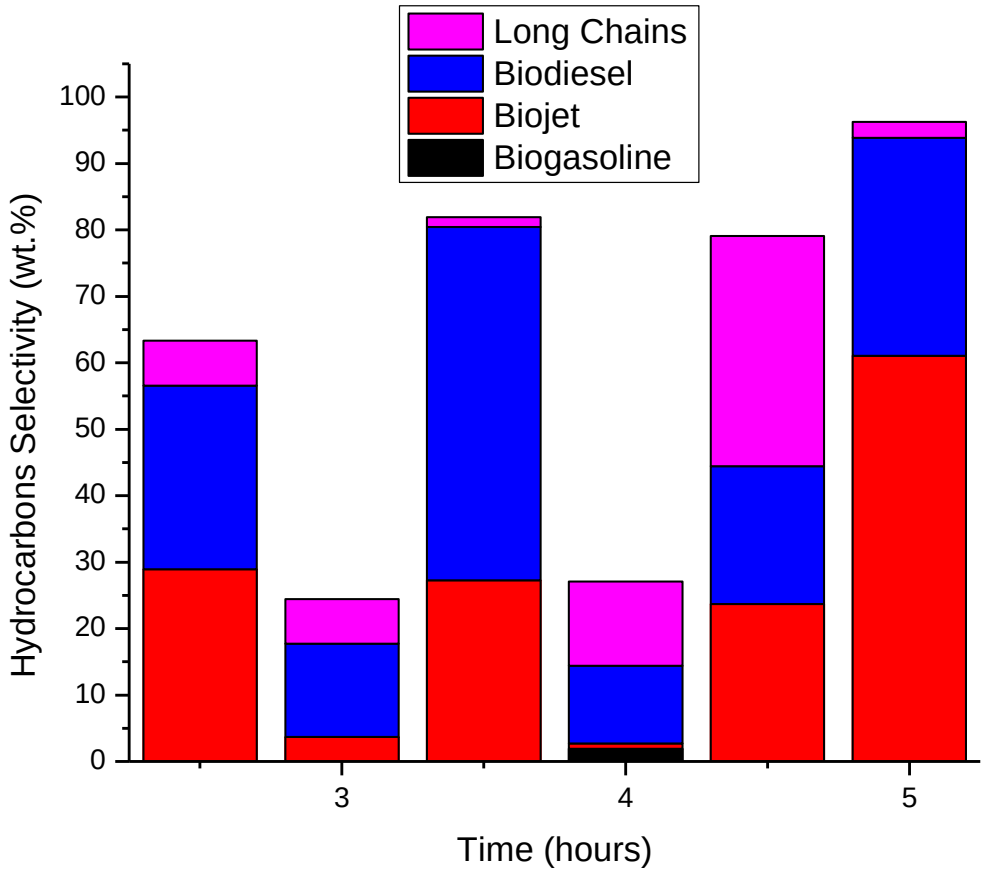
Time (hours)	Catalyst	Deoxygenation (%)	Alcohols (wt.%)	Ketones and Aldehydes (wt.%)	FFA (wt.%)	Esters (wt.%)	Hydrocarbons (wt.%)	C5-11 (wt.%)	C12-15 (wt.%)	C16-18 (wt.%)	C19+ (wt.%)
2,5	1Ni:1Co	58,5	15,31	0,68	5,59	15,07	63,34	0	28,92	24,56	9,86
	3Ni:2Co	58	15,12	9,48	5,17	8,78	61,36	1,33	35,65	17,23	7,15
3	1Ni:1Co	26,8	53,21	0,9	0	18,69	24,42	0,02	3,67	13,03	7,7
	3Ni:2Co	3,61	37,57	4,77	19,34	18,26	20,04	0,23	0,25	8,3	11,26
3,5	1Ni:1Co	76,11	3,68	1,37	0	12,87	81,95	0	27,28	48,83	5,77
	3Ni:2Co	58,5	16,34	1,72	0,66	16,39	63,9	0	41,95	19,35	2,6
4	1Ni:1Co	10,46	43,83	0,5	0,37	27,93	27,08	1,88	0,85	11,68	12,67
	3Ni:2Co	27,58	12,51	2,49	1,3	39,35	43,27	0,38	15,82	5,7	19,37

4,5	1Ni:1 Co	64,31	8,95	0,11	0	11,27	79,09	0	23,67	20,42	35
	3Ni:2 Co	-26,03	15,44	0	0,07	50,34	33,77	0,06	0,34	28,43	4,94
5	1Ni:1 Co	96,12	3,26	0,34	0,14	0	96,27	0	61,06	32,83	2,38
	3Ni:2 Co	61,71	18,94	0,89	3,75	10,65	65,77	0	38,22	21,77	5,78

C4: Hydrocarbons Selectivity with varying catalyst loading



C5: Hydrocarbons selectivity with reaction time



Appendix D: Design Expert

D1: ANOVA

Fit Statistics

Std. Dev.	24.19		**R^2**	0.4722
Mean	44.95		**Adjusted R^2**	0.3503
C.V. %	53.81		**Predicted R^2**	0.1958
			Adeq Precision	6.2895

D2: Optimization Solutions

Number	Temperature	Time	Loading	Deoxygenation	Desirability	
1	**320.000**	**5.500**	**1.250**	**73.060**	**0.461**	**Selected**
2	319.997	5.500	1.246	73.055	0.461	
3	320.000	5.500	1.240	73.052	0.461	
4	319.999	5.500	1.228	73.041	0.461	
5	320.000	5.499	1.221	73.033	0.461	
6	320.000	5.500	1.207	73.025	0.461	
7	320.000	5.500	1.204	73.023	0.460	
8	320.000	5.500	1.187	73.009	0.460	
9	320.000	5.500	1.184	73.007	0.460	
10	320.000	5.500	1.179	73.003	0.460	
11	320.000	5.500	1.169	72.995	0.460	
12	320.000	5.476	1.250	72.988	0.460	
13	320.000	5.500	1.142	72.973	0.459	
14	320.000	5.500	1.138	72.969	0.459	
15	320.000	5.500	1.127	72.960	0.459	
16	320.000	5.500	1.116	72.951	0.459	
17	320.000	5.500	1.099	72.938	0.459	
18	320.000	5.458	1.250	72.935	0.459	
19	320.000	5.495	1.105	72.929	0.459	

20	320.000	5.500	1.074	72.917	0.458	
21	320.000	5.500	1.068	72.913	0.458	
22	320.000	5.500	1.061	72.907	0.458	
23	320.000	5.500	1.055	72.902	0.458	
24	320.000	5.500	1.045	72.894	0.458	
25	320.000	5.500	1.037	72.888	0.458	
26	320.000	5.500	1.009	72.865	0.457	
27	320.000	5.500	1.006	72.862	0.457	
28	320.000	5.500	0.998	72.856	0.457	
29	320.000	5.500	0.961	72.826	0.457	
30	320.000	5.500	0.948	72.815	0.456	
31	320.000	5.448	1.134	72.810	0.456	
32	320.000	5.500	0.941	72.810	0.456	
33	320.000	5.500	0.926	72.797	0.456	
34	320.000	5.500	0.898	72.774	0.455	
35	320.000	5.499	0.875	72.753	0.455	
36	320.000	5.500	0.869	72.751	0.455	
37	320.000	5.500	0.824	72.714	0.454	
38	320.000	5.500	0.807	72.700	0.454	
39	320.000	5.500	0.803	72.698	0.454	
40	320.000	5.500	0.777	72.676	0.454	
41	320.000	5.500	0.773	72.673	0.453	
42	320.000	5.500	0.767	72.668	0.453	
43	320.000	5.500	0.750	72.654	0.453	
44	320.000	5.500	0.716	72.627	0.453	
45	320.000	5.500	0.711	72.623	0.452	
46	320.000	5.500	0.699	72.613	0.452	
47	320.000	5.500	0.696	72.611	0.452	
48	320.000	5.500	0.688	72.604	0.452	
49	320.000	5.500	0.678	72.596	0.452	

50	320.000	5.500	0.674	72.592	0.452	
51	320.000	5.500	0.668	72.588	0.452	
52	320.000	5.500	0.658	72.580	0.452	
53	320.000	5.500	0.633	72.560	0.451	
54	320.000	5.500	0.615	72.545	0.451	
55	320.000	5.499	0.609	72.537	0.451	
56	320.000	5.500	0.599	72.532	0.451	
57	320.000	5.500	0.588	72.523	0.450	
58	320.000	5.500	0.526	72.473	0.449	
59	320.000	5.500	0.518	72.466	0.449	
60	320.000	5.500	0.507	72.458	0.449	
61	319.782	5.500	0.500	72.275	0.445	
62	320.000	5.352	0.500	72.008	0.440	
63	320.000	4.976	1.250	71.493	0.430	
64	320.000	5.088	0.500	71.217	0.424	
65	320.000	5.045	0.500	71.091	0.422	
66	320.000	5.017	0.511	71.016	0.420	
67	320.000	4.989	0.500	70.921	0.418	
68	320.000	4.783	1.250	70.913	0.418	
69	320.000	4.961	0.500	70.839	0.417	
70	317.772	5.500	0.506	70.651	0.413	
71	320.000	4.816	0.500	70.405	0.408	
72	320.000	4.253	1.250	69.328	0.387	
73	320.000	4.417	0.500	69.210	0.384	
74	320.000	4.175	1.250	69.095	0.382	
75	320.000	4.284	0.500	68.811	0.376	
76	320.000	4.228	0.500	68.644	0.373	
77	320.000	3.973	1.249	68.488	0.370	
78	320.000	3.983	0.500	67.911	0.358	
79	319.997	3.916	0.500	67.708	0.354	

80	320.000	3.665	1.250	67.569	0.351	
81	320.000	3.654	1.250	67.535	0.351	
82	320.000	3.752	0.500	67.220	0.344	
83	320.000	3.239	1.250	66.293	0.326	
84	320.000	3.302	0.500	65.871	0.317	
85	320.000	3.041	1.250	65.700	0.314	
86	320.000	2.959	0.500	64.845	0.297	
87	320.000	2.709	0.701	64.259	0.285	
88	319.999	2.657	0.500	63.941	0.279	